AD-A121 379 IMPROVED DYNAMIC MODELS FOR AIR COMBAT ANALYSIS(U) 1/2
TECHNION - ISRAEL INST OF TECH HAIFA DEPT OF
AERONAUTICAL ENGINEERING N FARBER ET AL. JUL 82
UNCLASSIFIED AFWAL-TR-82-3057 F33615-81-K-3007 F/G 15/7 NL

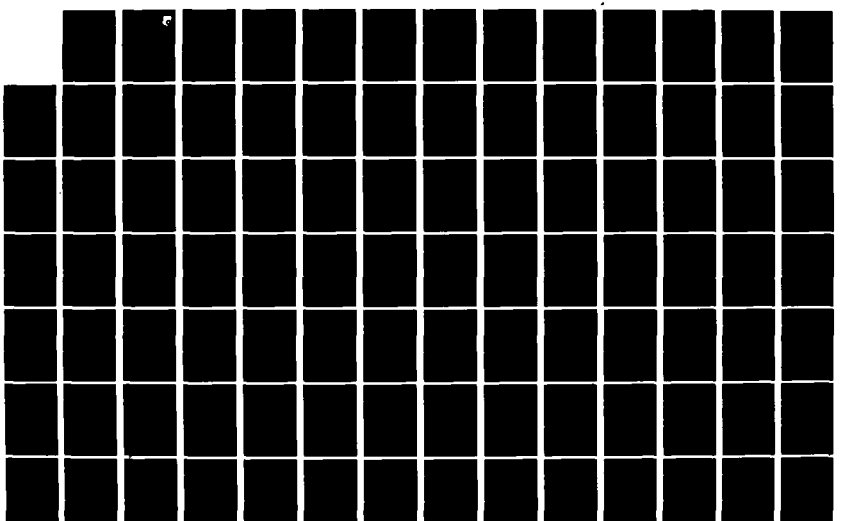

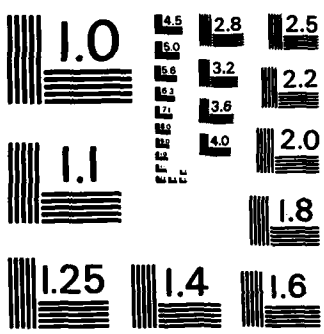

MICROCOPY RESOLUTION TEST CHART
NATIONAL BUREAU OF STANDARDS-1963-A

AFWAL-TR-82-3057

IMPROVED DYNAMIC MODELS FOR AIR COMBAT ANALYSIS

TECHNION UNIVERSITY
HAIFA, ISRAEL

July 1982

Final Report for Period 1 January 1981 - 31 December 1981

FLIGHT DYNAMICS LABORATORY
AIR FORCE WRIGHT AERONAUTICAL LABORATORIES
AIR FORCE SYSTEMS COMMAND
WRIGHT-PATTERSON AIR FORCE BASE, OHIO 45433

NOTICE

When Government drawings, specifications, or other data are used for any purpose other than in connection with a definitely related Government procurement operation, the United States Government thereby incurs no responsibility nor any obligation whatsoever; and the fact that the government may have formulated, furnished, or in any way supplied the said drawings, specifications, or other data, is not to be regarded by implication or otherwise as in any manner licensing the holder or any other person or corporation, or conveying any rights or permission to manufacture use, or sell any patented invention that may in any way be related thereto.

This report has been reviewed by the Office of Public Affairs (ASD/PA) and is releasable to the National Technical Information Service (NTIS). At NTIS, it will be available to the general public, including foreign nations.

This technical report has been reviewed and is approved for publication.

L. Earl Miller

L. EARL MILLER
Project Engineer

J. Christopher Boison

J. CHRISTOPHER BOISON
Chief, High Speed Aero Perf Br.
Aeromechanics Division

FOR THE COMMANDER

John R. Chevalier

JOHN R. CHEVALIER, Colonel, USAF
Chief, Aeromechanics Division
AF Wright Aeronautical Laboratories (AFSC)

If your address has changed, if you wish to be removed from our mailing list, or if the addressee is no longer employed by your organization please notify AFWAL/FIMG, *W-PAFB, OH 45433 to help us maintain a current mailing list.*

Copies of this report should not be returned unless return is required by security considerations, contractual obligations, or notice on a specific document.

Complete

SECURITY CLASSIFICATION OF THIS PAGE *(When Data Entered)*

REPORT DOCUMENTATION PAGE		READ INSTRUCTIONS BEFORE COMPLETING FORM
1. REPORT NUMBER AFWAL-TR-82-3057	2. GOVT ACCESSION NO.	3. RECIPIENT'S CATALOG NUMBER
4. TITLE *(and Subtitle)* IMPROVED DYNAMIC MODELS FOR AIR COMBAT ANALYSIS		5. TYPE OF REPORT & PERIOD COVERED Final Scientific Report Jan 81 - Dec 81
		6. PERFORMING ORG. REPORT NUMBER TAE
7. AUTHOR(s) N. Farber, M. Negrin and J. Shinar		8. CONTRACT OR GRANT NUMBER(s) F33615-K-3007
9. PERFORMING ORGANIZATION NAME AND ADDRESS Department of Aeronautical Engineering Technion, Israel Institute of Technology Haifa, 32000 - Israel		10. PROGRAM ELEMENT, PROJECT, TASK AREA & WORK UNIT NUMBERS 24040746
11. CONTROLLING OFFICE NAME AND ADDRESS U.S. Air Force Wright Aeronautical Laboratories/FIMG		12. REPORT DATE July 1982
		13. NUMBER OF PAGES 122
14. MONITORING AGENCY NAME & ADDRESS*(if different from Controlling Office)*		15. SECURITY CLASS. *(of this report)* Unclassified
		15a. DECLASSIFICATION/DOWNGRADING SCHEDULE

16. DISTRIBUTION STATEMENT *(of this Report)*

Approved for public release; distribution unlimited.

17. DISTRIBUTION STATEMENT *(of the abstract entered in Block 20, if different from Report)*

18. SUPPLEMENTARY NOTES

19. KEY WORDS *(Continue on reverse side if necessary and identify by block number)*

Air combat analysis, medium range air combat, air-to-air interception, differential games, feedback control strategies, singular perturbations, real time implementation.

20. ABSTRACT *(Continue on reverse side if necessary and identify by block number)*

This report summarizes a multi-year research effort to develop improved dynamic model for air combat analysis. Reaching this objective is demonstrated by providing a zero-order feedback solution to the three-dimensional medium range air-to-air interception engagement, formulated as a zero-sum differential game. Using realistic aerodynamic and propulsion models, control strategies are expressed in a feedback form expressing explicitly the dependence on the

(continued)

DD FORM 1 JAN 73 1473 EDITION OF 1 NOV 65 IS OBSOLETE

Complete

SECURITY CLASSIFICATION OF THIS PAGE *(When Data Entered)*

ABSTRACT (cont'd)

measurable state variables and aircraft performance parameters. The successive analysis is based on an innovative, variable modelling approach applying the method of forced singular perturbations. An imaginary air defence scenario serves as an illustrative example, showing the efficiency and the usefullness of the method for a rapid systematical parametric study. The accuracy of the zero-order feedback approximation and for most cases higher order terms may not be needed. Such corrective terms can be obtained, if necessary, by additional off-line computation. Computing the zero-order feedback strategies requires a minimal effort and presents therefore an extremely attractive candidate for real time implementation onboard of advanced fighter aircraft. It is, therefore, recommended to incorporate the implementation of the FSPT algorithm for optimal medium range air combat strategy in a future flight test program.

FOREWORD

This report was prepared by Technion University in Haifa, Israel under contract F33615-K-3007, project 24040746, for the Flight Dynamics Laboratory, Air Force Wright Aeronautical Laboratories, Wright-Patterson Air Force Base, Ohio. Dr. Earl Miller (AFWAL/FIMG) served as technical monitor for this contract.

The period of performance was January 1981 to December 1981.

The investigation was conducted by N. Faber, M. Negrin, and J. Shinar from the Department of Aeronautical Engineering.

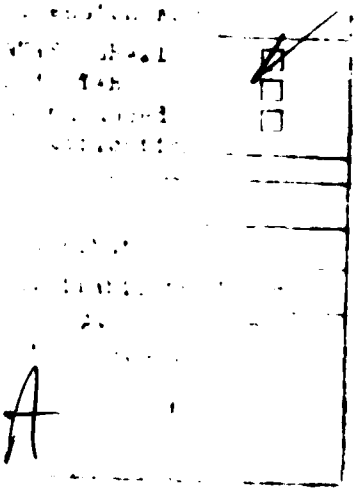

TABLE OF CONTENTS

TABLE OF CONTENTS (Cont'd)

TABLE OF CONTENTS (Cont'd)

LIST OF ILLUSTRATIONS

LIST OF SYMBOLS

a	- Speed of Sound
C_D, C_{D_0}, C_L	- Aerodynamic coefficients
C_S	- Specific fuel consumption
D	- Drag force
E	- Specific energy
g	- Acceleration of gravity
H, h	- Altitude
$\mathcal{H}$	- Hamiltonian
J	- Payoff function
K	- Induced drag parameter
L	- Lift force
ℓ	- Capture radius
M	- Mach number
m	- Aircraft mass
n	- Aerodynamic load factor
P_s	- Specific energy rate
q	- Dynamic pressure
R	- Turning radius
r	- Separation distance
S	- Wing surface
T	- Thrust
t	- Time
V	- Aircraft velocity
W	- Aircraft weight
X, Y	- Horizontal coordinates

Greek Letters

α	- Angle of attack
β_T	- Thrust tilt angle
γ	- Climb angle
ε	- Singular perturbation parameter
η	- Empirical constant

θ	- Line of sight angle in the vertical plane
λx, λy,...	- Adjoint variables
μ	- Aircraft bank angle
ξ	- Throttle parameter
ρ	- Air density
σ	- Sensitivity
τ	- Stretched time
χ	- Azimuth angle
ψ	- Line of sight angle in the horizontal plane.

Subscripts

E	- Evader
P	- Pursuer
0	- Initial value
f	- Final value
h	- Horizontal
I	- Induced

Superscripts

$( )^{o}$	- Reduced game
$( )^{i}$	- Outer boundary layer
$( )^{j}$	- Intermediate boundary layer
$( )^{k}$	- Inner boundary layer
$( )^{*}$	- Optimal value
$( )^{c}$	- Composite (zero-order) control
$( )^{L}$	- Value at local altitude

LIST OF ABBREVIATIONS

SPT	- Singular Perturbation Technique
FSPT	- Forced Singular Perturbation Technique
C.S.L.	- Combined Strategy Logic
ME1	- Main Equation 1.
IC	- Initial Conditions

SECTION I

INTRODUCTION

The research effort, conducted during the last years at the Department of Aeronautical Engineering at the Technion, developing improved models for air combat analysis, has shown that an analytical investigation of a complex dynamic problem can lead to meaningful and applicable results. USAF support of the research program guaranteed that the effort be focused on relevant air combat problems and made possible to complete the investigation in a relatively short time.

It has been a concensus for many years that the conflicting nature of air combat should be analyzed by a differential game approach. However, the inherent mathematical complexity of such game formulation with realistic dynamic models left little hope for a comprehensive investigation. In order to be able to obtain practically useful results it was first necessary to identify an analytical method of approximation which enables some order reduction of the mathematical model. The technique of multiple time scale singular perturbation seemed to be an attractive candidate based on its successful application in aircraft performance optimization problems.

The first phase of the research program was oriented to overcome the conceptual difficulty in applying the singular perturbation approximation to nonlinear zero-sum differential games [1]. In the sequel, a set of examples of gradually increasing complexity were solved leading to development of a consistent methodology. This methodology provides a uniformly valid zero-order solution in a feedback form for the control strategies of a realistic three-dimensional variable speed pursuit-evasion game. A basic operational scenario of future air warfare, the medium range air-to-air interception using advanced homing

missiles, serves as a suitable example to demonstrate the merits of this innovative approach.

The major effort of the investigation in the last year (sponsored by AFWAL Contract No. F33615-81-K-3007) was concentrated on developping a computer program. This program implements the variable modelling forced singular perturbation technique to solve the problem of medium range interception (using missiles) formulated as a perfect information zero-sum differential game.

The objective of this report is to document the results obtained during this last year and to outline the potential of the methodology developed for future applications. The report starts (Ch. 2) by summarizing the results obtained in the previous phases of the multi-year research effort, followed (Ch. 3) by the formulation of the three-dimensional medium range time optimal air-to-air interception game. The solution of this problem, presented in Ch. 6, is reached as a consequence of modelling considerations (described in Ch. 4) and the insight gained by solving first (in Ch. 5) the interception game in the vertical plane. In Ch. 7 an imaginary air defence scenario serves as an example to demonstrate the usefulness of the computationally efficient solution technique. In the following chapters the accuracy of the zero-order approximation is analysed and eventual corrections are discussed. The potential merits of applying the zero-order feedback solution for airborne implementation, as well as for rapid systematic performance analysis, are presented in the concluding chapter.

SECTION II

SUMMARY OF PRECEDING STUDIES

1. APPLICATION OF SPT FOR NONLINEAR DIFFERENTIAL GAMES

The application of singular perturbation technique (SPT) for solving certain types of pursuit-evasion problems formulated as non-linear, zero-sum differential games has been demonstrated in the past [1]. Motivation for using this approximation technique was explained by the necessity to overcome the high dimensionality (as well as the non-linear character) of realistic pursuit-evasion problems.

SPT is based on the assumption that some components of the state vector behave as "fast", compared to the other "slow" ones, leading to an eventual time scale separation. Using this approach, the original problem is separated into several subgames of lower dimensions, which can be solved analytically. This process is meaningful only if it is assumed that the original game has indeed a saddle point solution (an assumption which unfortunately cannot be verified).

Dealing with pursuit-evasion games, the reduced order game represents a "simple" pursuit, where the "fast" state variables, i.e., flight direction and velocities of both opponents, are considered as controls. The reduced order game has a smooth value function satisfying the sufficiency condition for saddle point optimality [1].

This game is unable to satisfy the initial and/or terminal conditions imposed in the original problem on those variables for which the dynamics is neglected in the reduced game.

In order to match these conditions several boundary layer games are required. The boundary layer games are usually decoupled into one-sided optimal control problems, for which satisfaction of "game optimality" is not required. Based on these subgames a uniformly valid composite solution is synthesized and it represents a suboptimal zero-order approximation for the exact solution of the original game (if such solution indeed exists).

The outcome of the original game using the suboptimal SPT strategy pair is defined as: Extended Value of the game. It was shown [1] that this extended value is bounded on both sides satisfying a week saddle inequality. Furthermore, it was proven [1] that if the perturbation parameter (ε) becomes very small the Extended Value of a singularly perturbed, zero-sum differential game approaches as a limit the exact Value of the game.

2. SPT SOLUTION OF THE "GAME OF TWO CARS"

The usefulness of SPT has been demonstrated, first, via the example of the "Game of Two Cars" (a 2-D, constant speed pursuit-evasion game). In this example, the original equations expressed in polar coordinates, were transformed in order to discover the existence of a small parameter (the ratio of aircraft's turning radius to the initial distance of separation R/r_0). As a result, the singularly perturbed differential, zero-sum differential game had a simple zero-order closed form solution. The strategy of each player is composed of three phases:

(a) a "hard" initial turn until the velocity vector is aligned with the line of sight;

(b) a subarc of line of sight guidance if the other player is still in phase (a);

(c) a straight line dash till capture.

This approximation was compared to the exact solution of the same problem given by Simakova [2].

In the exact solution the direction of the final dash is the common tangent of the turning circles of the players as determined by the initial conditions of the game. The optimal strategy of the players is to align their velocity vector with this tangent. If the initial conditions are such that both players finish their hard turn simultaneously the trajectories of the optimal and the SPT solution, and consequently the outcome of the game are identical. For any other initial conditions one of the players completes its "hard" turn earlier and following the suboptimal strategy of phase (b) deviates from the optimal one.

If it is the pursuer, the time of capture will be slightly longer than in the optimal game. If the evader reaches first the line of sight direction, the capture time of the SPT solution will be shorter than the Value predicted by Simakova. The differences, however, are small.

A quantitative example shows a remarkably good agreement between the outcome of this game using suboptimal strategies and the exact Value. Even for relatively large values of the perturbation parameter ($\varepsilon = 0.4$) the difference is only a few percent (the relative error in this example is between the order of ε^2 and ε^3).

3. VARIABLE SPEED MEDIUM RANGE INTERCEPTION GAME

3.1 Model A.

As a second step, a variable speed horizontal pursuit-evasion game of two airplanes, with realistic thrust and aerodynamic data has been analysed [3]. In this case it was difficult to show the existence of a small parameter of physical significance which can transform the system into a singularly perturbed structure. However, time scale separation of the variables was known to exist, therefore, a small parameter inserted artificially into the system, multiplying the derivatives of the "fast" variables.

This so-called Forced Singular Perturbation Technique (FSPT), has been used extensively for aircraft performance optimization [4-7]. FSPT was formally justified [8] as a legitimate technique to produce zero-order feedback solution for problems which exhibit genuine time scale separation.

Results of the constant speed model have shown, that if the initial separation is large compared to the turning radius of the players the line of sight dynamics is very "slow". Eventual speed variations are assumed to be next in the hierarchy while the directions of the players are considered as the "fastest" variables.

Assuming that capture range is greater than the pursuer's turning radius, a uniformly valid zero-order approximation of the optimal strategies has been obtained analytically in a feedback form.

The solution indicated that for large initial separation the optimal strategy terminates by a "tail chase" flown at maximum velocities. This reduced order solution is reached by both airplanes by performing a variable speed, full thrust, turning maneuver determined by a time optimal compromise between the lateral and longitudinal accelerations. Implementation of the suboptimal feedback strategies requires to measure only the relative angular position and the vehicle's own velocity. It seems, therefore, very attractive for real time on-board applications.

Numerical example solved in [3] confirmed the assumptions of time scale separation justifying the forced singular perturbation approach.

In this classical FSPT approach the hierarchy of the state variables (their respective role as being "slow" or "fast") is preserved for the whole duration of the game. Experience has shown, however, that in some nonlinear dynamic problems the relative rate of change of the variables may vary considerably in the course of the solution.

3.2 Model B.

The inherent property of the previous model (defined as model A) was the requirement for full thrust as a control strategy in all situations. Engineering insight indicates that such a model may not be representative in a case where one of the airplanes flies at a speed largely exceeding its own "corner velocity" (where the instantaneous turning rate is maximum) if its flight direction deviates considerably from the one required for optimality. It seems intuitively clear that such an airplane has to reduce its speed (to improve its turning rate) as rapidly as possible which implies, for horizontal flight, zero thrust as optimal control strategy. In this case speed variations cannot be more considered being "slow" as compared to the constrained turning rate. To properly model such situation it has been proposed [9] to declare velocity variations as the "fastest" dynamics in the SPT hierarchy. Turning dynamics were still considered "faster" than the variations of the line of sight and separation distance. This new SPT model (defined as model B), allows for variable throttle setting as optimal control strategy. The validity of this model is, however, conditional. When the

model dictates full thrust, deceleration rate becomes slower than turning rate and model A may be more representative.

3.3 Combined Strategy Logic

In [9] a variable modeling approach has been proposed. This model is based on a Combined Strategy Logic (C.S.L.) synthesized by using both A and B models. The first step of C.S.L. is to verify, using model B (for each player separately) whether the initial conditions of the engagement require a zero thrust subarc.

A negative answer leads to the use of model A for the respective player during the whole game. For a positive answer, model B is used until full thrust is required. Then the solution continues with model A. Since both models use the same reduced order game, the variable modeling computational scheme is only slightly more complex than the one using a single model.

4. THREE DIMENSIONAL CONSTANT SPEED MODEL

Real interception is a three-dimensional problem. Therefore, further extensions of the previous models are necessary. As a first step towards this goal, the 2-D constant speed model (the game of two cars) has been extended to include the effects of a 3-D flight [10].

Similarly to the 2-D, constant speed model it was assumed that turning rates of both aircraft are much faster than the rate of change of the line of sight. With this assumption a general solution (using vectorial notation) has been obtained. The solution indicates that the optimal strategy for each aircraft is to orient its angular velocity vector in a direction perpendicular to the plane defined by the line of sight and its current velocity vector.

The results of this strategy were the following:

(a) During the first stage of the engagement each aircraft moves in its own plane (defined by the line of sight and its velocity vector).

(b) As soon as one of the aircraft coincide its velocity vector with the line of sight, it keeps moving along this line.

(c) During the last stage both aircraft move along the line of sight.

One of the consequences of this solution is that a game which has progressed into a planar configuration will remain in it till termination. A fact supported by other references [11-13].

5. A CONCLUDING REMARK

The results summarized in this chapter have served as guidelines for the formulation and an appropriate solution of the real air combat problem of interest: "the 3-D medium range interception game", using a 3-D variable speed FSPT model.

SECTION III

FORMULATION OF THE 3-D MEDIUM RANGE TIME OPTIMAL, AIR-TO-AIR INTERCEPTION GAME

1. APPLICATION OF SPT FOR NONLINEAR DIFFERENTIAL GAMES

The motion of a point mass lifting vehicle over a flat non-rotating earth assuming symmetrical flight, is governed by the following set of nonlinear ordinary differential equations:

$$\dot{x} = V \cos\gamma \cos\chi \tag{3.1}$$

$$\dot{y} = V \cos\gamma \sin\chi \tag{3.2}$$

$$\dot{h} = V \sin\gamma \tag{3.3}$$

$$\dot{V} = g\left\{\frac{\xi\, T_{max}(h,V)\cos(\alpha + \beta_T) - D}{W} - \sin\gamma\right\} \tag{3.4}$$

$$\dot{\gamma} = \frac{g}{V}\left\{\frac{\xi\, T_{max}(h,V)\, \sin(\alpha + \beta_T) + L}{W} \cos\mu - \cos\gamma\right\} \tag{3.5}$$

$$\dot{\chi} = \frac{g}{V}\left\{\frac{\xi\, T_{max}(h,V)\, \sin(\alpha+\beta_T)+L}{W\cos\gamma} \sin\mu\right\} \tag{3.6}$$

$$\dot{m} = -\frac{1}{g} C_s(h,V,T) \tag{3.7}$$

$$L = \frac{1}{2}\rho(h)V^2\, S\, C_L(\alpha,M) \tag{3.8}$$

$$D = \frac{1}{2}\rho(h)V^2\, S\, C_D(M,C_L) \tag{3.9}$$

For a parabolic drag polar:

$$C_D(M,C_L) = C_{D_0}(M) + K(M)\, C_L^2(\alpha,M) \tag{3.10}$$

and aerodynamic load factor defined by:

$$n = \frac{L}{W} \triangleq \frac{\frac{1}{2}\rho(h)\ V^2\ C_L(\alpha,M)}{W/S} \tag{3.11}$$

The drag force can be expressed as:

$$D = D_0 + n^2\ D_I = D(h,V,n) \tag{3.12}$$

where D_0 is the zero lift drag and D_I the induced drag in level flight:

$$D_I = \frac{KW^2}{\frac{1}{2}\rho(h)\ V^2 S} \quad . \tag{3.13}$$

2. CONTROL CONSTRAINTS

The aircraft controls are throttle (ξ), angle of attack (α), bank angle (μ) and thrust tilt angle with respect to the aircraft longitudinal axis (β_T). α can be replaced as control variable by n (or C_L) according to the following rule:

Below "corner velocity" defined as:

$$V_C \triangleq \left[\frac{2n_{max}W}{\rho(h)\ S\ C_{L_{max}}(M_C)}\right]^{\frac{1}{2}} \tag{3.14}$$

The load factor is constrained by the maximum lift coefficient:

$$n \leq n_L(h,M) \triangleq \frac{1}{2}\rho(h)\ V^2\ S\ C_{L_{max}}(M)/W \tag{3.15}$$

Above the "corner velocity" the load factor is constrained by the aircraft structural properties:

$$n \leq n_{max} \tag{3.16}$$

Throttle constraints are:

$$0 \leq \xi \leq 1 \tag{3.17}$$

which are equivalent to the following constraints on the aircraft thrust:

$$0 \leq T \leq T_{max}(h,V) \tag{3.18}$$

Bank angle is constrained by:

$$-\pi \leq \mu \leq \pi \tag{3.19}$$

The thrust tilt angle constraints are:

$$\beta_{T_{min}} \leq \beta_T \leq \beta_{T_{max}} \tag{3.20}$$

3. STATE CONSTRAINTS

Minimum altitude limit:

$$h > 0 \tag{3.21}$$

Maximum dynamic pressure limit:

$$q = \frac{1}{2}\rho(h)V^2 \leq q_{max} \tag{3.22}$$

Maximum Mach number limit:

$$V \leq a(h)\, M_{max} \tag{3.23}$$

Loft ceiling (h_L) limit

$$\frac{1}{2}\rho(h_L)\, V^2 \geq \frac{W/S}{C_{L_{max}}(M)} \tag{3.24}$$

4. SIMPLIFIED EQUATIONS FOR THE 3-D GAME

For most cases fuel consumption during the interception engagement can be neglected, eliminating Eq. (3.7). Assuming that thrust is nearly aligned with aircraft longitudinal axis ($\beta_T \approx 0$) and that angles of attack are not excessive (implying $\cos\alpha \approx 1$, and $T_{max} \sin\alpha << L$) further simplications are obtained in Eqs. (3.4)-(3.6).

The game can be also formulated in relative coordinates, replacing the two sets of Eqs. (3.1)-(3.5) (for the pursuer and the evader) by only one (for the relative coordinates). However, only the horizontal components can be meaningfully expressed in this way since the aerodynamic and propulsive forces acting on the airplanes strongly depend on their respective altitudes. Consequently, the final set of differential equations describing the 3-D interception game is of 10 independent state variables.

$$(\dot{\Delta x}) = V_E \cos\gamma_E \cos\chi_E - V_P \cos\gamma_P \cos\chi_P \tag{3.25}$$

$$(\dot{\Delta y}) = V_E \cos\gamma_E \sin\chi_E - V_P \cos\gamma_P \sin\chi_P \tag{3.26}$$

$$\dot{h}_P = V_P \sin\gamma_P \tag{3.27}$$

$$\dot{h}_E = V_E \sin\gamma_E \tag{3.28}$$

$$\dot{V}_P = g\left[\frac{\xi_P T_{max_P} - D_{0_P} - n_P^2 D_{I_P}}{W_P} - \sin\gamma_P\right] \tag{3.29}$$

$$\dot{V}_E = g\left[\frac{\xi_E T_{max_E} - D_{0_E} - n_E^2 D_{I_E}}{W_E} - \sin\gamma_E\right] \tag{3.30}$$

$$\dot{\gamma}_P = \frac{g}{V_P}\left[n_P \cos\mu_P - \cos\gamma_P\right] \tag{3.31}$$

$$\dot{\gamma}_E = \frac{g}{V_E}\left[n_E \cos\mu_E - \cos\gamma_E\right] \tag{3.32}$$

$$\dot{\chi}_P = \frac{g}{V_P} \frac{n_P \sin \mu_P}{\cos \gamma_P} \tag{3.33}$$

$$\dot{\chi}_E = \frac{g}{V_E} \frac{n_E \sin \mu_E}{\cos \gamma_E} \tag{3.34}$$

Sometimes it is convenient to express relative geometry in spherical coordinates:

$$\dot{r} = -V_P \left[\cos \theta \cos \gamma_P \cos(\chi_P - \psi) + \sin \theta \sin \gamma_P\right] +$$

$$+ V_E \left[\cos \theta \cos \gamma_E \cos(\chi_E - \psi) + \sin \theta \sin \gamma_E\right] \tag{3.35}$$

$$\dot{\theta} = \frac{1}{r} \left\{-V_P \left[\cos \theta \sin \gamma_P - \cos \gamma_P \sin \theta \cos(\chi_P - \psi)\right] +\right.$$

$$\left. + V_E \left[\cos \theta \sin \gamma_E - \cos \gamma_E \sin \theta \cos(\chi_E - \psi)\right]\right\} \tag{3.36}$$

$$\dot{\psi} = \frac{1}{r \cos \theta} \left[-V_P \cos \gamma_P \sin(\chi_P - \psi) + V_E \cos \gamma_E \sin(\chi_E - \psi)\right] \tag{3.37}$$

In this case an additional differential equation is required for the altitude of one airplane (h_p for example), and the opponent's altitude (h_E in this case) is obtained from:

$$h_E = h_p + r \sin \theta \tag{3.38}$$

The relative geometry between the aircraft is depicted in Fig 3.1.

5. SIMPLIFIED MODELS

From the general model presented in 3.4 several simplified 2-D models can be derived.

5.1 Interception in the Horizontal Plane

Motion in the horizontal plane requires:

$$\gamma_P = \gamma_E = \theta = 0 \tag{3.39}$$

Therefore the aircraft bank angle is

$$\cos \mu = \frac{1}{n}$$

Equations of the line of sight variables in the horizontal plane are:

$$\dot{r} = -V_P \cos(\chi_P - \psi) + V_E \cos(\chi_E - \psi) \tag{3.40}$$

$$\dot{\psi} = \frac{1}{r}\left[-V_P \sin(\chi_P - \psi) + V_E \sin(\chi_E - \psi)\right] \tag{3.41}$$

Longitudinal acceleration of each aircraft is:

$$\dot{V} = \frac{g}{W}\left[\xi T_{max} - D_0 - n^2 D_I\right] \tag{3.42}$$

and its turning rate:

$$\dot{\chi} = \frac{g}{V}(n^2-1)^{\frac{1}{2}} \tag{3.43}$$

The turning rate constraints are:

(a) Below the "corner" velocity ($V \leq V_c$):

$$\dot{\chi} \leq g\left\{\left[\frac{\bar{q} V S C_{L_{max}}(M)}{2W}\right]^2 - \frac{1}{V^2}\right\} \tag{3.44}$$

(b) Above the corner velocity $(V \geq V_c)$:

$$\dot{\chi} \leq \frac{g}{V} \left(n_{max}^2 - 1\right)^{\frac{1}{2}} \tag{3 45}$$

This model was used as a basis of the 2-D, variable speed interception engagement reported in [3].

5.2 Interception in the Vertical Plane

In the vertical plane we have the following equations for the line of sight variables.

$$\dot{r} = -V_p \cos\left(\gamma_p - \theta\right) + V_E \cos\left(\gamma_E - \theta\right) \tag{3.46}$$

$$\dot{\theta} = \frac{1}{r}\left[-V_p \sin\left(\gamma_p - \theta\right) + V_E \sin\left(\gamma_E - \theta\right)\right] \tag{3 47}$$

Longitudinal acceleration of each aircraft is:

$$\dot{V} = g\left[\frac{\xi T_{max} - D_0 - n^2 D_I}{W} - \sin\gamma\right] \tag{3.48}$$

and its rate of climb is:

$$\dot{\gamma} = \frac{g}{V}\left(n - \cos\gamma\right) \tag{3.49}$$

The rate of climb constraints are similar to (3.44) and (3.45).

One of the most useful models for performance optimization in the vertical plane is the energy-state model. In this model the aircraft velocity is replaced by specific energy (E), defined by:

$$E \triangleq h + \frac{V^2}{2g} \tag{3.50}$$

This transformation of variables leads to the following equations for each aircraft.

$$\dot{\psi} = V \cos \gamma \tag{3.51}$$

$$\dot{h} = V \sin \gamma \tag{3.52}$$

$$\dot{E} = \left(\frac{\xi T_{max} - D}{W} \right) V \tag{3.53}$$

$$\dot{\gamma} = \frac{g}{V} (n - \cos \gamma) \tag{3.54}$$

Line of sight equations in this model are (3.46) and (3.47) while:

$$\chi_P - \psi_h = \chi_E - \psi_h = 0 \tag{3.55}$$

6. FORMULATION OF THE DIFFERENTIAL GAME AND THE NECESSARY CONDITIONS FOR OPTIMALITY

As mentioned in the introduction we deal with an interception problem in which roles are well defined. One airplane (P) is chasing the other (E) in a 3-D space. The problem can be thus formulated as a zero-sum, perfect information game Assuming that capture is guaranteed the payoff is capture time which P attempts to minimize and E to maximize.

Termination of the game is defined by reaching a separation distance ℓ representing the pursuer's firing envelope.

$$\left.\begin{aligned} \ell^2 - r^2(t_f) &= (\Delta x)^2 + (\Delta y)^2 + (h_p - h_E)^2 \\ |\dot{r}(t_f)| &< 0 \end{aligned}\right\} \tag{3.56}$$

If we assume the existence of a saddle point solution the necessary conditions of optimality can be applied.

First define the Hamiltonian:

$$\mathcal{H} = 1 + \lambda_x \dot{x} + \lambda_y \dot{y} + \lambda_{h_p} \dot{h}_p + \lambda_E \dot{h}_E + \lambda_{V_p} \dot{V}_p + \lambda_{V_E} \dot{V}_E +$$

$$+ \lambda_{\gamma_p} \dot{\gamma}_p + \lambda_{\gamma_E} \dot{\gamma}_E + \lambda_{\chi_p} \dot{\chi}_p + \lambda_{\chi_E} \dot{\chi}_E + \text{constraints} \qquad (3.57)$$

The necessary conditions of optimality include the adjoint equations and the respective transversality conditions.

The adjoint equations are:

$$\dot{\lambda}_x = -\frac{\partial \mathcal{H}}{\partial x} \quad ; \quad \lambda_x(t_f) = 2(x_p - x_E)_{t_f} \qquad (3.58)$$

$$\dot{\lambda}_y = -\frac{\partial \mathcal{H}}{\partial y} \quad ; \quad \lambda_y(t_f) = 2(y_p - y_E)_{t_f} \qquad (3.59)$$

$$\dot{\lambda}_{h_p} = -\frac{\partial \mathcal{H}}{\partial h_p} \quad ; \quad \lambda_{h_p}(t_f) = 2(h_p - h_E)_{t_f} \qquad (3.60)$$

$$\dot{\lambda}_{h_E} = \frac{\partial \mathcal{H}}{\partial h_E} \quad ; \quad \lambda_{h_E}(t_f) = -2(h_p - h_E)_{t_f} \qquad (3.61)$$

$$\dot{\lambda}_{V_p} = -\frac{\partial \mathcal{H}}{\partial V_p} \quad ; \quad \lambda_{V_p}(t_f) = 0 \qquad (3.62)$$

$$\dot{\lambda}_{V_E} = -\frac{\partial \mathcal{H}}{\partial V_E} \quad ; \quad \lambda_{V_E}(t_f) = 0 \qquad (3.63)$$

$$\dot{\lambda}_{\gamma_p} = -\frac{\partial \mathcal{H}}{\partial \gamma_p} \quad ; \quad \lambda_{\gamma_p}(t_f) = 0 \qquad (3.64)$$

$$\dot{\lambda}_{\gamma_E} = -\frac{\partial \mathcal{H}}{\partial \gamma_E} \quad ; \quad \lambda_{\gamma_E}(t_f) = 0 \qquad (3.65)$$

$$\dot{\lambda}_{\chi_p} = -\frac{\partial \mathcal{H}}{\partial \chi_p} \quad ; \quad \lambda_{\chi_p}(t_f) = 0 \qquad (3.66)$$

$$\dot{\lambda}_{\chi_E} = -\frac{\partial \mathcal{H}}{\partial \chi_E} \quad ; \quad \lambda_{\chi_E}(t_f) = 0 \qquad (3.67)$$

7. THE OPTIMAL STRATEGIES

Necessary conditions for optimality are expressed by Isaacs ME1:

$$\min_{\xi_P,\mu_P,n_P} \max_{\xi_E,\mu_E,n_E} \mathcal{H}(\xi_P,\xi_E,\mu_P,\mu_E,n_P,n_E) = 0 \ . \tag{3.68}$$

7.1 Pursuer

The optimal throttle control for $\lambda_{V_P} \neq 0$ is:

$$\xi_P^* = \frac{1}{2}\left(1 - \text{sign}\ \lambda_{V_P}\right) \tag{3.69}$$

For singular thrust arcs $\left(\lambda_{V_P} = \dot{\lambda}_{V_P} = 0\right)$ we have $0 \leq \xi_P^* \leq 1$. However, it can be shown that such singular arc is not optimal. Assuming that: $T_{max_P} \sin(\alpha+\beta_T)_P << L_P$, μ_P^* is determined by:

$$\text{tg}\ \mu_P^* = \frac{\lambda_{\chi_P}/\cos\ \gamma_P}{\lambda_{\gamma_P}} \tag{3.70}$$

n_P^* is determined by:

$$n_P^* = W_P \left(\lambda_{\chi_P}^2 + \lambda_{\gamma_P}^2 \cos^2\ \gamma_P\right)^{\frac{1}{2}} \frac{1/\cos\ \gamma_P}{2\lambda_{V_P} V_P} \tag{3.71}$$

Equation (3.71) is valid only if the constraints on the load factor [(3.15) and (3.16)] are not violated, otherwise

$$n_P^* = \inf\left(n_P^*, n_{L_P}, n_{max_P}\right) \tag{3.72}$$

7.2 Evader

Similar expressions are obtained for the evader (maximizer)

$$\xi_E^* = \frac{1}{2}(1 + \text{sign } \lambda_{V_E}) \tag{3.73}$$

$$\text{tg } \mu_E^* = \frac{\lambda_{\chi_E}/\cos \gamma_E}{\lambda_{\gamma_E}} \tag{3.74}$$

$$n_E^* = W_E \left(\lambda_{\chi_E}^2 + \lambda_{\gamma_E}^2 \cos^2 \gamma_E\right)^{\frac{1}{2}} \frac{1/\cos \gamma_E}{2\lambda_{V_E} V_E} \tag{3.75}$$

and if the load factor is violated

$$n_E^* = \inf\left(n_E^*, n_{L_E}, n_{max_E}\right) \tag{3.76}$$

8. A CONCLUDING REMARK

The set of necessary conditions for game optimality include 20 differential equations (for the state and adjoint variables) and 6 expressions for the control strategies, leading to solve a nonlinear two point boundary value problem. For this very complex problem the merits of an analytical approximation, based on application of a forced singular perturbation technique, can be fully appreciated. As a first step of such analysis some important modelling considerations are discussed in the next chapter.

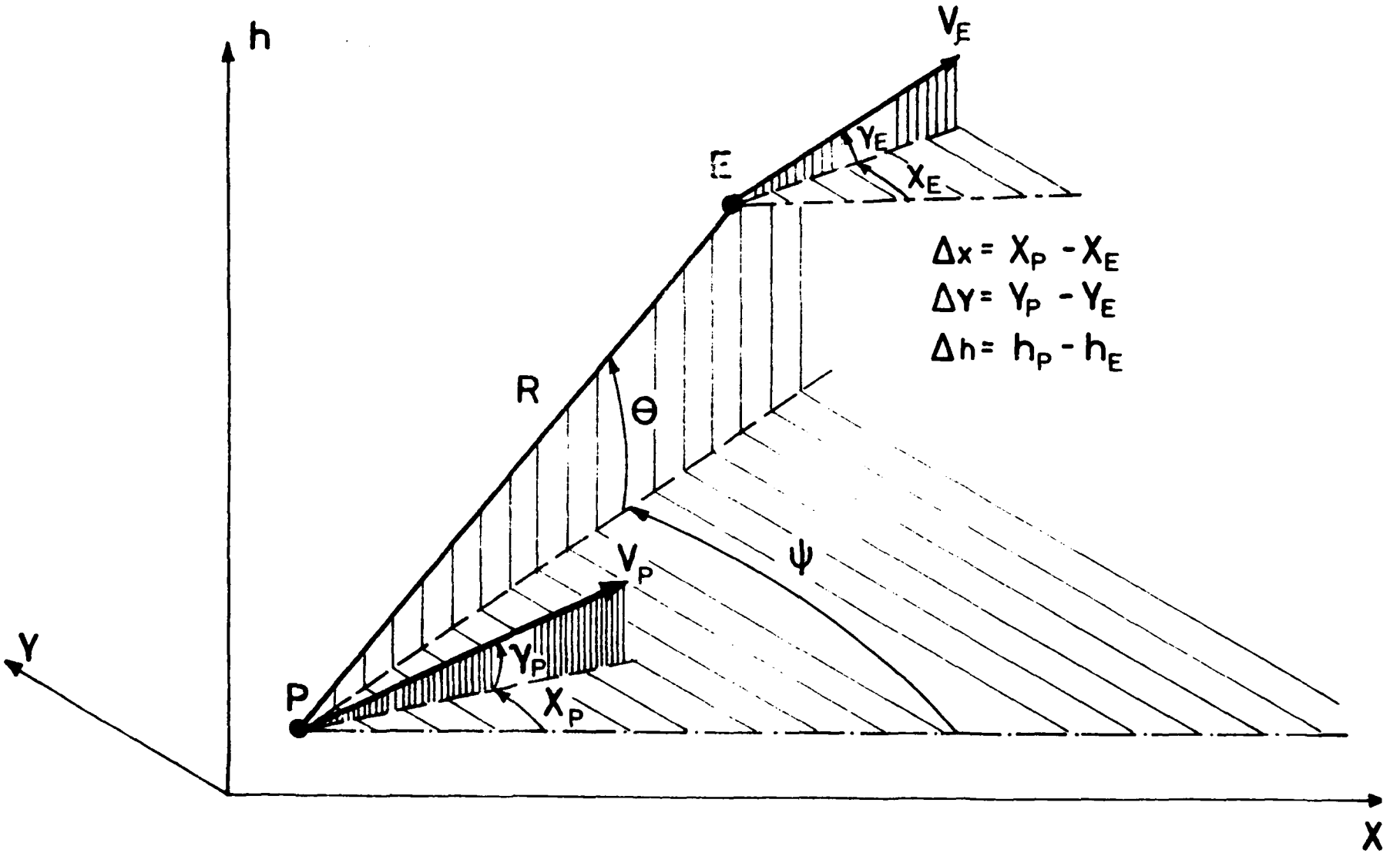

Fig. 3.1: Geometry of the 3-D interception.

SECTION IV

SPT MODELLING CONSIDERATION

The most appealing feature of an SPT solution lies in its potential to provide feedback control strategies. Whenever such solution cannot be obtained the SPT approximation loses substantially from its attractiveness. Implementation of SPT for solving the multi-dimensional nonlinear medium range interception problems in a feedback form depends on several factors.

(a) The ability to transform the original problem to a set of multiple time scale (multiple boundary layer) problems preferably of a single state variable in each layer. Such transformation has to be based on observing an actual time scale separation of the original problem and it requires a considerable insight and sound engineering judgement.

(b) Terminal boundary layers have to be avoided. Previous studies [14, 15] have indicated that if the solution includes a terminal boundary layer, this part cannot be implemented in a real feedback form, even if the open loop solution of the problem can be computed. For an on-line implementation, intending to reproduce the open loop solution, the initial boundary layer control strategy (which is uniformly valid for the boundary layer as well as for the free stream) has to be switched to a different terminal boundary layer strategy at a precise instant as required by the open loop matching condition. The exact timing is critical in order to satisfy the prescribed end conditions. Being in the "free stream" no state feedback information can be used to determine the conditions for the boundary layer initiation Moreover, even if it is correctly started the terminal boundary layer trajectory computed in the real (forward) time direction is unstable with respect to disturbances in

the state variables. For these reasons it is adviced to avoid formulations which lead to a terminal boundary layer.

(c) Use of zero order approximations only. It was shown [15, 16] that first or higher order correction terms improving the zero-order approximation have to be computed by integration along the zero-order trajectory. It is clearly an off-line process. Therefore feedback implementation of SPT is inherently limited to the zero-order solution. These guidelines will be used later during the analysis of the 3-D, variable speed interception model.

The extension of 2-D constant velocity to 3-D constant velocity was possible, because in a constant speed model turning performance is independent of the position coordinates. For example, the extension of 2-D constant velocity to 2-D horizontal variable velocity was possible because (h=const.) and $\dot{V}=f(V)$.

In a realistic 3-D modelling altitude plays a much more important role than merely an additional position coordinate because of the following reasons:

I. Maximum thrust is function of both Mach number and altitude.

II. Induced drag (caused by aircraft maneuver) is inversely proportional to air density, i.e., the capability to increase specific energy diminishes with altitude.

III. Stall speed is an altitude dependent variable (which increases with altitude).

IV. At low altitudes any attempt of an evading aircraft to escape a descending pursuer (attacking from higher altitude), according to the line of sight strategy can lead to violation of the ground state constraint (3.21).

V. At high altitudes any attempt to execute a maneuver with a relatively high load factor can force the aircraft (pursuer or evader) to cross the boundary of its dynamic flight envelope.

Observing these effects it seems that a direct extension of the results of a 2-D [illegible] speed model to a 3-D one (or alternatively adding the variable speed feature to the 3-D constant speed model as done for the horizontal case) may not be appropriate.

In order to understand properly the influence of the above mentioned effects it is proposed, first, to analyse an interception engagement in the vertical plane.

In the past, energy-state modelling has been offered as an easily implementable approach towards aircraft performance optimization in the vertical plane. The energy-state approximation is based on the observation that in many aircraft maneuvers the specific energy E, defined in (3.50), varies slowly compared to the other state variables [16]. Thus the use of a reduced order model where the "fast" variables are assumed to be pseudo-controls seems to be justified.

This approximation has provided an excellent insight leading to an improved understanding of high performance aircraft trajectory optimization problems. However, energy-state solutions have had only a limited value for direct airborne applications. As an inherent property of the reduced order model, discontinuities of the "fast" state variables (like altitude) are required. Moreover, the model can not satisfy part of the initial and terminal conditions of the real problem.

A way to overcome these inconveniences is by application of singular perturbation technique or (in the absence of a small parameter of physical significance) by use of the forced singular perturbation technique (FSPT).

In the next chapter:

(a) The suitability of the vertical plane medium range interception model to a FSPT formulation will be checked.

(b) The model will be solved in detail.

SECTION V

FSPT SOLUTION FOR MEDIUM RANGE INTERCEPTION IN THE VERTICAL PLANE

1. GENERAL CONSIDERATIONS AND EQUATIONS OF MOTION

Investigating the suitability of this problem to a FSPT formulation, it is first necessary to identify "fast" and "slow" variables in the equations of motion. For this purpose we assume the following:

(a) Medium range interception is characterized by a separation distance largely exceeding the aircraft turning radii. As a result, the rate of change of the relative geometry (expressed by the line of sight components) is the slowest variable in the model.

(b) Based on engineering observations, specific energy is slow variable compared with V or h [17]. Therefore, use of E,h instead of V,h is essential towards legitimate use of FSPT.

(c) The fastest variable in this model is the climb angle γ (since h is an integral of γ).

Applying these considerations to the vertical plane interception (whose geometry is depicted in Fig. 5.1), the equations of motion (with ε inserted artificially) are:

$$\dot{r}_h = -V_p \cos \gamma_p + V_E \cos \gamma_E \quad ; \qquad r_h(t=0) = r_{h_0} \tag{5.1}$$

r_h is the horizontal distance between the aircraft.

$$\epsilon \dot{E}_p = \frac{V_p}{W_p} \left(\xi_p T_{max_p} - D_{0_p} - n_p^2 D_{I_p} \right) \quad ; \; E_p(t=0) = E_{p_0} \tag{5.2}$$

$$\epsilon \dot{E}_E = \frac{V_E}{W_E} \left(\xi_E T_{max_E} - D_{0_E} - n_E^2 D_{I_E} \right) \quad ; \; E_E(t=0) = E_{E_0} \tag{5.3}$$

$$\epsilon^2 \dot{h}_p = V_p \sin \gamma_p \quad ; \qquad h_p(t=0) = h_{p_0} \tag{5.4}$$

$$\epsilon^2 \dot{h}_E = V_E \sin \gamma_E \quad ; \qquad h_E(t=0) = h_{E_0} \tag{5.5}$$

$$\epsilon^3 \dot{\gamma}_p = \frac{g}{V_p} \left(n_p - \cos \gamma_p \right) \; ; \qquad \gamma_p(t=0) = \gamma_{p_0} \tag{5.6}$$

$$\epsilon^3 \dot{\gamma}_E = \frac{g}{V_E} \left(n_E - \cos \gamma_E \right) \; ; \qquad \gamma_E(t=0) = \gamma_{E_0} \tag{5.7}$$

Termination of the game is defined by:

$$|r|_{t_f} \triangleq \left| \left[r_h^2 + (h_p - h_E)^2 \right]^{\frac{1}{2}} \right|_{t_f} = \ell \tag{5.8}$$

$$|\dot{r}|_{t_f} < 0 \tag{5.9}$$

where: ℓ - Pursuer's capture range.

The natural payoff is time of capture which the pursuer tries to minimize and the evader to maximize.

Before starting the formal solution several additional assumptions ought to be made.

(a) Interception time is long enough to allow each aircraft to reach its optimum altitude (at which maximum velocity can be achieved). Later on it will be shown that this phase corresponds to the reduced game solution.

(b) Pursuer's capture range is greater than its turning radius. Therefore the "end game" phase disappears and the interception terminates with a "tail chase" configuration.

2. THE NECESSARY CONDITIONS FOR OPTIMALITY

The Hamiltonian of this problem is defined first:

$$\mathcal{H} = 1 + \lambda_{r_h}(-V_P \cos\gamma_P + V_E \cos\gamma_E) + \lambda_{E_P}\frac{V_P}{W_P}(\xi_P T_{max_P} - D_{0_P} - n_P^2 D_{I_P}) +$$

$$+ \lambda_{E_E}\frac{V_E}{W_E}(\xi_E T_{max_E} - D_{0_E} - n_E^2 D_{I_E}) + \lambda_{h_P} V_P \sin\gamma_P + \lambda_{h_E} V_E \sin\gamma_E +$$

$$+ \lambda_{\gamma_P}\frac{g}{V_P}(n_P - \cos\gamma_P) + \lambda_{\gamma_E}\frac{g}{V_E}(n_E - \cos\gamma_E) + \text{constraints} = 0 \qquad (5.10)$$

The adjoint equations are:

$$\dot{\lambda}_{r_h} = -\frac{\partial\mathcal{H}}{\partial r_h} = 0 \rightsquigarrow \lambda_{r_h} = \text{const.} = \frac{-1}{\dot{r}_h(t_f)} \qquad (5.11)$$

$$\varepsilon\dot{\lambda}_{E_P} = -\left.\frac{\partial\mathcal{H}}{\partial E_P}\right|_{h_P = \text{const.}} = -\frac{g}{V_P}\frac{\partial\mathcal{H}}{\partial V_P} \quad ; \quad \lambda_{E_P}(t_f) = 0 \qquad (5.12)$$

$$\varepsilon\dot{\lambda}_{E_E} = -\left.\frac{\partial\mathcal{H}}{\partial E_E}\right|_{h_E = \text{const.}} = -\frac{g}{V_E}\frac{\partial\mathcal{H}}{\partial V_E} \quad ; \quad \lambda_{E_E}(t_f) = 0 \qquad (5.13)$$

$$\varepsilon^2 \dot{\lambda}_{h_P} = - \left.\frac{\partial \mathcal{H}}{\partial h_P}\right|_{E_P=\text{const.}} = - \frac{\partial \mathcal{H}}{\partial h_P} + \frac{g}{V_P} \frac{\partial \mathcal{H}}{\partial V_P} \quad ; \quad \lambda_{h_P}(t_f) = 2(h_P - h_E)_{t_f} \tag{5.14}$$

$$\varepsilon^2 \dot{\lambda}_{h_E} = - \left.\frac{\partial \mathcal{H}}{\partial h_E}\right|_{E_E=\text{const.}} = - \frac{\partial \mathcal{H}}{\partial h_E} + \frac{g}{V_E} \frac{\partial \mathcal{H}}{\partial V_E} \quad ; \quad \lambda_{h_E}(t_f) = -2(h_P - h_E)_{t_f} \tag{5.15}$$

$$\varepsilon^3 \dot{\lambda}_{\gamma_P} = - \frac{\partial \mathcal{H}}{\partial \gamma_P} \quad ; \quad \lambda_{\gamma_P}(t_f) = 0 \tag{5.16}$$

$$\varepsilon^3 \dot{\lambda}_{\gamma_E} = - \frac{\partial \mathcal{H}}{\partial \gamma_E} \quad ; \quad \lambda_{\gamma_E}(t_f) = 0 \tag{5.17}$$

Optimal strategies are derived from Isaacs MEl.

$$\min_{\xi_P, n_P} \max_{\xi_E, n_E} \mathcal{H} = 0 \quad .$$

2.1 Pursuer

$$\xi_P^* = \frac{1}{2}(1 - \text{sign}\ \lambda_{E_P}) \qquad \lambda_{E_P} \neq 0 \tag{5.18}$$

It can be shown that singular arcs ($\lambda_{E_P} = \dot{\lambda}_{E_P} = 0$) are not optimal.

n_P^* is calculated from $\frac{\partial \mathcal{H}}{\partial n_P} = 0$.

$$n_P^* = \frac{\lambda_{\gamma_P}}{\lambda_{E_P}} \frac{W_P g}{2 D_{I_P} V_P^2} \tag{5.19}$$

Equation (5.19) is valid only if the constraints of the load factor are not violated. A more general expression for n_P^* is:

$$n_P^* = \inf(n_P^*, n_{L_P}, n_{\max_P}) \tag{5.20}$$

2.2 Evader

$$\xi_E^* = \frac{1}{2}\,(1 + \text{sign}\ \lambda_{E_E}) \qquad \lambda_{E_E} \neq 0 \tag{5.21}$$

Similar to the pursuer, singular thrust arcs are not optimal in this case. n_E^* is calculated from $\frac{\partial \mathcal{H}}{\partial n_E} = 0$.

$$n_E^* = \frac{\lambda_{\gamma_E}}{\lambda_{E_E}} \frac{W_E g}{2D_{I_E} V_E^2} \quad , \tag{5.21a}$$

or, when constraints are taken into consideration:

$$n_E^* = \inf(n_E^*, n_{L_E}, n_{max_E}) \tag{5.22}$$

3. THE REDUCED GAME

By setting $\varepsilon = 0$ in equations (5.2) ÷ (5.7) and (5.11) ÷ (5.17) the reduced game is obtained. Denoting all variables of the reduced game by the superscript "o" we get from (5.2) ÷ (5.7):

$$\left.\begin{aligned} \xi_P^o\, T_{max_P} - D_{0_P}^o - n_P^{o2}\, D_{I_P}^o &= 0 \\ \xi_E^o\, T_{max_E} - D_{0_E}^o - n_E^{o2}\, D_{I_E}^o &= 0 \end{aligned}\right\} \tag{5.23}$$

$$\left.\begin{aligned} V_P^o \sin \gamma_P^o = 0 \rightsquigarrow \gamma_P^o &= 0 \\ V_E^o \sin \gamma_E^o = 0 \rightsquigarrow \gamma_E^o &= 0 \end{aligned}\right\} \tag{5.24}$$

$$\left.\begin{aligned} \frac{g}{V_P^o}\,(n_P^o - \cos\gamma_P^o) = 0 \sim n_P^o = \cos\gamma_P^o = 1 \\ \frac{g}{V_E^o}\,(n_E^o - \cos\gamma_E^o) = 0 \sim n_E^o = \cos\gamma_E^o = 1 \end{aligned}\right\} \tag{5.25}$$

$$\left.\frac{\partial \mathcal{H}^o}{\partial E_P}\right|_{h_P=\text{const.}} = \left.\frac{\partial \mathcal{H}^o}{\partial E_E}\right|_{h_E=\text{const.}} = 0 \tag{5.26}$$

$$\left.\frac{\partial \mathcal{H}^o}{\partial h_P}\right|_{E_P=\text{const.}} = \left.\frac{\partial \mathcal{H}^o}{\partial h_E}\right|_{E_E=\text{const.}} = 0 \tag{5.27}$$

$$\frac{\partial \mathcal{H}^o}{\partial \gamma_P} = \frac{\partial \mathcal{H}^o}{\partial \gamma_E} = 0. \tag{5.28}$$

The controls in this game are the specific energy and altitude of each aircraft. These controls are obtained by min-max of the reduced game Hamiltonian.

$$\mathcal{H}^o = 1 + \lambda_{r_h}^o\,(-V_P^o + V_E^o) = 0 \tag{5.29}$$

From (5.11) and (5.9) it follows that $\lambda_{r_h}^o > 0$. Using this fact and performing maximization-minimization of the Hamiltonian:

$$h_P^o, E_P^o = \underset{h_P, E_P}{\arg\min}\ \{\mathcal{H}^o\} \tag{5.30}$$

$$h_E^o, E_E^o = \underset{h_E, E_E}{\arg\max}\ \{\mathcal{H}^o\} \tag{5.31}$$

we obtain:

$$h_P^o, E_P^o = \underset{h_P, E_P}{\arg\max}\{V_P^o\} \tag{5.32}$$

$$h_E^{\upsilon}, E_E^o = \underset{h_E, E_E}{\arg \max} \{V_E^o\} \tag{5.33}$$

In other words, to find the altitude and energy level at which each aircraft flies during the reduced game one has to search the whole range of energies and altitudes of each aircraft's flight envelope.

Since $\gamma_p^o = \gamma_E^o = 0$ the reduced game is characterized by flight at constant altitude at which maximum velocity can be achieved. This velocity is determined by:

$$V_p^o = \underset{V_p}{\sup \arg} \{\xi_p^o T_{max} - D_{0_p}^o - D_{I_p}^o = 0\} \tag{5.34}$$

$$V_E^o = \underset{V_E}{\sup \arg} \{\xi_E^o T_{max} - D_{0_E}^o - D_{I_E}^o = 0\} \tag{5.35}$$

From which we obtain: $\xi_p^o = \xi_E^o = 1$. And finally

$$\lambda_{r_h}^o = - \frac{1}{V_p^o + V_E^o} \quad . \tag{5.36}$$

4. THE OUTER BOUNDARY LAYER (ENERGY BOUNDARY LAYER)

The equations of motion in the outer boundary layers (separately controlled by each player) are obtained through the stretching transformation: $\tau_i = t/\varepsilon$.

Denoting all variables in the outer boundary layer by the superscript "i" we have, setting $\varepsilon = 0$ and using the matching conditions:

$$\frac{dr_h^i}{d\tau_i} = 0 \rightsquigarrow r_h^i(\tau_i) = r_{h_0} \tag{5.37}$$

$$\frac{dE_p^i}{d\tau_i} = \frac{V_p^i}{W_p^i} (\xi_p^i T_{max_p}^i - D_{0_p}^i - n_p^{i2} D_{I_p}) \quad ; \quad E_p^i(\tau_i=0) = E_{p_0} \tag{5.38}$$

$$\frac{dE_E^i}{d\tau_i} = \frac{V_E^i}{W_E^i}\left(\xi_E^i T_{max_E}^i - D_{0_E}^i - n_E^{i2} D_{I_E}\right) \quad ; \quad E_E^i(\tau_i=0) = E_{E_0} \tag{5.39}$$

$$0 = \varepsilon \frac{dh_P^i}{d\tau_i} = V_P^i \sin \gamma_P^i \sim \gamma_P^i = 0 \tag{5.40}$$

$$0 = \varepsilon \frac{dh_E^i}{d\tau_i} = V_E^i \sin \gamma_E^i \sim \gamma_E^i = 0 \tag{5.41}$$

$$0 = \varepsilon^2 \frac{d\gamma_P^i}{d\tau_i} = \frac{g}{V_P^i}\left(n_P^i - \cos \gamma_P^i\right) \sim n_P^i = 1 \tag{5.42}$$

$$0 = \varepsilon^2 \frac{d\gamma_E^i}{d\tau_i} = \frac{g}{V_E^i}\left(n_E^i - \cos \gamma_E^i\right) \sim n_E^i = 1 \tag{5.43}$$

$$\frac{d\lambda_{r_h}^i}{d\tau_i} = 0 \sim \lambda_{r_h}^i(\tau_i) = \lambda_{r_{h_0}}^o \tag{5.44}$$

$$\frac{d\lambda_{E_P}^i}{d\tau_i} = -\frac{g}{V_P^i}\frac{\partial \mathcal{H}^i}{\partial V_P^i} \tag{5.45}$$

$$\frac{d\lambda_{E_E}^i}{d\tau_i} = \frac{g}{V_E^i}\frac{\partial \mathcal{H}^i}{\partial V_E^i} \tag{5.46}$$

$$0 = \varepsilon \frac{d\lambda_{h_P}^i}{d\tau_i} = -\left.\frac{\partial \mathcal{H}^i}{\partial h_P^i}\right|_{E_P=\text{const.}} \tag{5.47}$$

$$0 = \varepsilon \frac{d\lambda_{h_E}^i}{d\tau_i} = -\left.\frac{\partial \mathcal{H}^i}{\partial h_E^i}\right|_{E_E=\text{const.}} \tag{5.48}$$

$$0 = \varepsilon^2 \frac{d\lambda_{\gamma_P^i}}{d\tau_i} = - \frac{\partial \mathcal{H}^i}{\partial \gamma_P^i} \tag{5.49}$$

$$0 = \varepsilon^2 \frac{d\lambda_{\gamma_E^i}}{d\tau_i} = - \frac{\partial \mathcal{H}^i}{\partial \gamma_E^i} \tag{5.50}$$

In this boundary layer we still have:

$$\gamma_P^i = \gamma_E^i = 0 \quad n_P^i = n_E^i = 1$$

Each aircraft has to change its energy level from its initial value (E_{P_0} or E_{E_0}) to the value dictated by the outer solution (E_P^o or E_E^o). To do it optimally, it is necessary that at each energy level the aircraft will be at an optimal altitude (considered as control in this boundary layer). This altitude is calculated (for both aircraft), by minimization-maximization of the Hamiltonian ($\mathcal{H}^i$).

$$\mathcal{H}^i = 1 + \lambda^o_{r_{h_0}} (-V_P^i + V_E^i) + \lambda^i_{E_P} P^i_{S_P}\Big|_{n_P^i=1} + \lambda^i_{E_E} P^i_{S_E}\Big|_{n_E^i=1} = 0, \tag{5.51}$$

where $P_S \triangleq \dot{E}$ is the specific power.

Substituting $\lambda^o_{r_{h_0}}$ (5.36) into (5.51) we obtain:

$$\mathcal{H}^i = \frac{V_P^o - V_P^i}{V_P^o - V_E^o} + \lambda^i_{E_P} P^i_{S_P}\Big|_{n_P^i=1} - \frac{V_E^o - V_E^i}{V_P^o - V_E^o} + \lambda^i_{E_E} P^i_{S_E}\Big|_{n_E^i=1} = 0 \tag{5.52}$$

Since the Hamiltonian is separable (with respect to the players controls):

$$\lambda^i_{E_P} = \frac{V_P^i - V_P^o}{V_P^o - V_E^o} \quad \frac{1}{P^i_{S_P}} < 0 \tag{5.53}$$

$$\lambda^i_{E_E} = \frac{-V^i_E + V^o_E}{V^o_P - V^o_E} \quad \frac{1}{P^i_{S_E}} > 0 \tag{5.54}$$

The optimal altitudes (h^i_P, h^i_E) are:

$$h^i_P = \arg\min_{h_P} \mathcal{H}^i \tag{5.55}$$

$$h^i_E = \arg\max_{h_E} \mathcal{H}^i \tag{5.56}$$

Expressed more specifically,

$$h^i_P = \arg\max_{h_P} \left\{ \frac{P^i_{S_P}}{V^o_P - V^i_P} \right\} \tag{5.57}$$

$$h^i_E = \arg\max_{h_E} \left\{ \frac{P^i_{S_E}}{V^o_E - V^i_E} \right\} \tag{5.58}$$

From (5.53), (5.54):

$$\xi^i_P = \xi^i_E = 1 \ . \tag{5.59}$$

5. THE INTERMEDIATE BOUNDARY LAYER (ALTITUDE BOUNDARY LAYER)

The equations of motion in the intermediate boundary layer (separately controlled by the players) are obtained through the stretching transformation $\tau_j = t/\varepsilon^2$. Denoting all variables in this boundary layer by the superscript "j" we have, setting $\varepsilon = 0$ and using the matching conditions:

$$\frac{dr^j_h}{d\tau_j} = 0 \sim r^j_h = r_{h_0} \tag{5.60}$$

$$\frac{dE_P^j}{d\tau_j} = 0 \sim E_P^j(\tau_j=0) = E_{P_0} \tag{5.61}$$

$$\frac{dE_E^j}{d\tau_j} = 0 \sim E_E^j(\tau_j=0) = E_{E_0} \tag{5.62}$$

$$\frac{dh_P^j}{d\tau_j} = V_P^j \sin \gamma_P^j \quad ; \quad h_P^j(\tau_j=0) = h_{P_0} \tag{5.63}$$

$$\frac{dh_E^j}{d\tau_j} = V_E^j \sin \gamma_E^j \quad ; \quad h_E^j(\tau_j=0) = h_{E_0} \tag{5.64}$$

$$0 = \varepsilon \frac{d\gamma_P^j}{d\tau_j} = \frac{g}{V_P^j}(n_P^j - \cos \gamma_P^j) \sim n_P^j = \cos \gamma_P^j \tag{5.65}$$

$$0 = \varepsilon \frac{d\gamma_E^j}{d\tau_j} = \frac{g}{V_E^j}(n_E^j - \cos \gamma_E^j) \sim n_E^j = \cos \gamma_E^j \tag{5.66}$$

$$\frac{d\lambda_{r_h}^j}{d\tau_j} = 0 \sim \lambda_{r_h}^j(\tau_j) = \lambda_{r_{h_0}}^o \tag{5.67}$$

$$\frac{d\lambda_{E_P}^j}{d\tau_j} = 0 \sim \lambda_{E_P}^j(\tau_j) = \lambda_{E_{P_0}}^i \tag{5.68}$$

$$\frac{d\lambda_{E_E}^j}{d\tau_j} = 0 \sim \lambda_{E_E}^j(\tau_j) = \lambda_{E_{E_0}}^i \tag{5.69}$$

$$\frac{d\lambda_{h_P}^j}{d\tau_j} = -\frac{\partial \mathcal{H}^j}{\partial h_P^j} + \frac{g}{V_P^j}\frac{\partial \mathcal{H}^j}{\partial V_P^j} \tag{5.70}$$

$$\frac{d\lambda^j_{h_E}}{d\tau_j} = - \frac{\partial \mathcal{H}^j}{\partial h^j_E} + \frac{g}{V^j_E} \frac{\partial \mathcal{H}^j}{\partial V^j_E} \tag{5.71}$$

$$0 = \varepsilon \frac{d\lambda^j_{\gamma_P}}{d\tau_j} = - \frac{\partial \mathcal{H}^j}{\partial \gamma^j_P} \tag{5.72}$$

$$0 = \varepsilon \frac{d\lambda^j_{\gamma_E}}{d\tau_j} = - \frac{\partial \mathcal{H}^j}{\partial \gamma^j_E} \tag{5.73}$$

Velocities in this boundary layer are calculated by:

$$V^j = \{2g(E^j - h^j)\}^{\frac{1}{2}} \tag{5.74}$$

According to (5.72), (5.73) the path angles (γ^j_P, γ^j_E) become the controls of this boundary layer. Their role is to transfer the airplanes from their current state (h^j_P, h^j_E) to the required "optimal" altitudes (h^i_P, h^i_E) determined by (5.57), (5.58).

The Hamiltonian of this boundary layer is:

$$\mathcal{H}^j = 1 + \lambda^o_{r_{h_0}} (-V^j_P \cos \gamma^j_P + V^j_E \cos \gamma^j_E) + \lambda^i_{E_{P_0}} \frac{V^j}{W^j} (T^j_P - D^j_P) + \lambda^i_{E_{E_0}} \frac{V^j}{W^j} (T^j_E - D^j_E) +$$

$$+ \lambda^j_{h_P} V^j_P \sin \gamma^j_P + \lambda^j_{h_E} V^j_E \sin \gamma^j_E = 0. \tag{5.75}$$

Using (5.72), (5.73) we have:

$$\lambda^o_{r_{h_0}} V^j_P \sin \gamma^j_P + \lambda^j_{h_P} V^j_P \cos \gamma^j_P = 0 \tag{5.76}$$

$$-\lambda^o_{r_{h_0}} V^j_E \sin \gamma^j_E + \lambda^j_{h_E} V^j_E \cos \gamma^j_E = 0. \tag{5.77}$$

After using (5.29), we obtain:

$$\lambda^j_{h_P} = \frac{-tg\ \gamma^j_P}{V^o_P - V^o_E} \tag{5.78}$$

$$\lambda^j_{h_E} = \frac{tg\ \gamma^j_E}{V^o_P - V^o_E} \tag{5.79}$$

Substituting $\lambda^o_{r_{h_0}}$ (5.29), $\lambda^i_{E_{P_0}}$ (5.53), $\lambda^i_{E_{E_0}}$ (5.54), $\lambda^j_{h_P}$ (5.78), $\lambda^j_{h_E}$ (5.79) into the Hamiltonian, noting that $\mathcal{H}^j = 0$ and using the fact that the Hamiltonian is separable into two parts (exclusively controlled by the pursuer or the evader) we have:

$$\gamma^j_P = \cos^{-1}\left\{\frac{V^j_P\ P^i_{S_{P_0}}}{V^o_P(P^i_{S_{P_0}} - P^j_{S_P}) + V^i_{P_0}\ P^j_{S_P}}\right\} \text{sign}\ (h^i_P - h^j_P) \tag{5.80}$$

$$\gamma^j_E = \cos^{-1}\left\{\frac{V^j_E\ P^i_{S_{E_0}}}{V^o_E(P^i_{S_{E_0}} - P^j_{S_E}) + V^i_{E_0}\ P^j_{S_E}}\right\} \text{sign}\ (h^i_E - h^j_E) \tag{5.81}$$

It has been shown in [18] that the arguments in equations (5.80) and (5.81) are bounded between zero and one.

.6. THE INNER BOUNDARY LAYER (TURNING BOUNDARY LAYER)

The equations of motion in the inner boundary layer (separately controlled by each player) are obtained through the stretching transformation $\tau_k = t/\varepsilon^3$. Denoting all variables in this boundary layer by the superscript "k" we have, setting $\varepsilon = 0$ and using the matching conditions:

$$\frac{dr^k_h}{d\tau_k} = 0 \sim r^k_h(\tau_k) = r_{h_0} \tag{5.82}$$

$$\frac{dE_P^k}{d\tau_k} = 0 \sim E_P^k(\tau_k) = E_{P_0} \tag{5.83}$$

$$\frac{dE_E^k}{d\tau_k} = 0 \sim E_E^k(\tau_k) = E_{E_0} \tag{5.84}$$

$$\frac{dh_P^k}{d\tau_k} = 0 \sim h_P^k(\tau_k) = h_{P_0} \tag{5.85}$$

$$\frac{dh_E^k}{d\tau_k} = 0 \sim h_E^k(\tau_k) = h_{E_0} \tag{5.86}$$

$$\frac{d\gamma_P^k}{d\tau_k} = \frac{g}{V_P^k}(n_P^k - \cos\gamma_P^k) \quad ; \quad \gamma_P^k(0) = \gamma_{P_0} \tag{5.87}$$

$$\frac{d\gamma_E^k}{d\tau_k} = \frac{g}{V_E^k}(n_E^k - \cos\gamma_E^k) \quad ; \quad \gamma_E^k(0) = \gamma_{E_0} \tag{5.88}$$

$$\frac{d\lambda_{r_h}^k}{d\tau_k} = 0 \sim \lambda_{r_h}^k(\tau_k) = \lambda_{r_{h_0}}^o \tag{5.89}$$

$$\frac{d\lambda_{E_P}^k}{d\tau_k} = 0 \sim \lambda_{E_P}^k(\tau_k) = \lambda_{E_{P_0}}^i \tag{5.90}$$

$$\frac{d\lambda_{E_E}^k}{d\tau_k} = 0 \sim \lambda_{E_E}^k(\tau_k) = \lambda_{E_{E_0}}^i \tag{5.91}$$

$$\frac{d\lambda_{h_P}^k}{d\tau_k} = 0 \sim \lambda_{h_P}^k(\tau_k) = \lambda_{h_{P_0}}^j \tag{5.92}$$

$$\frac{d\lambda^k_{h_E}}{d\tau_k} = 0 \rightarrow \lambda^k_{h_E}(\tau_k) = \lambda_{h_{E_0}} \tag{5.93}$$

$$\frac{d\lambda^k_{\gamma_P}}{d\tau_k} = -\frac{\partial \mathcal{H}^k}{\partial \gamma_P} \tag{5.94}$$

$$\frac{d\lambda^k_{\gamma_E}}{d\tau_k} = -\frac{\partial \mathcal{H}^k}{\partial \gamma_E} \tag{5.95}$$

Velocities in this boundary layer are given by: $V^k_{(t_f)} = V^j_0 = V_0$

The Hamiltonian of this boundary layer is:

$$\mathcal{H}^k = 1 + \lambda^o_{r_{h_0}}\left(-V_{P_0}\cos\gamma^k_P + V_{E_0}\cos\gamma^k_E\right) + \lambda^i_{E_{P_0}}\frac{V_{P_0}}{W_P}\left(T_{max_P} - D_{0_P} - n^{k^2}_P D_{I_P}\right)_0 +$$

$$+ \lambda^i_{E_{E_0}}\frac{V_{E_0}}{W_E}\left(T_{max_E} - D_{0_E} - n^{k^2}_E D_{I_E}\right)_0 + \lambda^j_{h_{P_0}} V_{P_0}\sin\gamma^k_P + \lambda^j_{h_{E_0}} V_{E_0}\sin\gamma^k_E +$$

$$+ \lambda^k_{\gamma_P}\frac{g}{V_{P_0}}\left(n^k_P - \cos\gamma^k_P\right) + \lambda^k_{\gamma_E}\frac{g}{V_{E_0}}\left(n^k_E - \cos\gamma^k_E\right) \quad . \tag{5.96}$$

In this boundary layer, n^k_P and n^k_E are the controls. Expressions for their optimal values are obtained as follows:

$$\frac{\partial \mathcal{H}^k}{\partial n^k_P} = 0 \quad ; \quad \frac{\partial \mathcal{H}^k}{\partial n^k_E} = 0 \tag{5.97}$$

From which:

$$n^k_P = \frac{\lambda^k_{\gamma_P}}{\lambda^i_{E_{P_0}}}\frac{gW_P}{2D_{I_{P_0}}V^2_{P_0}} \tag{5.98}$$

$$n_E^k = \frac{\lambda_{\gamma_E}^k}{\lambda_{E_{E_0}}^i} \frac{gW_E}{2D_{I_{E_0}} V_{E_0}^2} \tag{5.99}$$

Substituting: $\lambda_{r_h}^o$ (5.36), $\lambda_{E_{P_0}}^i$ (5.53), $\lambda_{E_{E_0}}^i$ (5.54), $\lambda_{h_{P_0}}^j$ (5.78), $\lambda_{h_{E_0}}^j$ (5.79) into the Hamiltonian, using its separability (with respect to each aircraft controls) $\lambda_{\gamma_P}^k$ and $\lambda_{\gamma_E}^k$ can be extracted from it and substituted into (5.98) and (5.99).

$$n_P^k = \cos \gamma_P^k + \left\{ \frac{V_{P_0}^i}{\cos \gamma_{P_0}^j \left(V_{P_0}^o - V_{P_0}^i\right)} \frac{\left(T_P^i - D_P^i\right)_0}{D_{I_{P_0}}} \left[1 - \cos\left(\gamma_{P_0}^j - \gamma_P^k\right)\right] + \right.$$

$$\left. + \cos^2 \gamma_P^k - \cos^2 \gamma_{P_0}^j \right\}^{\frac{1}{2}} \operatorname{sign}\left(\gamma_{P_0}^j - \gamma_P^k\right) \tag{5.100}$$

$$n_E^k = \cos \gamma_E^k + \left\{ \frac{V_{E_0}^i}{\cos \gamma_{E_0}^j \left(V_{E_0}^o - V_{E_0}^i\right)} \frac{\left(T_E^i - D_E^i\right)_0}{D_{I_{E_0}}} \left[1 - \cos\left(\gamma_{E_0}^j - \gamma_E^k\right)\right] + \right.$$

$$\left. + \cos^2 \gamma_E^k - \cos^2 \gamma_{E_0}^j \right\}^{\frac{1}{2}} \operatorname{sign}\left(\gamma_{E_0}^j - \gamma_E^k\right) \tag{5.101}$$

7. FEEDBACK SOLUTION OF THE PROBLEM

Uniformly valid feedback expressions for n_P and n_E can be obtained if we replace the initial (stationary) values of the various variables in (5.100), (5.101) by their current (measurable) values.

The pursuer's aerodynamic load factor will be expressed as follows:

$$n_p = \cos \gamma_p + \left\{ \frac{1}{\cos \gamma_p^j} \frac{V_p^i}{V_p^o - V_p^i} \frac{\left(\xi_p T_{max_p} - D_{0_p} - D_{I_p}\right)^i}{D_{I_p}} \left[1 - \cos (\gamma_p^j - \gamma_p)\right] + \right.$$

$$\left. + \cos^2 \gamma_p - \cos^2 \gamma_p^j \right\}^{\frac{1}{2}} \cdot \text{sign} (\gamma_p^j - \gamma_p) \qquad (5.102)$$

The term $(\cos^2\gamma_p - \cos^2\gamma_p^j)$ is small compared with the first one under the root sign as long as $\gamma_p \neq \gamma_p^j$. When $\gamma_p \to \gamma_p^j$ the solution has to approach asymptotically a straight line path at γ_p^j. These two arguments justify cancellation of this term.

We get finally:

$$n_p = \cos \gamma_p + \left\{ \frac{1}{\cos\gamma_p^j} \frac{V_p^i}{V_p^o - V_p^i} \frac{\left(\xi_p T_{max_p} - D_{0_p} - D_{I_p}\right)^i}{D_{I_p}} \left[1 - \cos (\gamma_p^j - \gamma_p)\right] \right\}^{\frac{1}{2}} \cdot$$

$$\cdot \text{sign} (\gamma_p^j - \gamma_p) \qquad (5.103)$$

where:

V_p^o - pursuer's maximum velocity in a straight level flight within its flight envelope.

$$V_p^o = \max_{E_p, h_p} \arg \left\{ T_{max_p} - D_{0_p} - D_{I_p} = 0 \right\} \qquad (5.104)$$

The superscript "i" is used to denote variables obtained at h^i (and the current specific energy level) defined by:

$$h_p^i(E) = \arg \max_{h_p} \left[\frac{P_{S_p}^i(E)}{V_p^o - V_p^i(E)} \right] \qquad (5.105)$$

$P_{S_p}^i(E)$ - Pursuer's specific power at straight level flight at an altitude h_p^i.

V_P^i is calculated from:

$$V_P^i = \left\{2g(E_p - h_p^i)\right\}^{\frac{1}{2}} \tag{5.106}$$

The flight path angle γ_P^j at which the aircraft has to fly in order to reach the altitude h^i is expressed in feedback form as follows:

$$\gamma_P^j = \cos^{-1}\left[\frac{V_P^i \, P_{S_P}^i}{V_P^o\left(P_{S_P}^i - P_{S_P}\right) + V_P^i \, P_{S_P}}\right] \text{sign}(h^i - h) \tag{5.107}$$

P_{S_P} - Pursuer's specific power.

The pursuer's optimal throttle remain as in (5.59):

$$\xi_P = 1.$$

Similar results hold for the evader.

8. TERMINAL PHASE OF THE VERTICAL INTERCEPTION MODEL

According to the solution presented in this chapter the interception terminates at the free stream conditions, i.e., both airplanes fly horizontally ($\gamma = 0$) at their maximum speed at their respective optimal altitudes (h_p^o, h_E^o). If $h_p^o \neq h_E^o$ (which is generally true) the transversality conditions on $\lambda_{h_p}(t_f)$ and $\lambda_{P_E}(t_f)$ (5.14), (5.15) are not satisfied by (5.78) and (5.79). Relating to practical terms, if the altitude gap $|h_p^o - h_E^o|$ is too large, weapon firing may not be convenient. Moreover, since the choice of optimal altitude h_p^o is independent of the position of the other airplane, such strategy cannot be considered feedback optimal for the pursuer. Even if $|\Delta h^o| \ll \ell$, the evader could avoid capture by flying at a non-optimal altitude out of the firing envelop. For all these reasons the energy state FSPT model

requires a terminal boundary layer. As it was mentioned previously (Ch. 4) feedback control of a terminal boundary layer is not feasible. This difficulty can be overcome by using a dual modelling approach for the pursuer only. The evader has to fly always at its optimal altitude.

If altitude influence could have been neglected (which is unfortunately not true), the pursuer's strategy would have been, similarly to the horizontal case, a line of sight pursuit. It seems therefore reasonable to propose for the pursuer a weighted combination of these control strategies obtained from two different FSPT models. This idea is presented mathematically by the following expression for the pursuer's aerodynamic load factor,

$$n_{P_V} = \beta \hat{n}_P + (1-\beta)\bar{n}_P \tag{5.108}$$

where:

$$\beta = \left[\frac{\bar{r}_0 - r}{\bar{r}_0 - \bar{r}_f}\right]^n \tag{5.109}$$

$\hat{n}_P$ - Pursuer's vertical plane load factor derived from line of sight model;

$\bar{n}_P$ - Pursuer's vertical plane load factor derived from energy-state model;

n - Empirical constant.

The time varying weighting factor β ensures a smooth transition and enforces the condition of capture (i.e., convenient weapon firing). It is easy to see that when $r = r_0$ (at the beginning of the interception)

$$\beta = 0 \sim n_{P_V} = \bar{n}_P$$

i.e., energy-state model is used exclusively. When $r = r_f$ (at termination)

$$\beta = 1 \sim n_{P_V} = \hat{n}_P ,$$

i.e., line-of-sight model is used exclusively. At intermediate values of r ($r_0 < r < r_f$) n_{P_V} is determined by (5.108).

The value of $m = 2$ was found acceptable based on some numerical experimentation. In Figure 5.2 the final time vs. m is depicted (for the example that will be presented in detail in Chapter 7) showing that for $m = 2$ the pursuer minimizes the capture time.

It can be summarized that the solution of the vertical interception game is a pair of uniformly valid strategies expressed differently for the pursuer and for the evader. These results will be interpreted in the next chapter in relation to the 3-D variable speed medium range interception game.

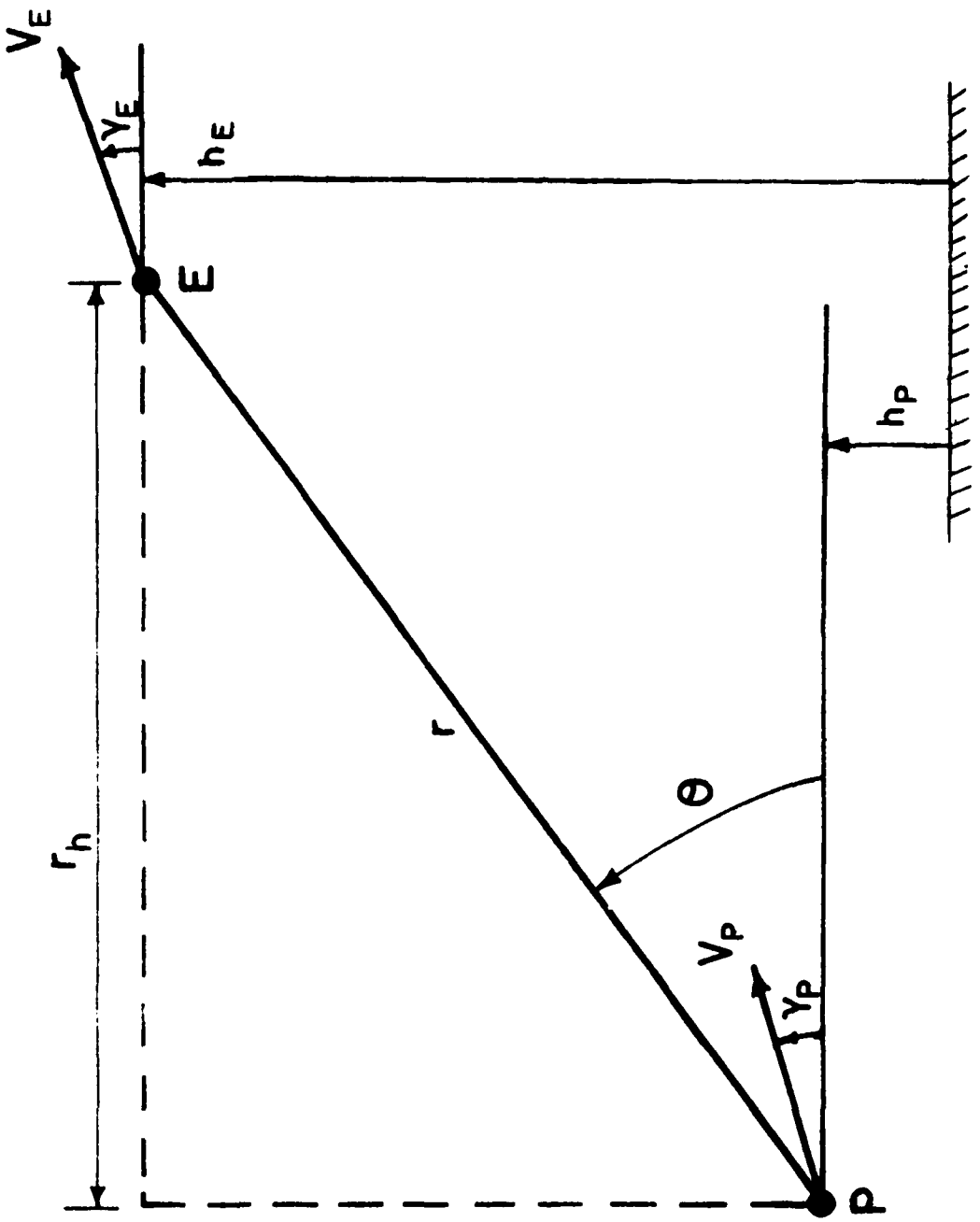

Fig. 5.1: Geometry of the vertical plane interception.

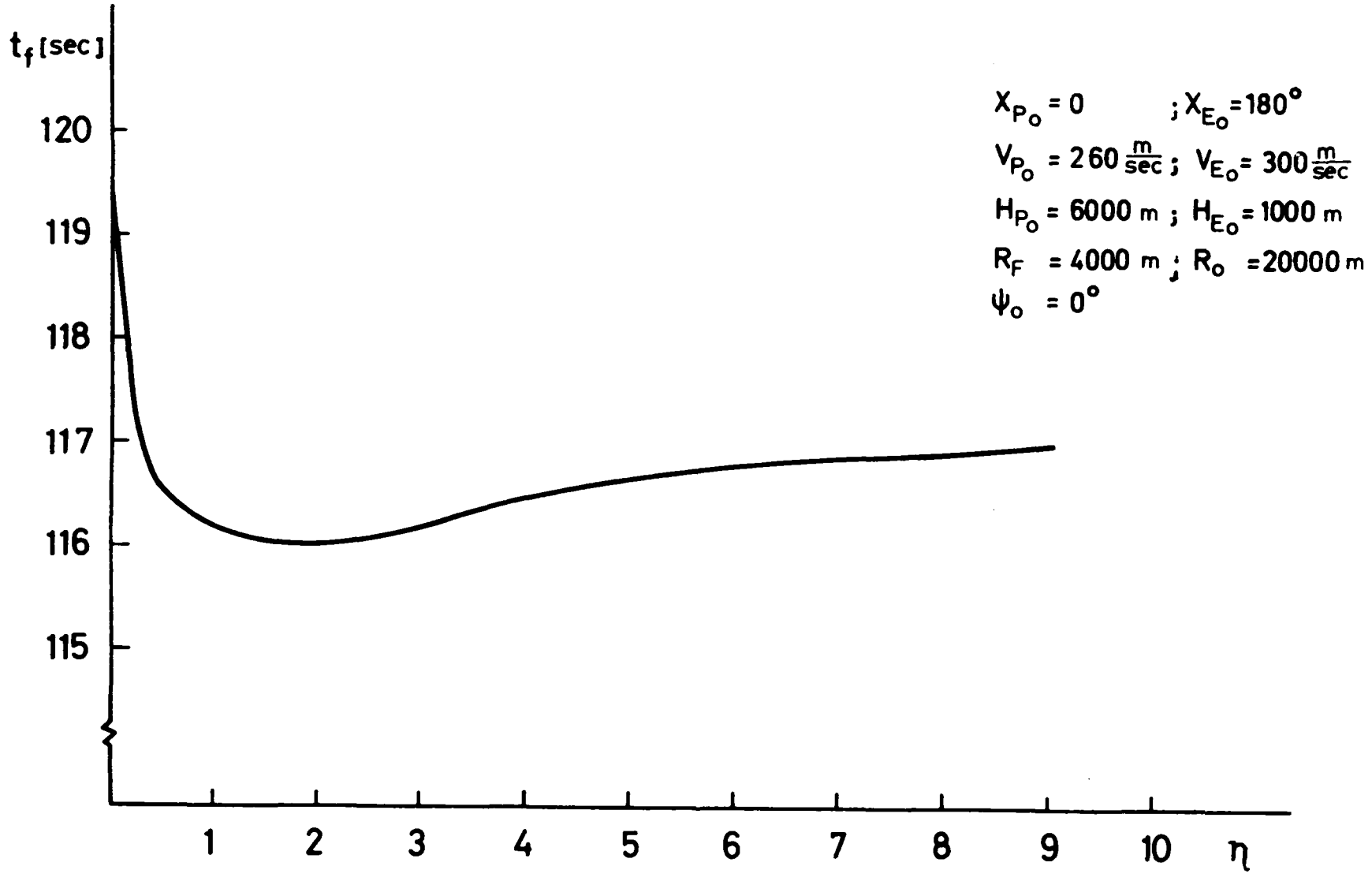

Fig. 5.2. Final time as function of η.

SECTION VI

FSPT STRATEGIES FOR THE 3-D INTERCEPTION

1. REVIEW OF THE MODELLING CONSIDERATIONS

As explained in Chapter 4, the implementation of the method of forced singular perturbations to solve the original 3-D variable speed problem can by no means be considered as a straightforward extension of previous results. The relative complexity of the FSPT game analysis for the vertical interception presented in Chapter 5, compared to the horizontal case [2] clearly indicates that a much more careful modelling approach may be required. For an enhaced insight it is useful to recall the models used in the 2-D (horizontal and vertical) problems.

TABLE 1: FSPT Models for Horizontal and Vertical Interception

Horizontal Interception (Model A)	Vertical Interception
$\dot{r} = \dot{r}_h = -V_P \cos(\chi_P - \psi) + V_E \cos(\chi_E - \psi)$	$\dot{r}_h = -V_P \cos\gamma_P + V_E \cos\gamma_E$
$\dot{\psi} = \frac{1}{r_h}\left[-V_P \sin(\chi_P - \psi) + V_E \sin(\chi_E - \psi)\right]$	———
$\varepsilon\dot{V}_P = \left(\frac{T_P - D_P}{W_P}\right)g$	$\varepsilon E_P = \left(\frac{T_P - D_P}{W_P}\right) V_P$
$\varepsilon\dot{V}_E = \left(\frac{T_E - D_E}{W_E}\right)g$	$\varepsilon E_E = \left(\frac{T_E - D_E}{W_E}\right) V_E$
———	$\varepsilon^2\dot{h}_P = V_P \sin\gamma_P$
———	$\varepsilon^2\dot{h}_E = V_E \sin\gamma_E$
$\varepsilon^2\dot{\chi}_P = \frac{g}{V_P}\left(n_P^2 - 1\right)^{\frac{1}{2}}$	$\varepsilon^3\dot{\gamma}_P = \frac{g}{V_P}\left(n_P - \cos\gamma_P\right)$
$\varepsilon^2\dot{\chi}_E = \frac{g}{V_E}\left(n_E^2 - 1\right)^{\frac{1}{2}}$	$\varepsilon^3\dot{\gamma}_E = \frac{g}{V_E}\left(n_E - \cos\gamma_E\right)$

Inspection of Table 1 suggests the following hierarchy for the 3-D model.

a) Horizontal components of the relative geometry ($\Delta x, \Delta y$ or r_h, ψ) are no doubt the variables of the reduced game for a medium range interception.

b) Since in the horizontal model (model A) speed can be expressed by specific energy, there is no contradiction between the two models to appoint the specific energy as the first (slowest) boundary layer variable.

c) The experience with energy state models certainly requires to admit that altitudes vary faster than specific energy.

d) The flight path angle is a definitely faster variable than altitude (since h is the integral of γ).

e) Turning dynamics in both planes seem to belong to the same level of hierarchy, being the components of the same variable: the aircraft total angular velocity vector $\vec{\omega}$ given by

$$\omega^2 = \dot{\gamma}^2 + (\dot{\chi} \cos \gamma)^2 \tag{6.1}$$

Substituting to (6.1):

$$\dot{\gamma} = \frac{g}{V} (n_V - \cos \gamma) \quad ; \quad n_V \triangleq n \cos \mu \tag{6.2}$$

and

$$\dot{\chi} = \frac{g n_h}{V \cos \gamma} \quad ; \quad n_h \triangleq n \sin \mu \tag{6.3}$$

leads to:

$$\omega^2 = \frac{g^2}{V^2} \left[n^2 - 2n \cos \gamma \cos \mu + \cos^2 \gamma \right] \tag{6.4}$$

Taking into account that the total aerodynamic load factor "n" is a constrained control variable by (3.15) and (3.16) the coupling between the horizontal and vertical components must not be overlooked.

However, for unconstrained load factor the exact optimal solution (i.e., Eqs.(3.70)-(3.71) can be expressed by defining

$$n_h^* \triangleq \frac{W}{2\lambda_V V D_i}\left(\frac{\lambda_x}{\cos\gamma}\right) \tag{6.5}$$

$$n_V^* \triangleq \frac{W}{2\lambda_V V D_i}\lambda_\gamma \tag{6.6}$$

as:

$$n^* = (n_h^{*2}+n_V^{*2})^{\frac{1}{2}} \tag{6.7}$$

$$tg\ \mu^* = n_h^*/n_V^* \tag{6.8}$$

These expressions suggest that, for $\cos\gamma \approx 1$, the vectorial composition of the two perpendicular 2-D solutions can be a reasonable approximation for a 3-D problem subject to properly imposed cons raints.

Based on this insight it is therefore proposed that the zero-order FSPT solution of the three-dimensional variable speed medium range interception game will be synthesized by this approach.

2. OPTIMAL CONTROL STRATEGIES FOR 3-D MEDIUM RANGE INTERCEPTION

The zero-order composite FSPT strategies of the aircraft can be now summarized.

For both players the optimal throttle setting is always maximal.

$$(\xi_P^c)_{3D} = (\xi_E^c)_{3D} = 1 \tag{6.9}$$

Let us note in this conjunction that a model B [3] type solution is not necessary in the 3-D case. Airplanes can loose speed rapidly (if it is required) by exchanging kinetic energy to altitude without giving up total specific energy.

The aerodynamic load factor and the respective bank angle are given by

$$n_{P_{3D}}^{c} = \min \left\{ n_{P_{max}}, n_{P_L}, \left(n_{h_P}^2 + n_{V_P}^2 \right)^{\frac{1}{2}} \right\} \tag{6.10}$$

$$\text{tg } \mu_P^c = n_{h_P} / n_{V_P} \tag{6.11}$$

with similar expressions for the evader. The horizontal load factor expression is the same for both players as derived in [3]

$$n_h = \left\{ \frac{V}{V_{L-V}} \cdot \frac{T_{max} - D_0 - D_i}{D_I} \left[1 - \cos(\chi - \psi) \right] \right\}^{\frac{1}{2}} \text{sign}(\psi - \chi) \tag{6.12}$$

It has been however remembered that the vertical maneuvering strategy of the pursuer is different from the evader's. n_{V_P} is given by Eqs. (5.109)-(5.110), while n_{V_E} is simply $\bar{n}_E$ expressed by Eq.(5.103).

SECTION VII

A DEMONSTRATIVE EXAMPLE

1. AIR DEFENSE SCENARIO

In order to demonstrate the applicability of the zero-order feedback solution as outlined in Chapter 6 an imaginary air defense scenario was selected.

Aircraft "A" (the pursuer in the game), an agile air superiority fighter of high thrust to weight ratio, patrols to defend a small area from an eventual attack of a tactical bomber "B" (the evader) penetrating at a low altitude at high subsonic speed.

Some basic information on both aircraft is given in Table 7.1. Aerodynamic and thrust data of aircraft "A" was obtained and used in the computer program in a tabular form as shown in Table 7.2. The data of aircraft "B" is expressed by a polynomial approximation in the computer program and depicted in Figs. 7.1 and 7.4.

Comparison of the flight envelopes for both aircraft (Fig. 7.5) shows a definite advantage of "A" in low altitude. "B" has however a higher maximum speed and maximum altitude.

It is assumed that the interception game starts by simultaneous detection followed by an immediate bomb load release by the penetrating "B". Since "A" is equipped with a superior weapon system, "B" wishes to enhance the survival probability by optimal evasion. The interception is successful if the pursuer can reach the firing range of its missiles in finite time. If such defined "capture" can take place, the objective of the pursuer is to minimize the time of capture and the evader wants the maximize it. Due to the differences in aircraft flight envelopes (see Fig. 7.5), capture is not always guaranteed.

This scenario serves as basis for the following studies.

a Detailed time history of a characteristic single engagement analyzing aircraft strategies.

b. Parametric study of the influence of initial conditions, weapon and airplane characteristics on the outcome of the interception.

Such a systematical investigation, requiring to solve a large number of "optimal" engagements, could be performed with the limited computational resources only due to the inherent efficiency of the feedback solution.

2. TIME HISTORY OF A CHARACTERISTIC ENGAGEMENT

The initial and end conditions of this engagement are summarized in Table 7.3 and the projection of the initial geometry are depicted in Fig. 7.6 In figures 7.7 – 7.13 the time histories of the control and state variables are depicted. Based on these results several observations can be made.

a) During the initial phase of the engagement, the pursuer performs a sharp diving turn increasing its velocity and closing the angular difference with the line of sight. At the same time the evader engages in a sharp climbing turn at almost constant velocity.

b) About 35 seconds after the maneuver started, both azimuth angles χ_P and χ_E approach the line of sight azimuth angle ψ and the aircraft maneuvers in the horizontal plane are almost completed.

c) From that point till the end of the interception the aircraft fly, only with the intention to increase their velocity.

d) At about t = 60 sec, the evader starts diving in order to change its velocity from subsonic to supersonic, while at the same time the pursuer, flying already at supersonic velocity, climbs toward the evader. This maneuver "seems" to be non reasonable, however, according with energy-state model this is the best way for the evader, to increase its specific energy and velocity, required to escape.

e) It should be noticed that the pursuer has more favorable initial conditions than the evader, since its initial dive maneuver serves two goals at the same time, increases its velocity and brings closer to the evader.

f) Another interesting point to be noticed is that although the maneuver starts with the evader being at 5000 meters lower than the pursuer, at t = 32 sec both aircraft are at the same altitude, 3000 meters, and from that moment until termination of the interception the evader flies at higher altitude than the pursuer.

g) As one can see, capture occurred in this example, before any one of the aircraft reached the "outer" (steady state) conditions, i.e., $V^{o} = V_{max}$ Since the strategies of both aircraft are based on the assumption of reaching maximum velocity during the reduced game, and these maximum velocities are not achieved, the accuracy of the FSPT approximation might be degraded This will be discussed in Chapter 10.

Observing the time histories the following conclusions can be made:

1 The results confirm the assumptions of the FSPT modelling about time scale separation

2. After the horizontal turn is completed the behaviour of both airplanes are dominated by the energy state model requirements. This fact can be clearly seen in Figs. 7 14, 7.15 where the optimal "energy climb" profiles

$h^1(E)$ and the actual trajectories are plotted into the flight envelope maps 3 Due to the small altitude difference between the airplanes the line of sight strategy used by the pursuer at the terminal phase cannot be noticed

3. PARAMETRIC INVESTIGATION

The qualitative and quantitative outcome of the game, i e.,

(i) can capture be achieved?

(ii) the value of the "time of capture".

depend on the parameters of the airplanes and the weapon system as well as on the initial conditions. For a brief but systematical analysis the influence of the following were considered.

First the influence of initial range, pursuer's initial heading and missile firing range (capture radius) on the qualitative outcome was investigated. In Fig 7 16 the relevant capture zone projections for different firing ranges are depicted. It shows that for the set of initial conditions kept constant, capture can be attained even in the most unfavourable conditions for the pursuer ($\chi_{P_0} = 180°$).

Figs. 7.17, 7.18 show the influence of the initial altitude on the time of capture, indicating that almost independently of initial range and capture radius the best altitude for patrolling is between 7-8 km This gives to the pursuer a 2:1 advantage in specific energy. The results show that if $h_{P_0} < 3$ km or the energy ratio is lower than 1.15 no capture occurs.

Fig 7.19 answers the question about the optimal penetration speed of the evader to maximize the time of capture. The results show that the almost transonic speed is the best. It is also shown that for initial speed lower

than 250 m/sec the evader cannot follow the optimal strategy without violating ground clearance.

Fig. 7.20 shows the influence of thrust to weight ratio of the airplanes. It seems to be a parameter of major importance since the turning phase of the interception is relatively short. Using an example which under nominal conditions has a time of capture of t_f = 216 sec, it is shown that a 5% improvement of pursuer's thrust to weight ratio (or equivalently 5% degradation for the evader) can reduce this capture time by about 30%. The slope of the curve for the nominal value indicates that navigation to the opposite direction (increasing thrust for the evader) does not allow capture.

TABLE 7.1. Aircraft Data

Aircraft	A	B
$W[Kg_f]$	12700	20000
$S[m^2]$	27.87	49.246
$W/S[kg_f/m^2]$	455.7	406
T_0/W	0.86	0.47
n_{max}	6	5
M_{max}	2	2.1

TABLE 7.2. "A" AIRCRAFT THRUST AND AERODYNAMIC DATA

h[m] \ M	0.6	0.8	1	1.2	1.4	1.6	1.8	2
0	11022	11793	13109	15060	15105	14970	13562	12111
3050	8618	9526	10523	12247	12973	13517	12292	11340
6100	6260	7258	8255	9571	10205	11431	11340	10796
9150	4173	5035	6124	7258	8210	8845	9117	9027
12200	2540	3084	3946	4853	5534	6033	6396	6622
15250	1406	1769	2268	2722	3220	3493	3719	3856

Thrust $[Kg_f]$

M	0.6	0.8	1	1.2	1.4	1.6	1.8	2
C_{D_0}	0.0175	0.0181	0.035	0.043	0.043	0.045	0.046	0.046
K	0.12	0.12	0.15	0.19	0.25	0.29	0.34	0.38
$C_{L_{max}}$	1.5	1.5	1.55	1.3	0.95	0.75	0.65	0.6

$$D = q(C_{D_0} + KC_L^2) \qquad C_L = w/\tfrac{1}{2}\rho V^2 S$$

TABLE 7.3. INITIAL CONDITIONS OF THE INTERCEPTION

r_0[m]	ψ_0	θ_0
20000	0°	14.44°

	$V_0\left[\frac{m}{sec}\right]$	h_0[m]	γ	χ
Pursuer	260	6000	0°	145°
Evader	300	1000	0°	180°

FINAL CONDITION OF THE INTERCEPTION

$r_f = 4000$ [m].

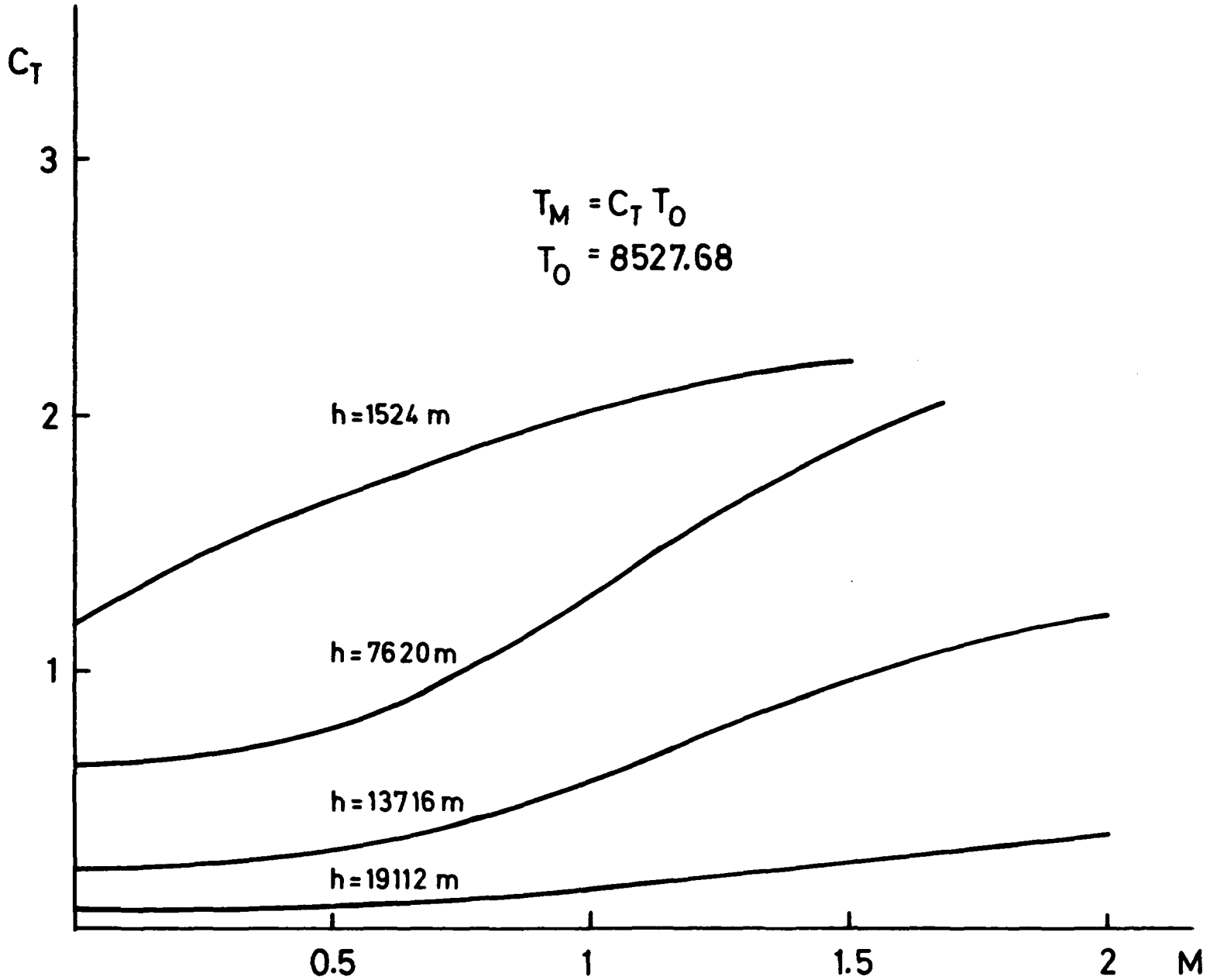

Fig. 7.1: Aircraft's A thrust coefficient.

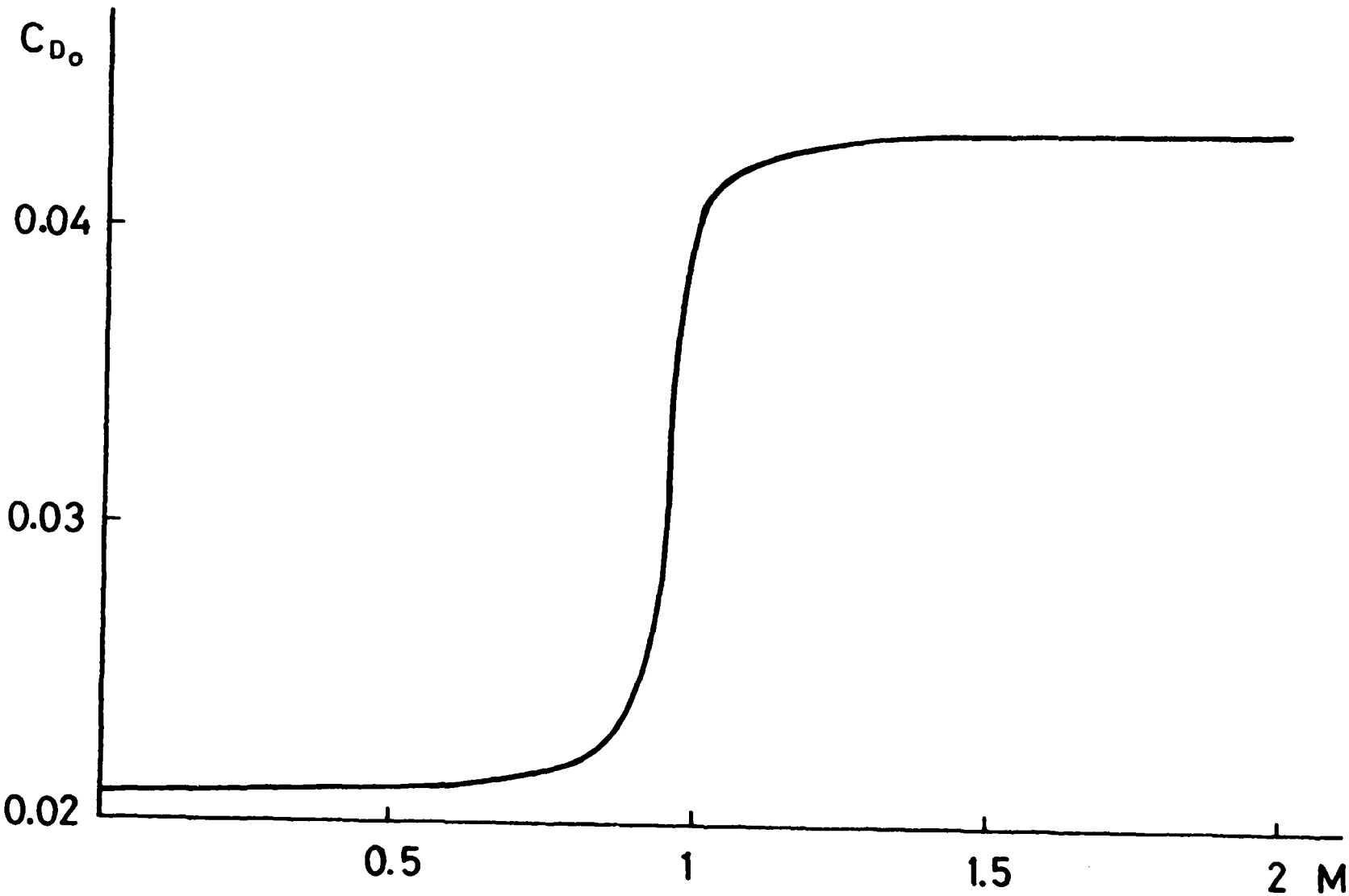

Fig. 7.2: Aircraft's A parasitic drag coefficient.

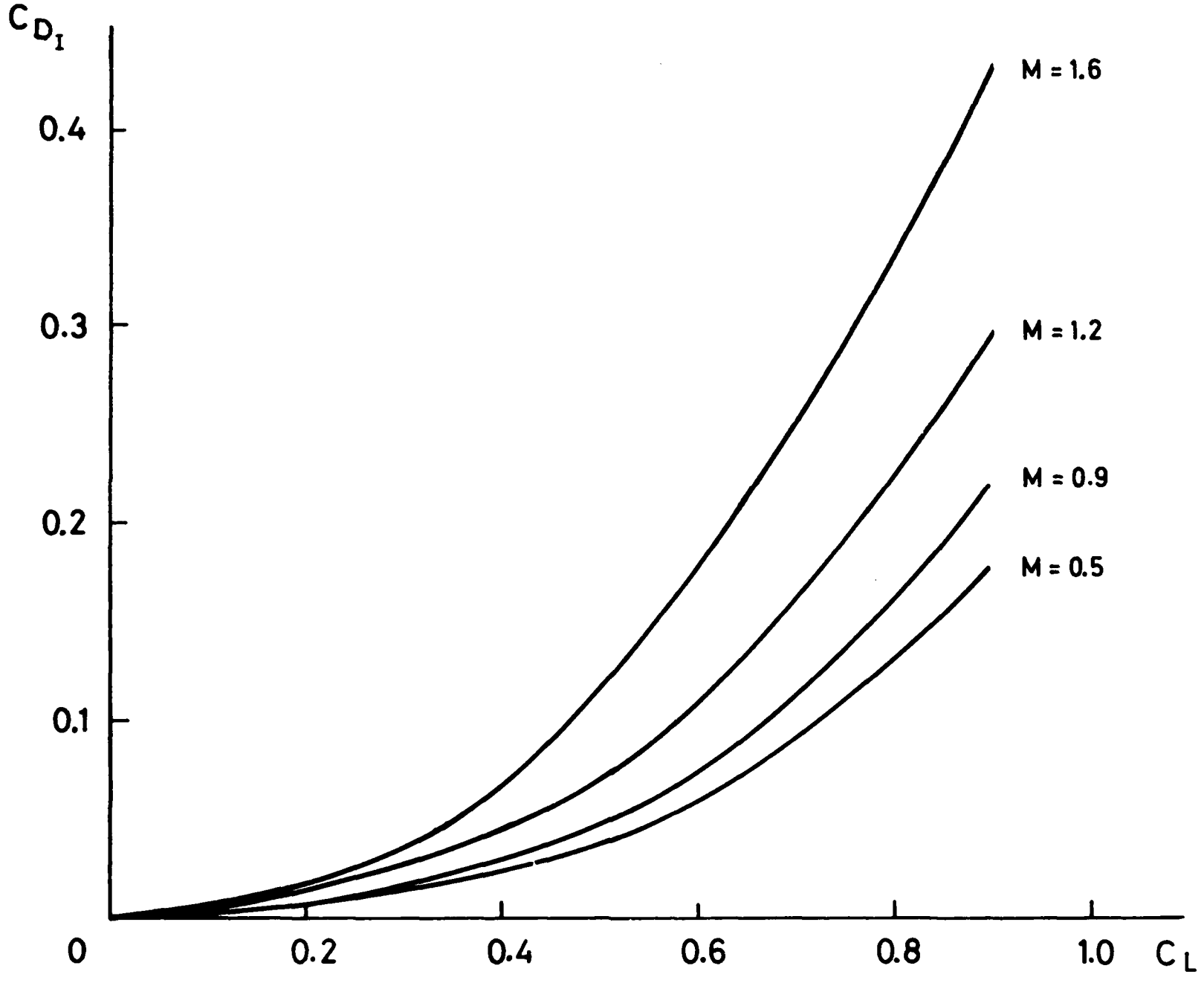

Fig. 7.3: Aircraft's A induced drag coefficient.

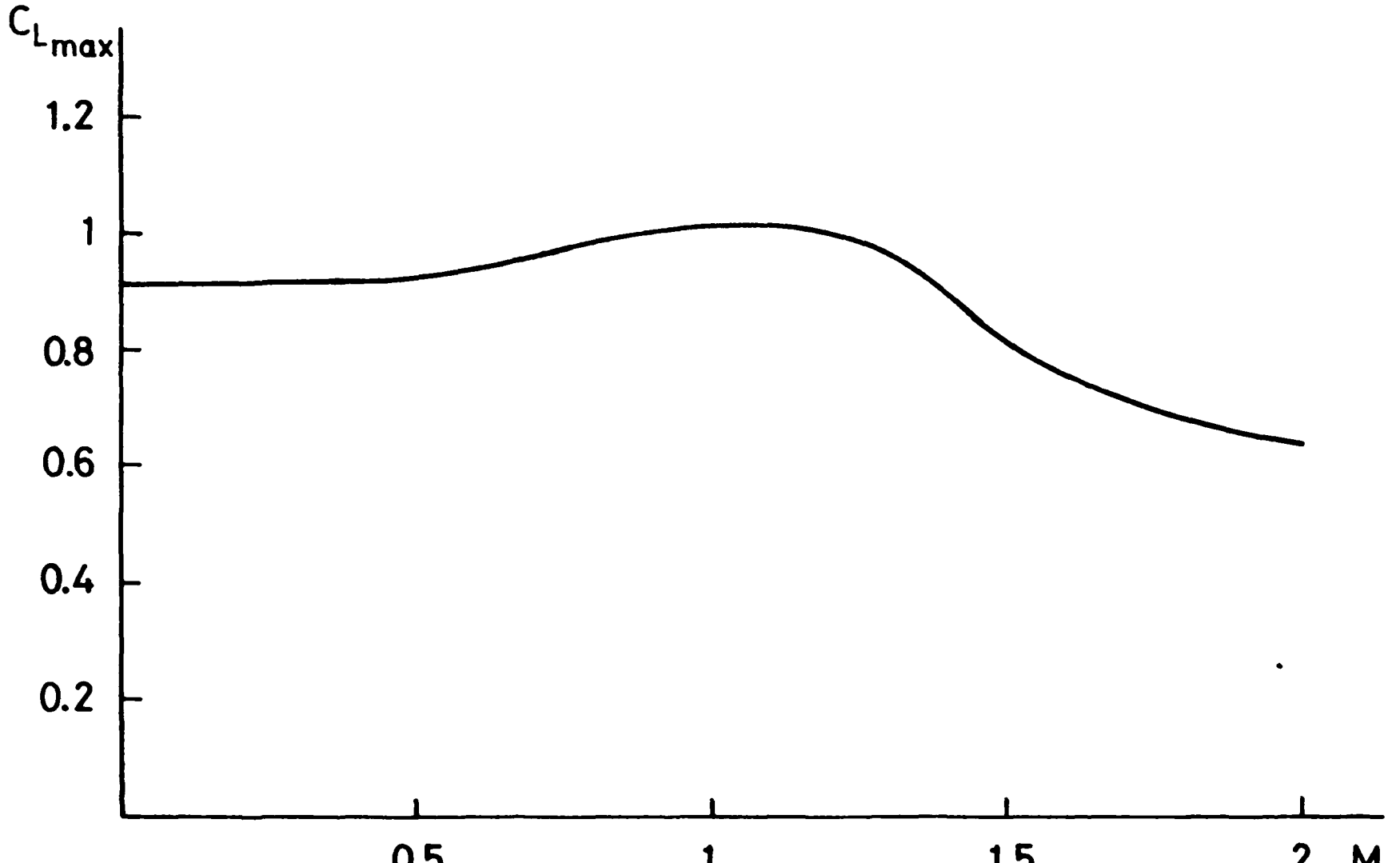

Fig. 7.4: Aircraft's A maximum lift coefficient.

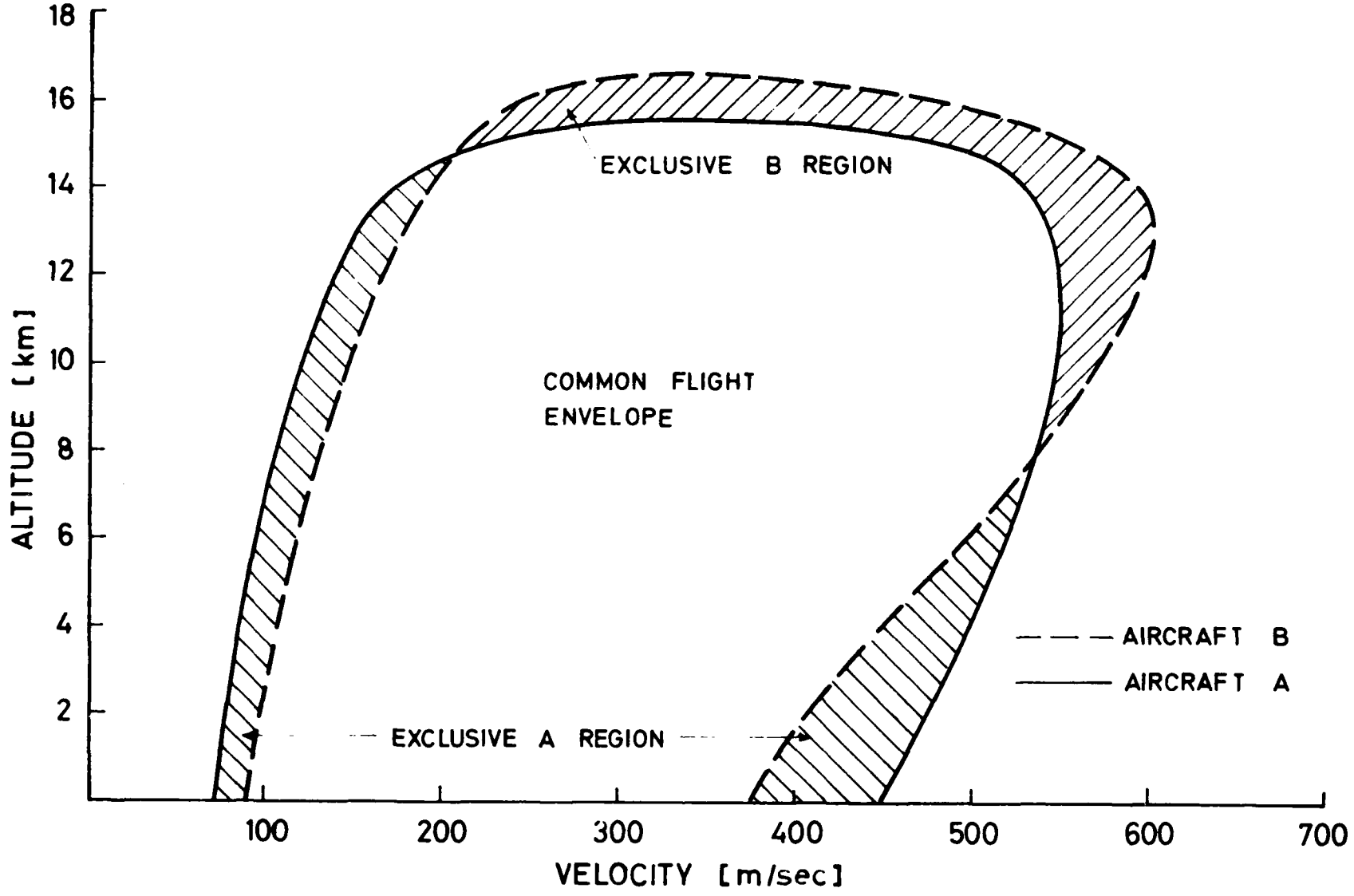

Fig. 7.5: Aircraft's A and B flight enveloppes.

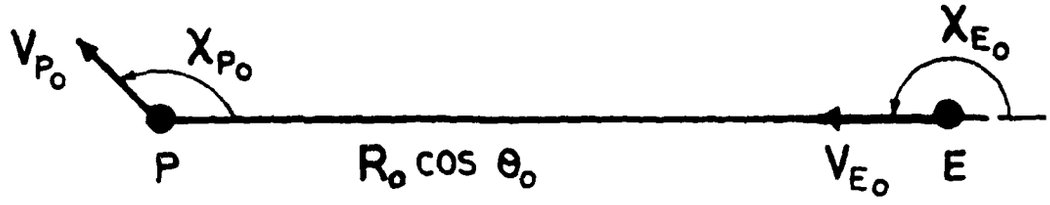

Fig. 7.6a: Projection of IC in the horizontal plane.

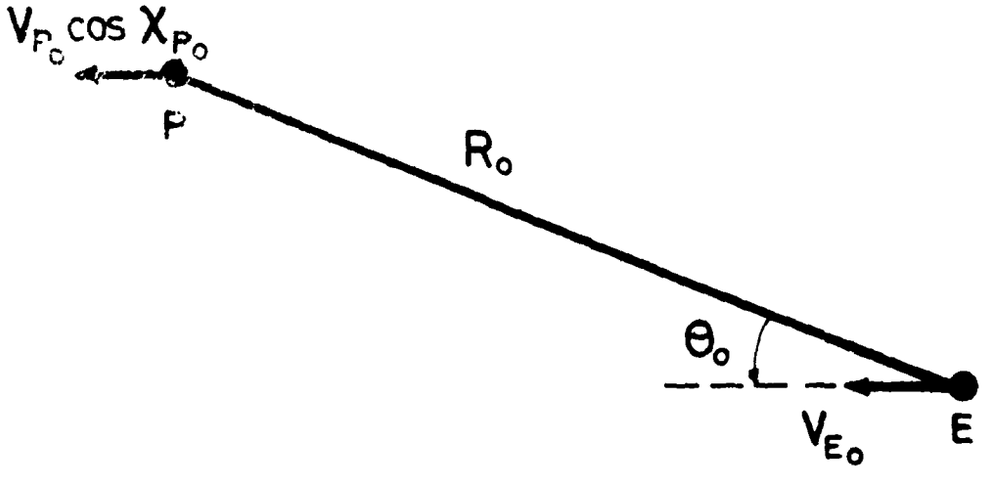

Fig. 7.6b: Projection of IC in the vertical plane containing the line of sight.

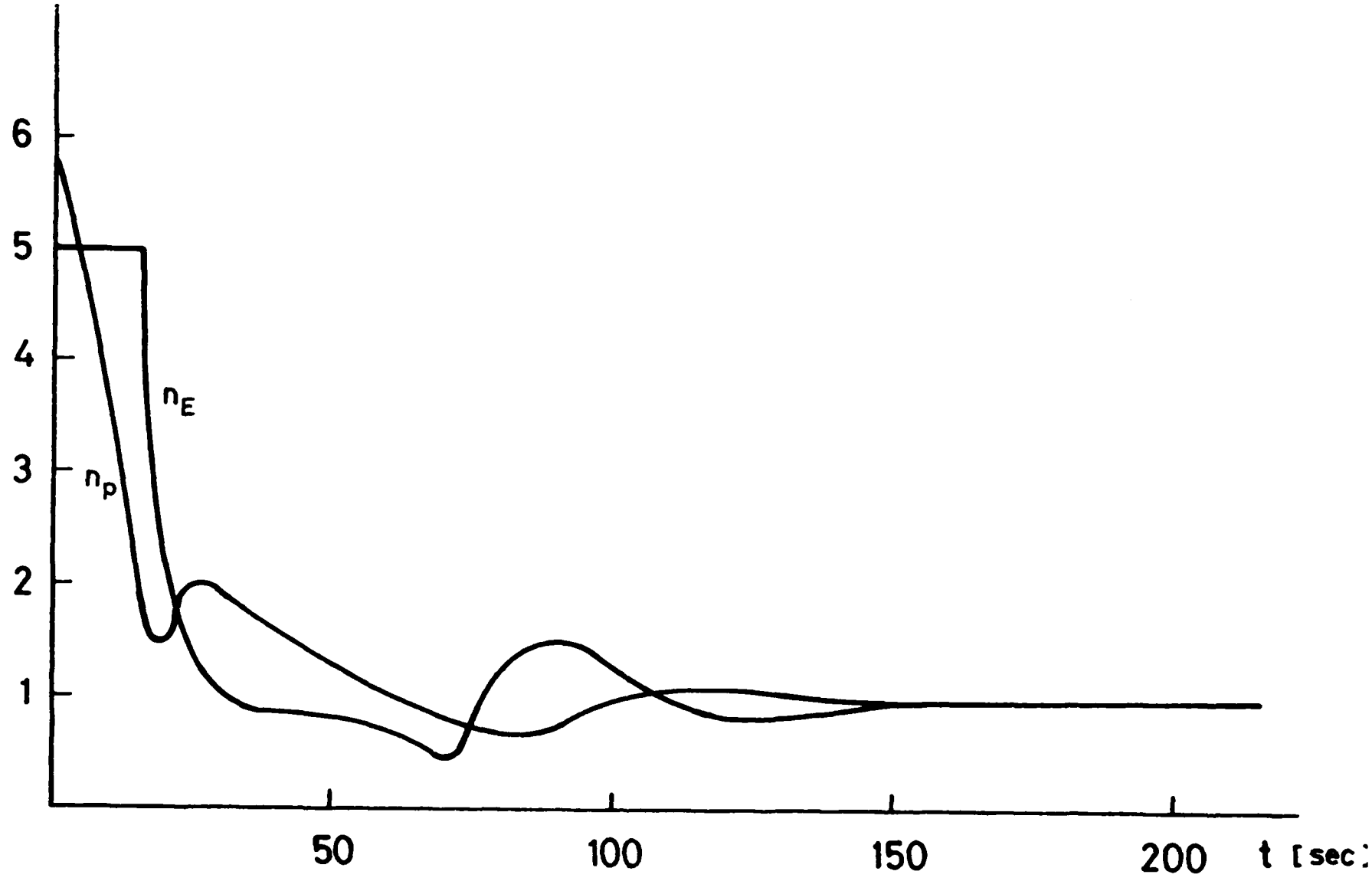

Fig. 7.7: Time history of the aerodynamic load factors.

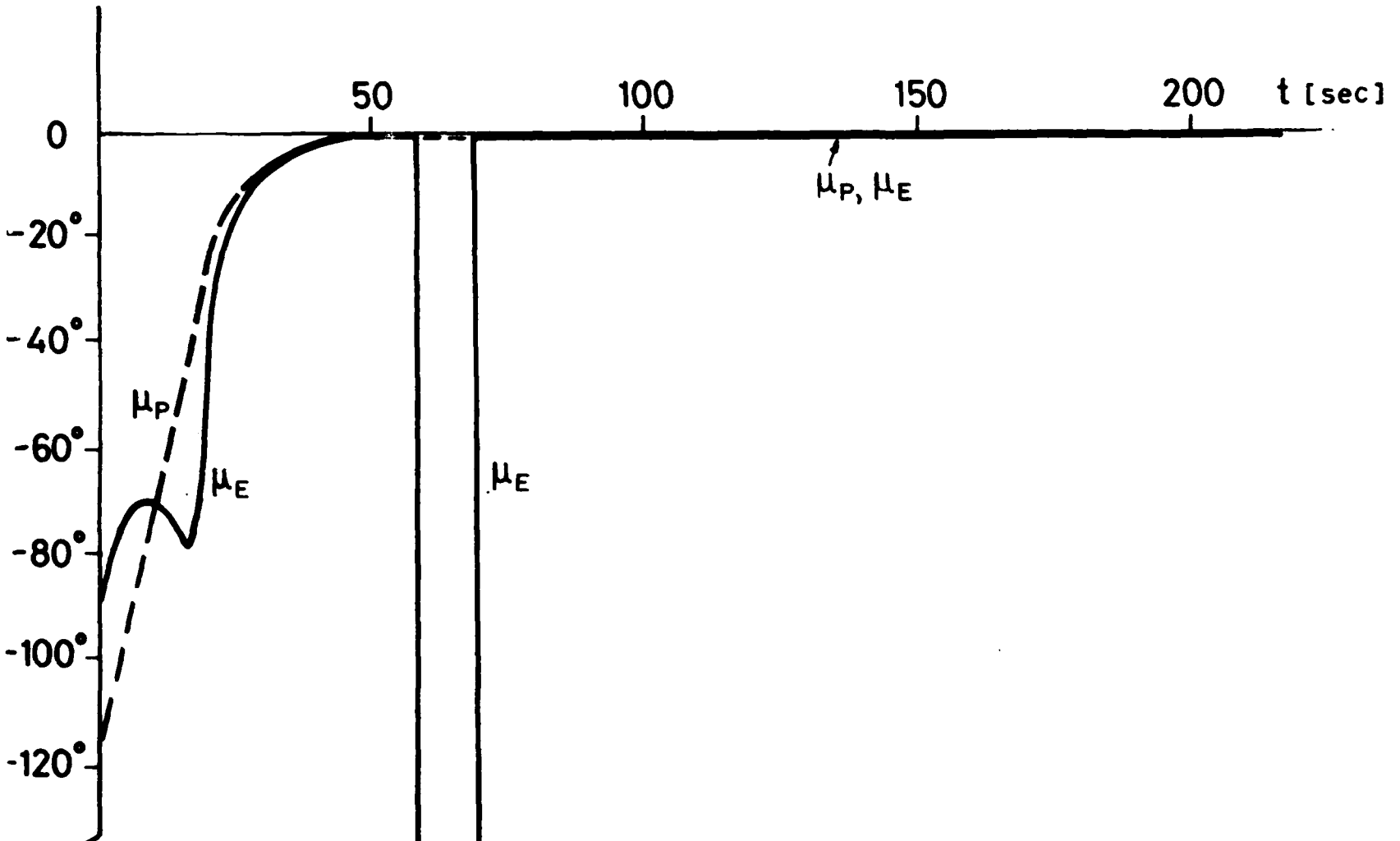

Fig. 7.8: Time history of the bank angles (positive for left turn).

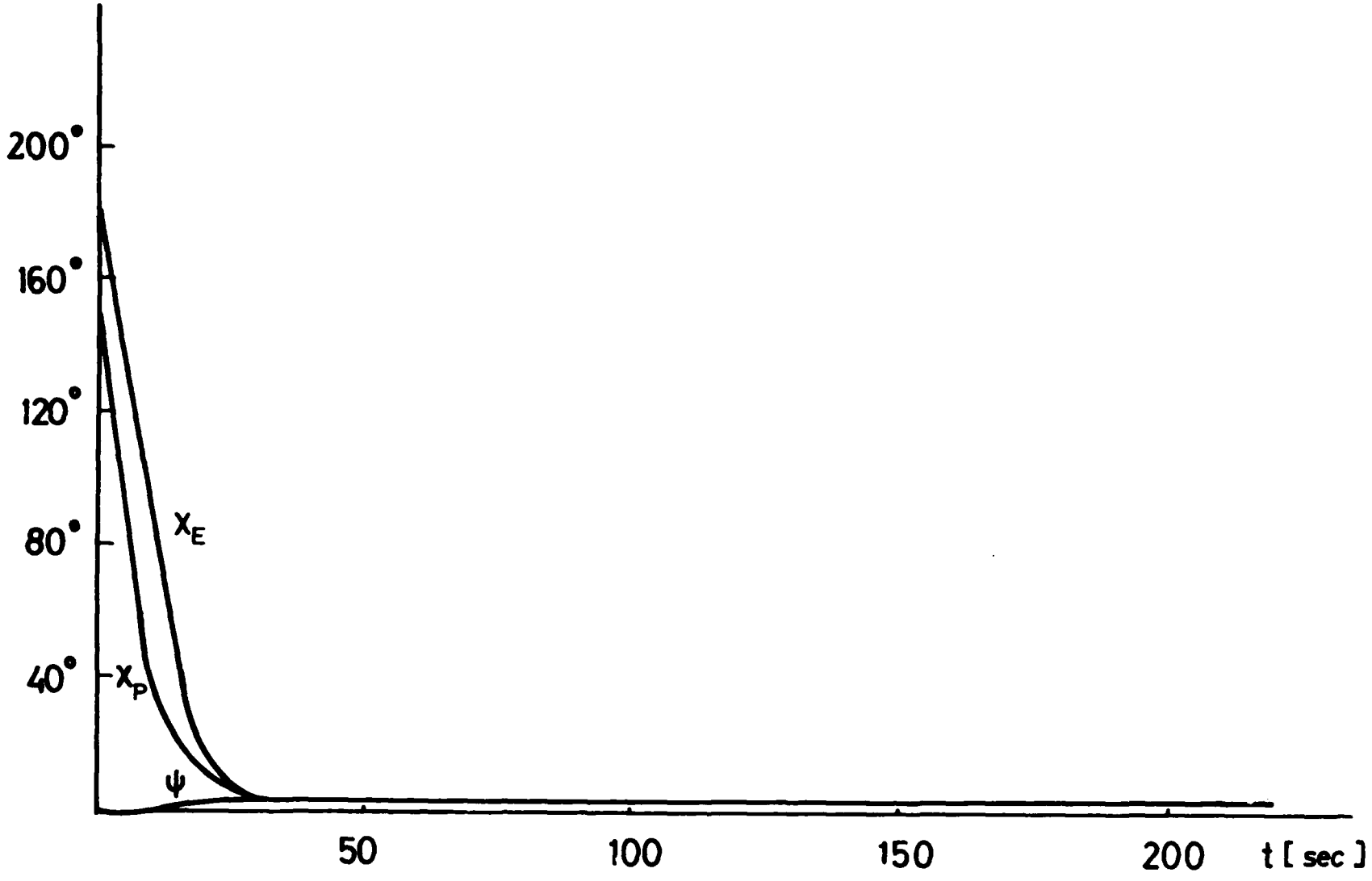

Fig. 7.9: Time history of azimuth and horizontal line of sight angles.

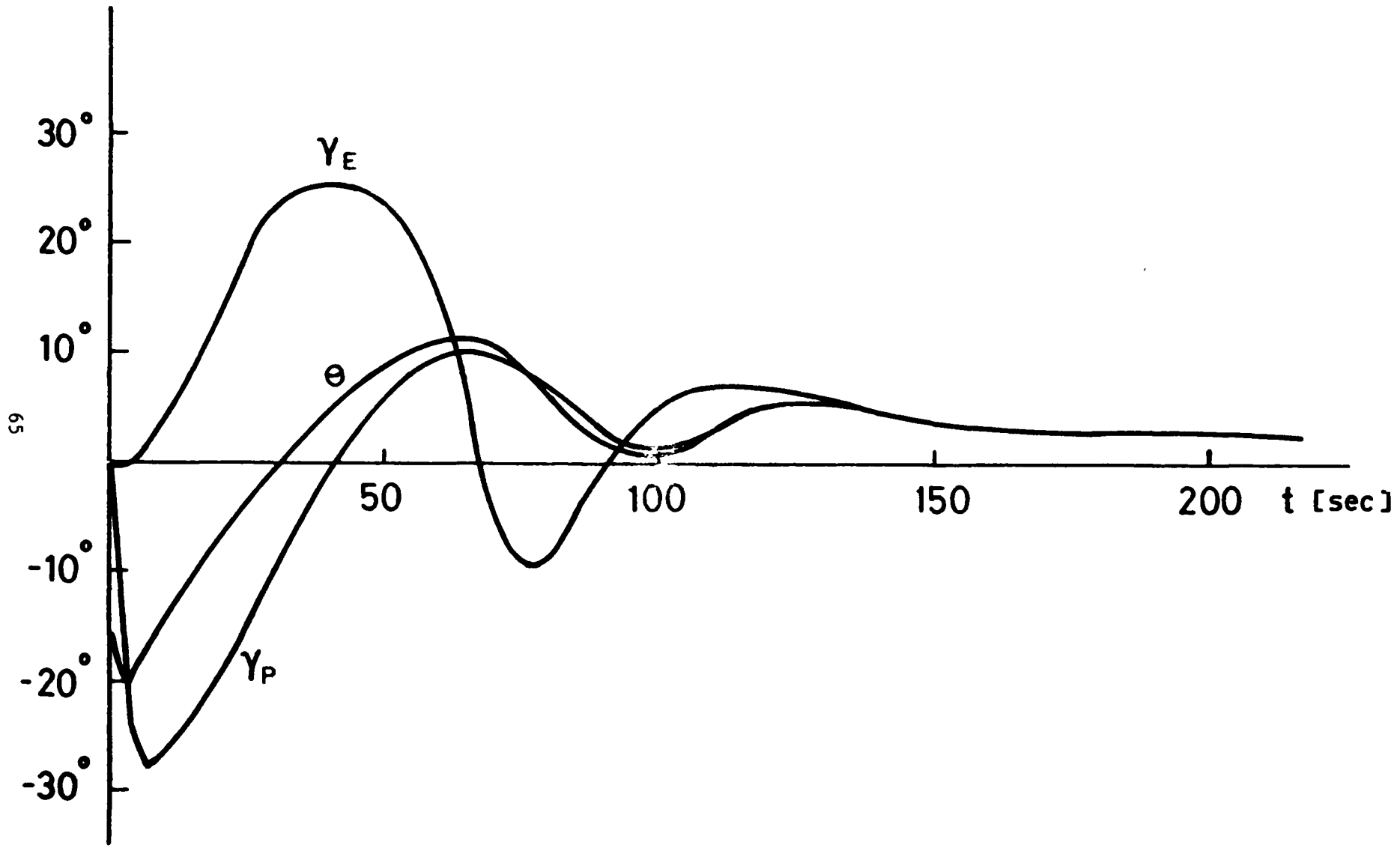

Fig. 7.10: Time history of flight path and vertical line of sight angles.

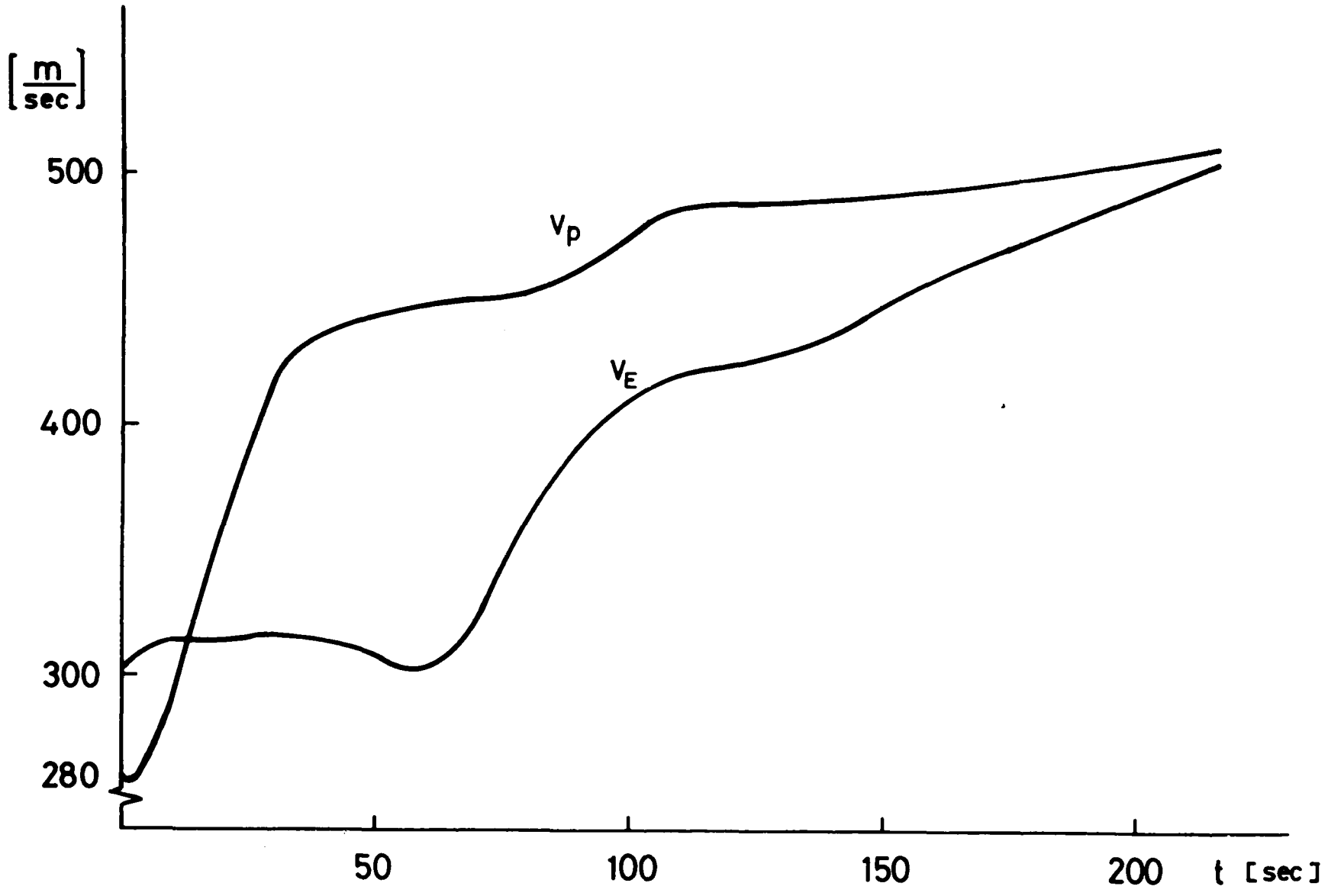

Fig. 7.11: Time history of the velocities.

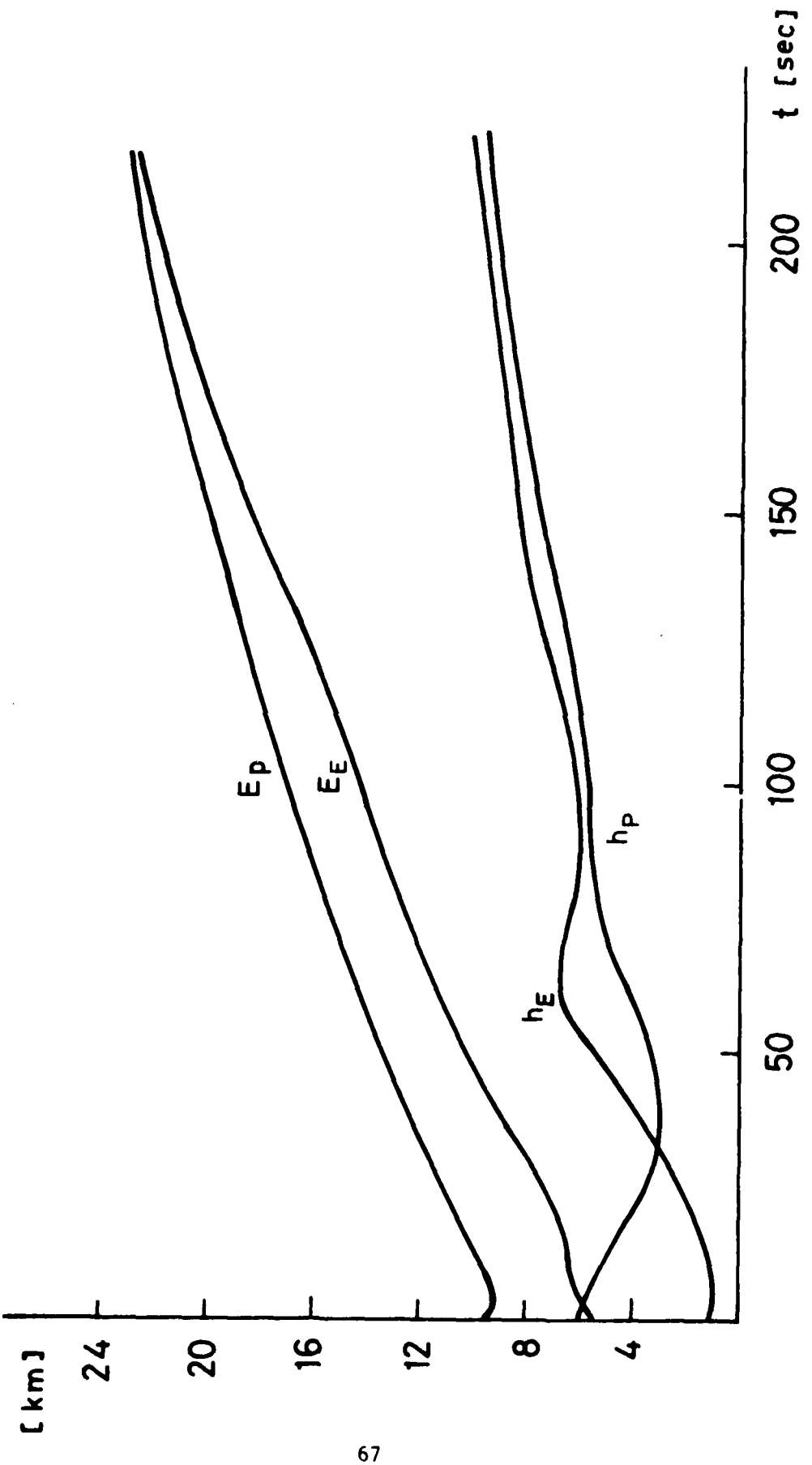

Fig. 7.12: Time history of altitudes and specific energies.

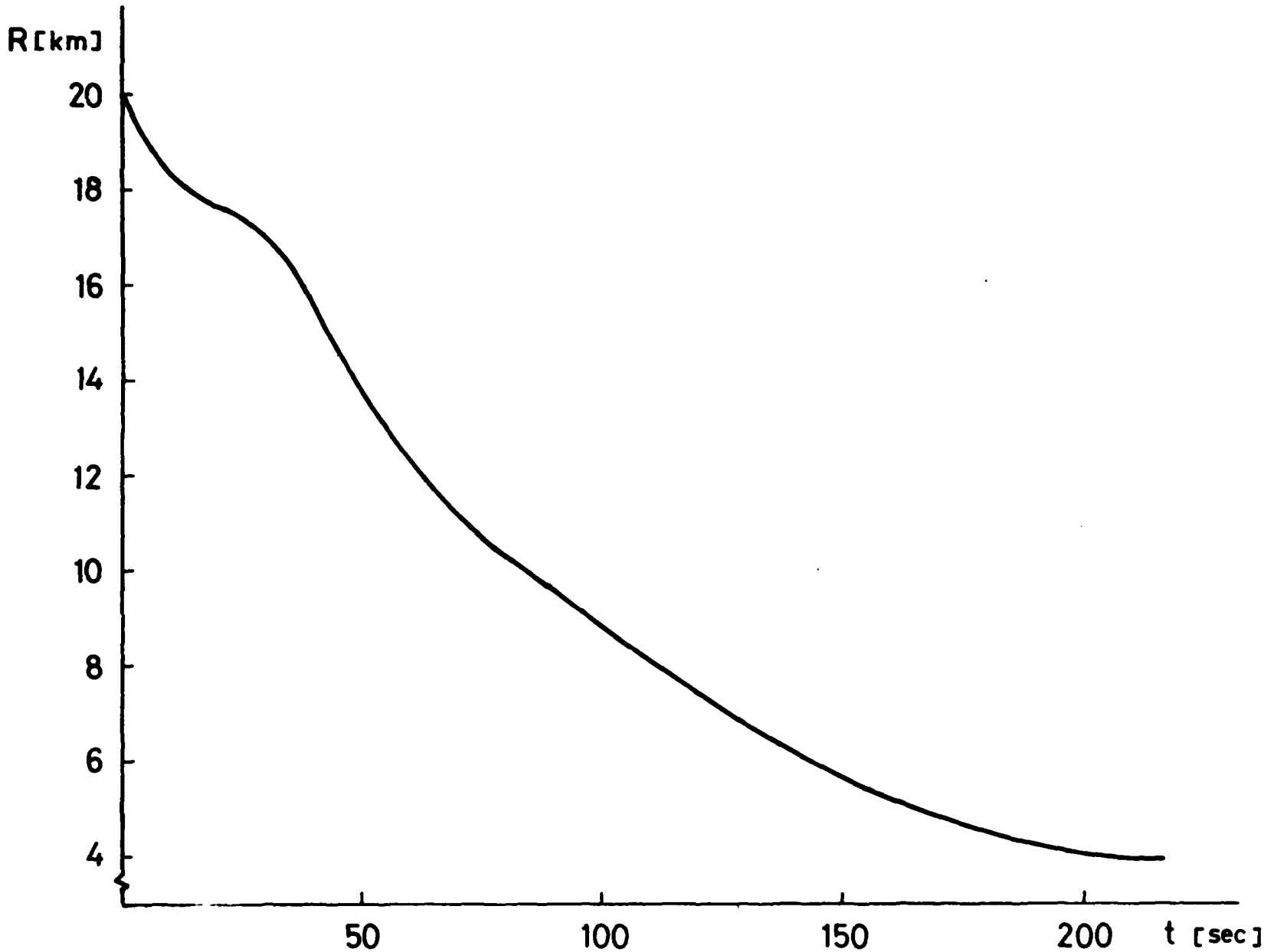

Fig. 7.13: Time history of separation distance.

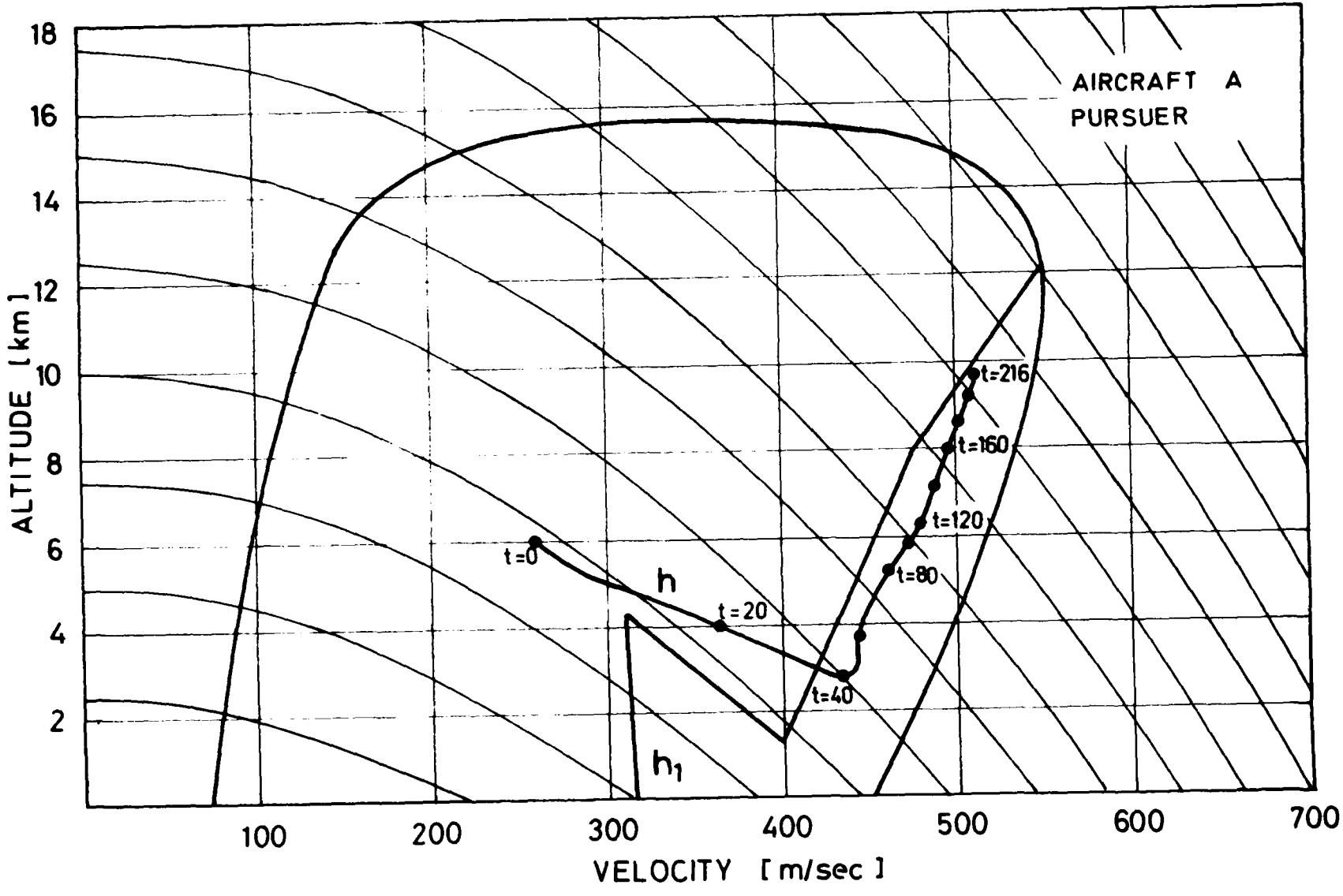

Fig. 7.14. Aircraft's A optimal and actual altitude paths.

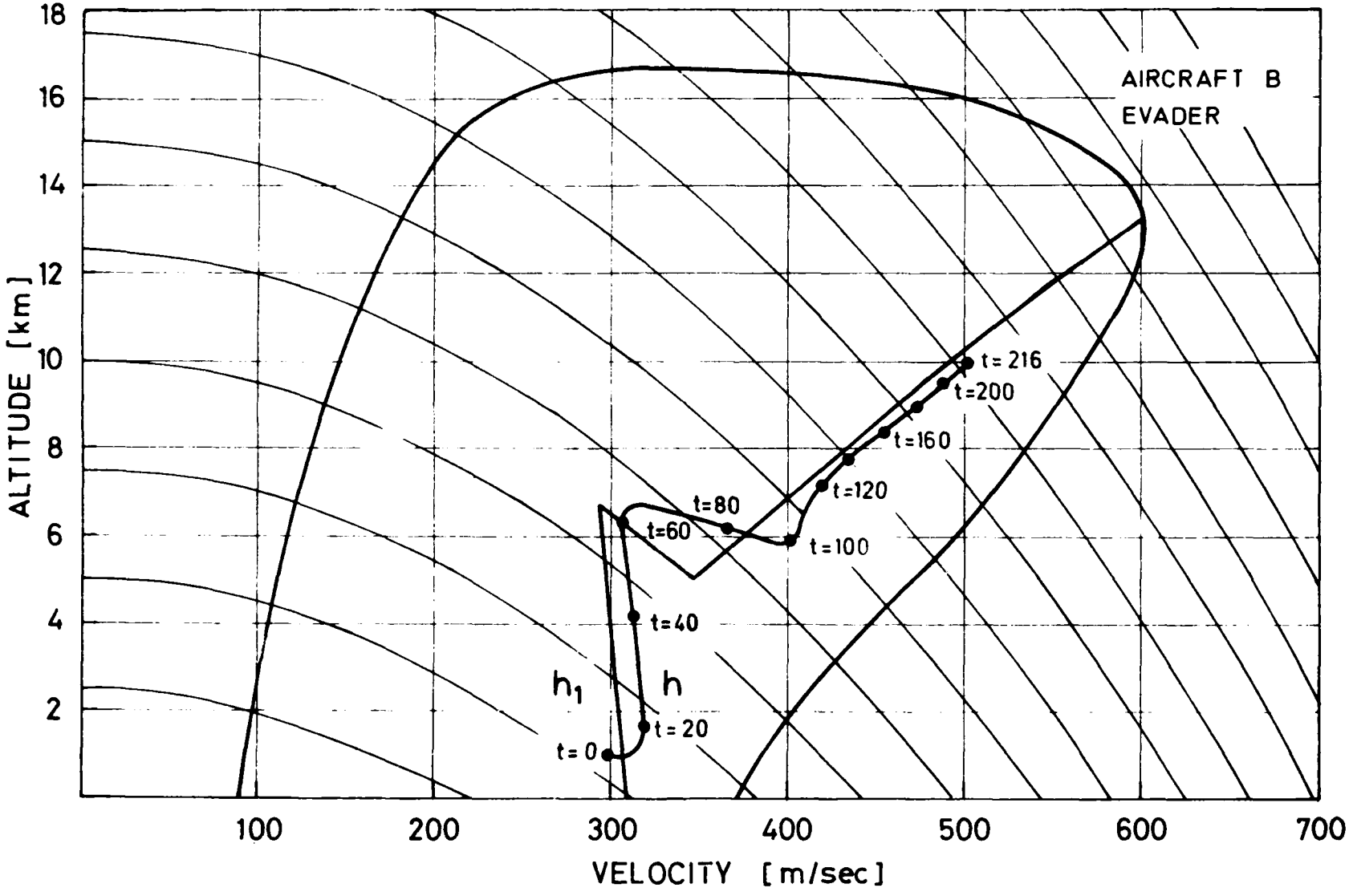

Fig. 7.15. Aircraft's B optimal and actual altitude paths.

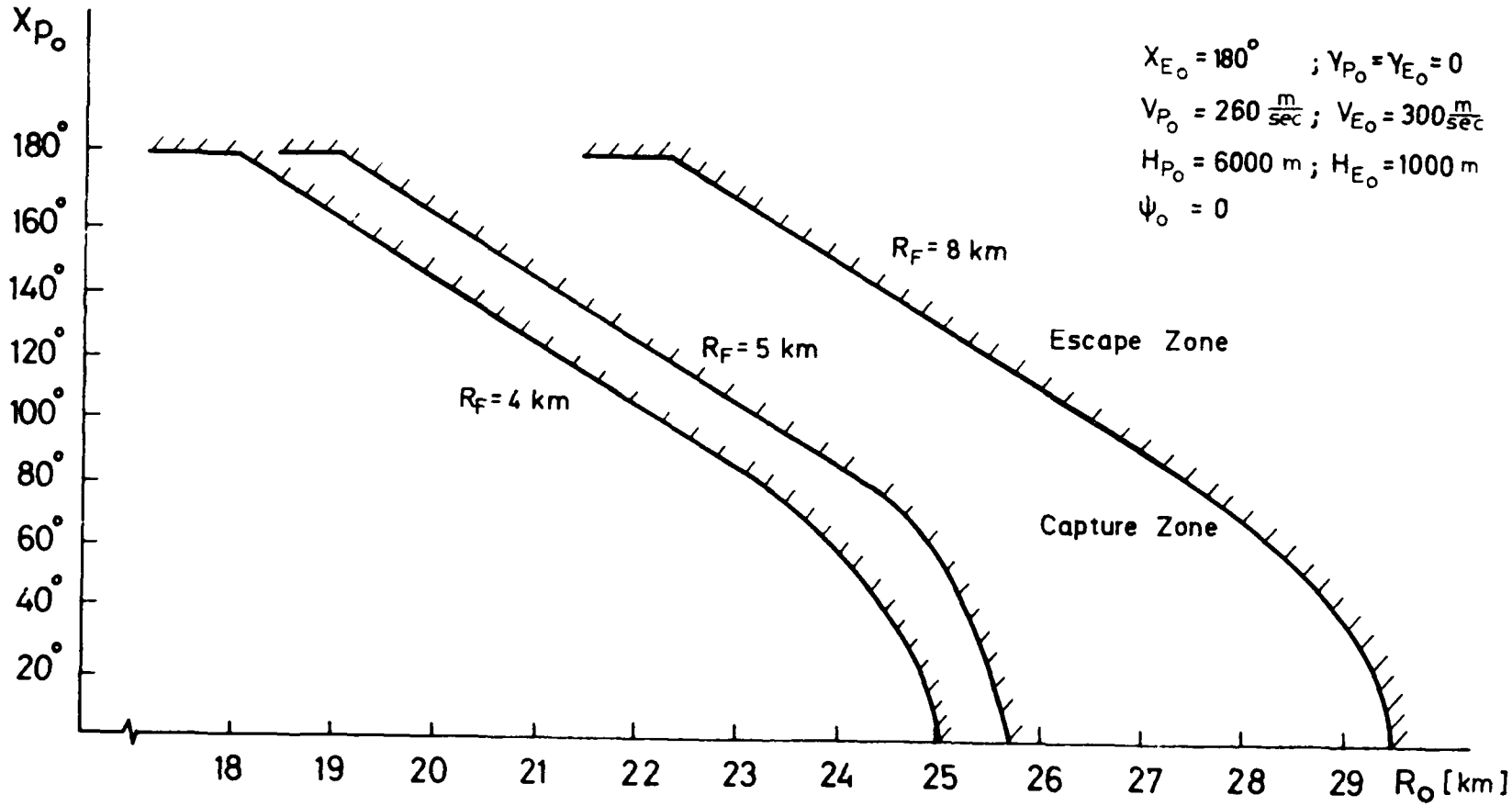

Fig. 7.16: Effect of pursuer's initial range variation on initial heading.

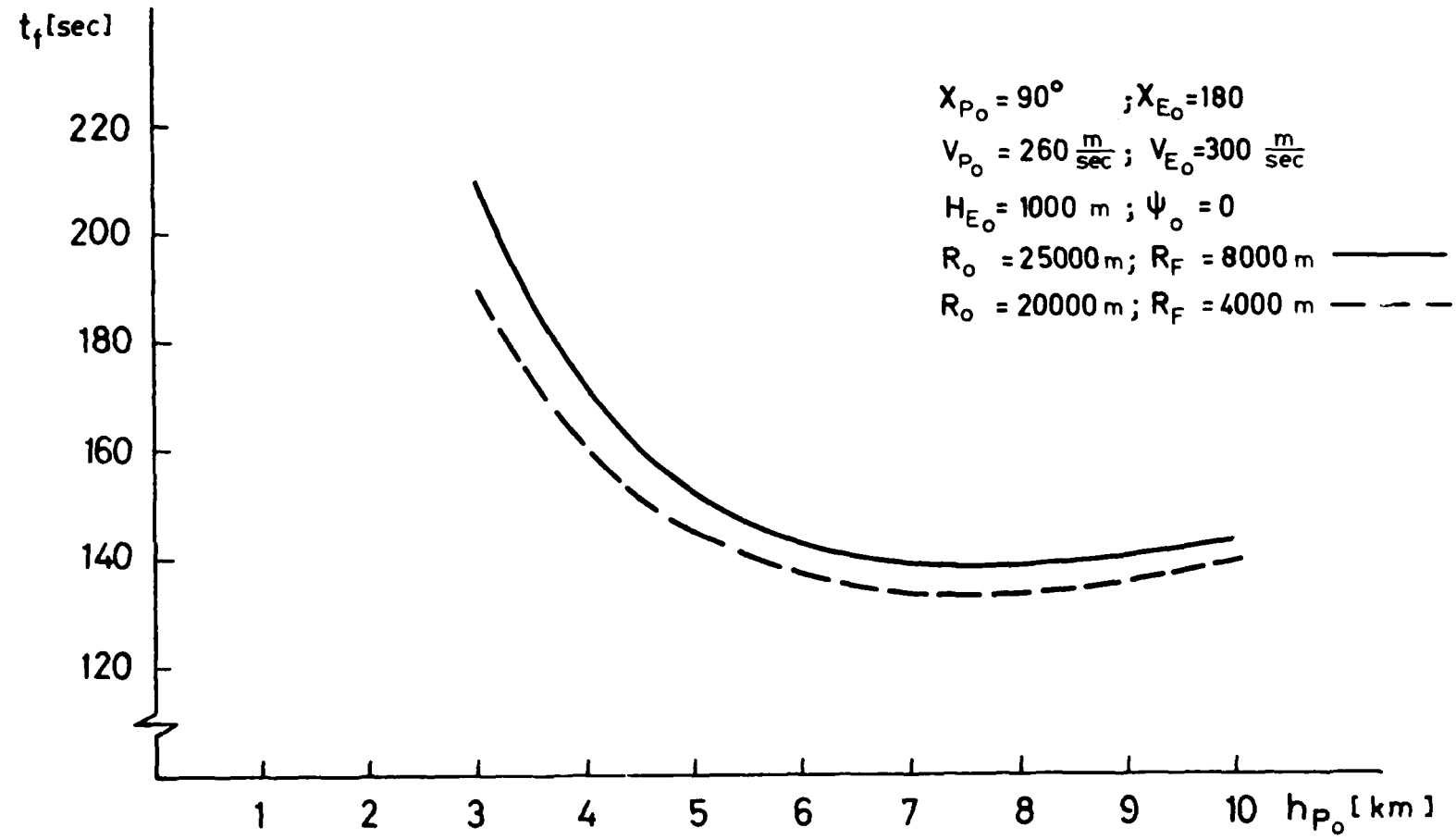

Fig. 7.17: Effect of pursuer's initial altitude variation on capture time.

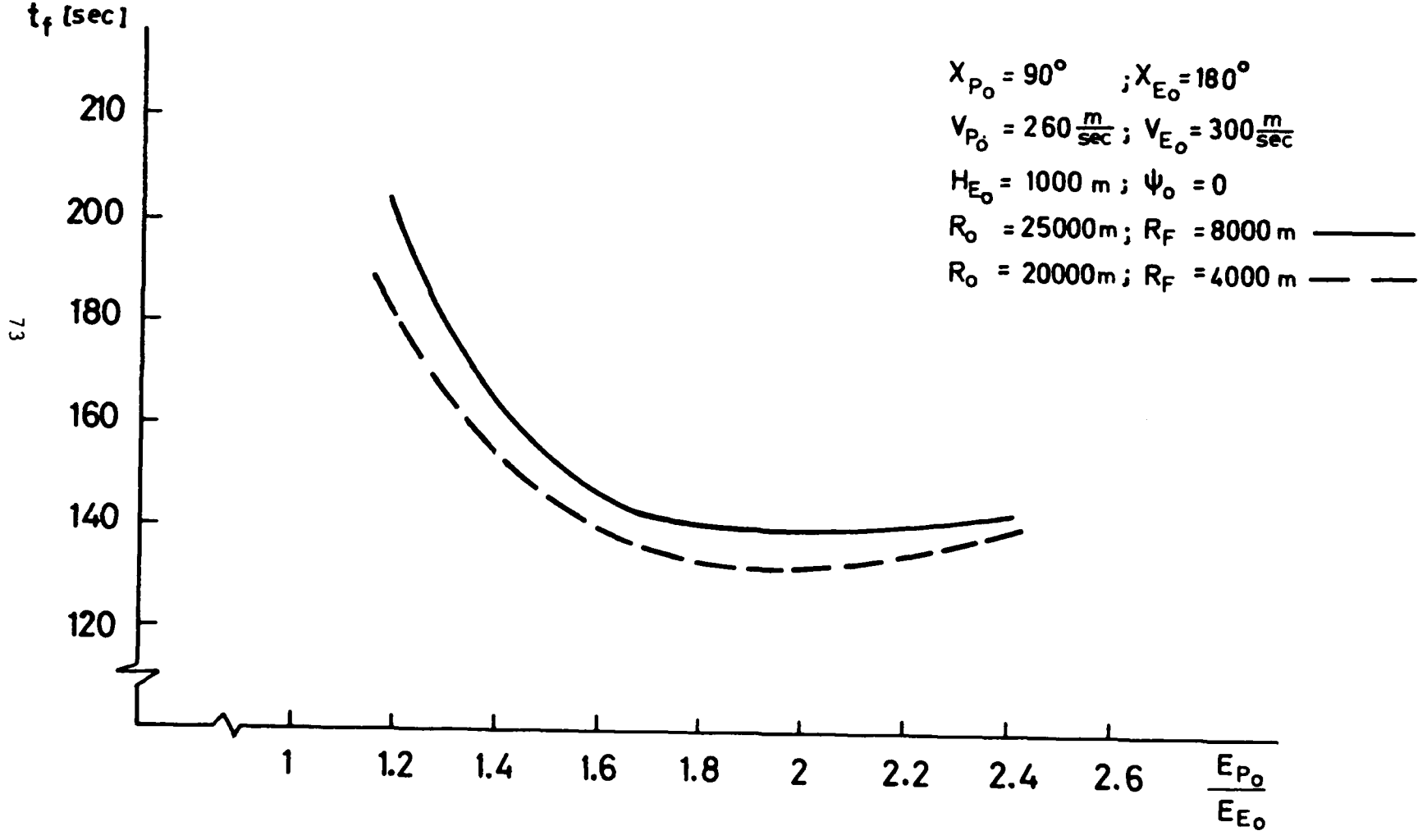

Fig. 7.18: Effect of pursuer's initial specific energy variation on capture time.

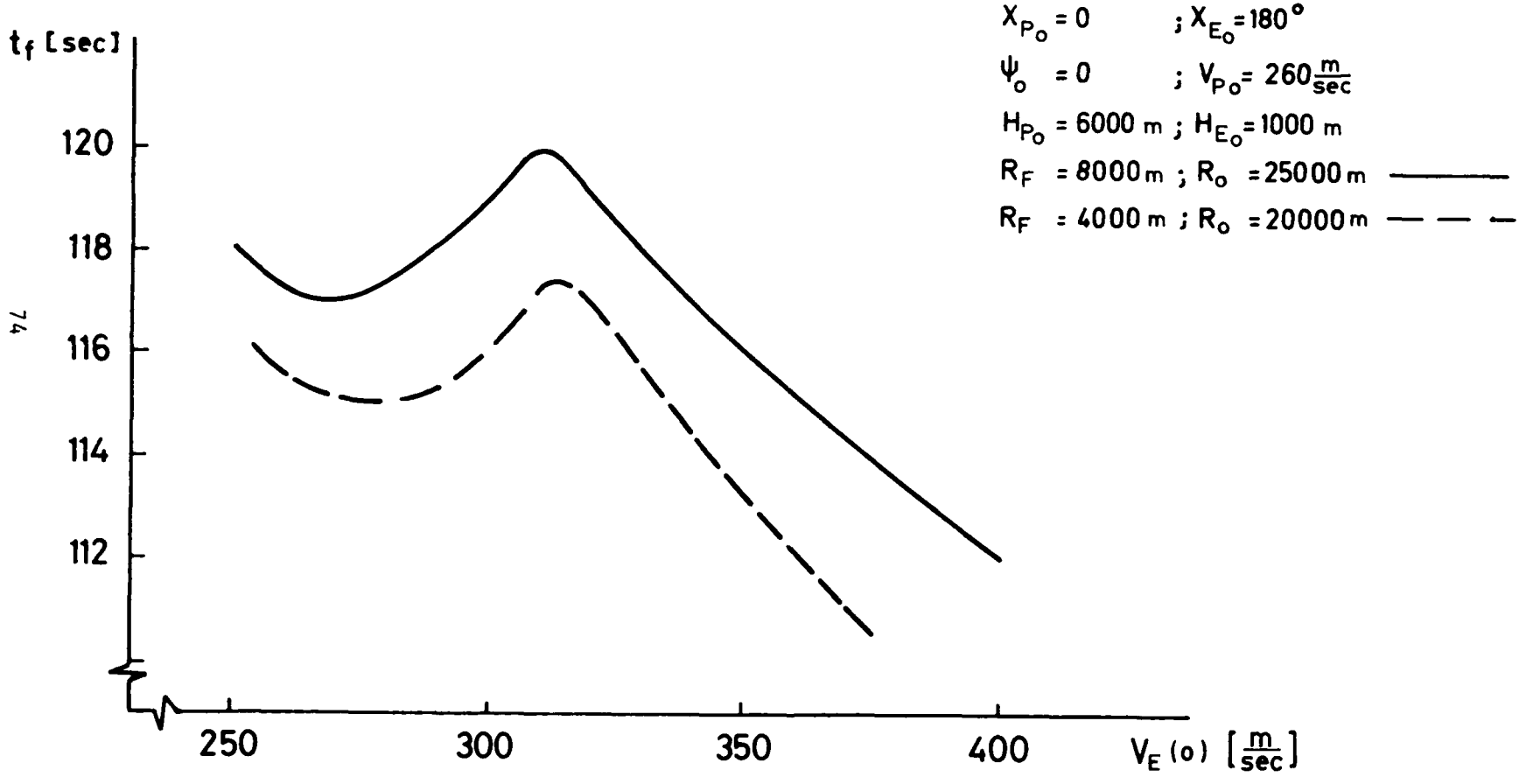

Fig. 7.19: Effect of evader's initial velocity variation on capture time.

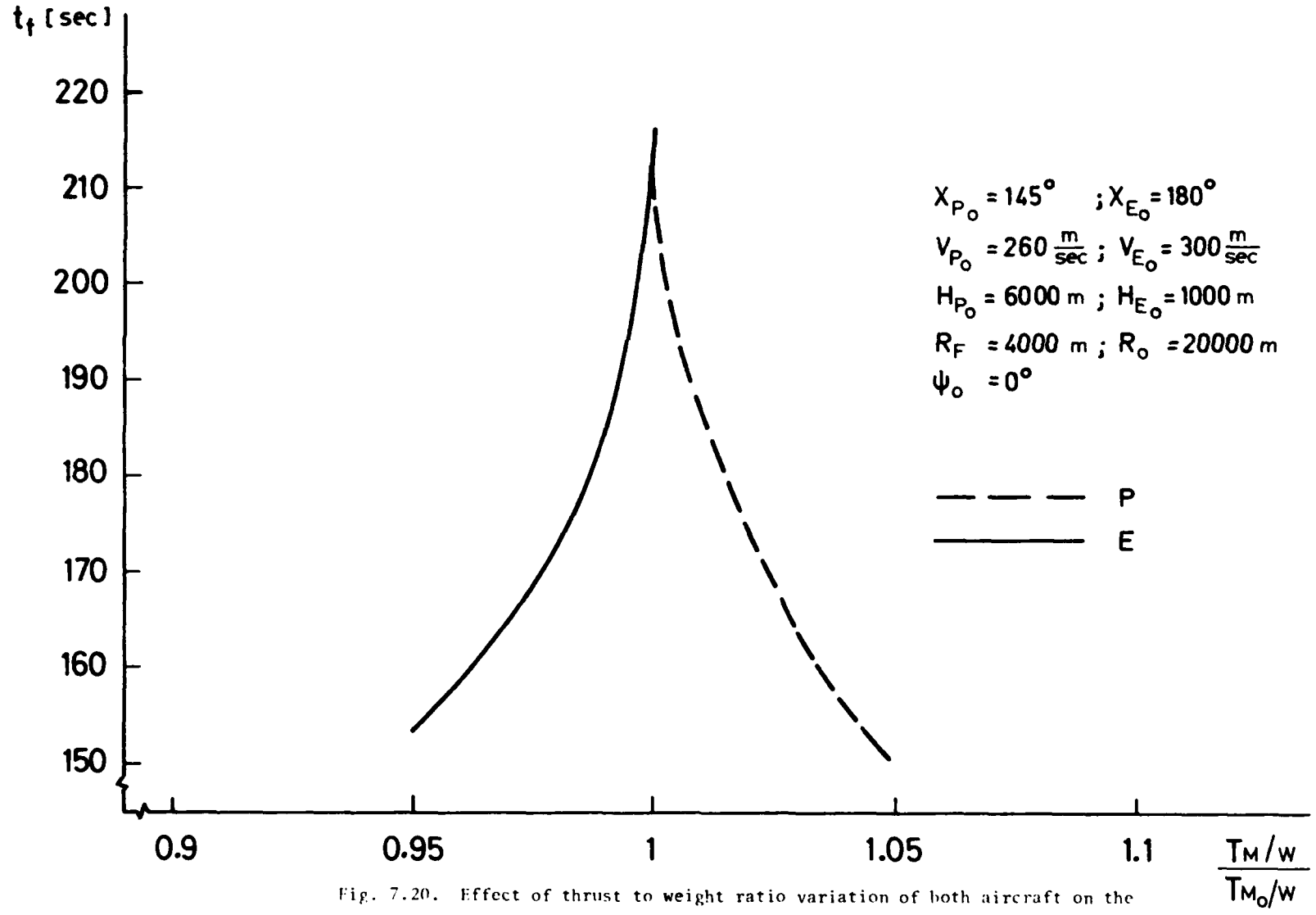

Fig. 7.20. Effect of thrust to weight ratio variation of both aircraft on the capture time.

SECTION VIII

ACCURACY ASSESSMENT OF THE ZERO-ORDER FSPT SOLUTION

An important test for the usefulness of any approximation is its accuracy. Accuracy depends generally on satisfaction of the simplifying assumptions made in order to obtain an analytically treatable problem. The solution of the medium range interception game by the method of forced singular perturbations, presented in previous chapters, seems to demonstrate that the basic hypothesis of time scale separation of variables has been a valid and justified assumption. This time scale separation is however not perfect and as a consequence the accuracy of the zero-order feedback approximation cannot be expected to be absolute.

The accuracy of any approximation has to be established by comparison to the results of the exact solution. Unfortunately, there is no operating numerical algorithm to solve the non-linear two-point boundary layer problem formulated by the necessary conditions of saddle point optimality for a 3-D time optimal variable speed pursuit-evasion game.

In the last decade several computer programs were developed in order to satisfy this obvious need [20-27] but most of them are not operative. The few that are in operating conditions [Jarmark, Enjalbar] are limited to solve fixed time games. Moreover, they exhibit serious difficulties of convergence for relatively long flight times as in the case of a medium range interception.

As a consequence of the state of art of reliable numerical game solutions, this report cannot include a quantitative assessment of accuracy of the zero-order FSPT feedback solution for the 3-D medium range air-to-air interception game. It must be mentioned, however, that the one sided optimal control version of the same 3-D medium range interception engagement (assuming a known

evader control strategy, as for example, straight flight) has been also solved by the similar FSPT approach [18]. This optimal control approximation has been numerically validated by comparing to the results obtained by a very accurate multiple shooting algorithm [19]. For the computations, the aerodynamic and propulsion model of aircraft "B", in this report, was used. The results of this comparison were presented in an invited paper at the JACC 1981 [19] The comparison showed an excellent qualitative similarity in the time history of the main variables and an accuracy of the order of 1% (or better).

Very recently a numerical comparison was carried out at NASA Ames Research Center between the zero-order FSPT approximation and the exact solution for a variable speed horizontal pursuit-evasion game. Results of the comparison are summarized in a forthcoming document [28]. For this comparison the exact solution was obtained by backward (retrograde) integration of the state and adjoint equations expressed in the coordinate frame of the final line of sight. This method was proposed to obtain "open-loop optimal" extremal trajectories in several recent papers [29-31]. The outcome of a systematic comparison for a large set of different initial conditions has demonstrated that for all cases where the geometrical perturbation parameter, defined by the ratio of the evaders' minimum turning radius at the initial flight conditions to the initial range of separation is sufficiently small (less than 0.1) the accuracy of the zero-order FSPT solution is 1% or better.

Although these last results of game comparison were obtained for a two-dimensional case (there is no similar open loop solution for the 3-D game) they are consistent with the results of [19].

It can be therefore asserted that the zero order FSPT approach is a valid method of analysis for the medium range air-to-air interception game (since in

this case the conditions of geometric time scale separation are almost always satisfied) even if presently no direct numerical assessment can be accomplished.

The accuracy of 1% or better, indicated in both related comparisons, seems to be satisfactory for all practical purposes such as a parametric study presented in Ch. 7 or for a real time airborn implementation. The accuracy of regular state variable measurements and estimates of performance parameters does not attain that level any longer. Consequently, the computation of first and higher order terms of the FSPT solution may not be necessary. Nevertheless, since such correction terms may be required for some special cases, the technique of their derivation, which has been a part of the research program, is presented in the next chapter.

SECTION IX

OFF-LINE FIRST-ORDER CORRECTIONS

1. GENERAL DISCUSSION

Comparing the expressions for optimal control strategies of the exact optimal saddle point solution to the expressions of the zero-order multiple time scale FSPT approximation, it can be directly observed that the functional structure (i.e., the dependence on the state and the adjoint variables) is identical. The only difference is that in the FSPT solution some of the adjoint variables are approximated by a simplified state feedback expression, obtained by assuming a time scale separation of the state variables. Improving the zero-order feedback solution means to use a better estimate for the adjoints. Consequently, the control strategy will be also improved.

For computation of the higher order terms the method of matched asymptotic expansion can be used. It has to be however remembered that since we deal with a feedback solution, the state variables are assumed to be accurately measured. Only the adjoint variables and the controls have to be expanded. Such an expansion is different from usual open loop expansions.

As it will be shown in this chapter, the computation of the first order correction terms has to be carried out by integration along the previously obtained zero-order trajectory. It is clearly an "off-line" operation and cannot be considered as a part of a real time implementation. It has however its engineering value if off-line computation is not prohibitive and if additional accuracy is required.

In order to demonstrate the complexity involved in such operation, in the following parts of this chapter the example of horizontal medium range interception (solved to zero-order in [3]) is selected. In the sequel the non-dimensional notation of [3] will be used.

2. LIST OF SYMBOLS FOR THE NON-DIMENSIONAL HORIZONTAL GAME

$\mathcal{H}$ - Hamiltonian

J_r, J_θ, ... - Components of the adjoint vector

N - Mach dependent coefficient

R - Aircraft turning radius

r - Separation distance

$\tilde{r}$ - Normalized separation distance $\left(\tilde{r} \triangleq \frac{r}{R_{P_{min}}}\right)$

t - Time

$\tilde{t}$ - Normalized time $\left(\tilde{t} \triangleq \frac{V_{C_P}}{R_{P_{min}}}\right)$

V - Aircraft true airspeed

v - Normalized velocity $\left(v \triangleq \frac{V}{V_C}\right)$

Γ - Ratio of minimum turning radii $\left(\Gamma \triangleq \frac{R_{P_{min}}}{R_{E_{min}}}\right)$

ϵ - Small parameter

η - Normalized turning rate $\left(\eta \triangleq \frac{\dot{\varphi}}{\dot{\varphi}_C}\right)$

θ - Line of sight angle

Λ - Normalized acceleration $(\Lambda \triangleq \phi - N\eta^2)$

σ - Stretched time in the inner boundary layer $(\sigma \triangleq \tilde{t}/\epsilon^2)$

τ - Stretched time in the outer boundary layer $(\tau \triangleq \tilde{t}/\epsilon)$

ϕ - Aircraft straight line normalized acceleration

φ - Velocity vector angle

Ω - Ratio of corner velocities $\left(\Omega \triangleq \frac{V_{P_{min}}}{V_{E_{min}}}\right)$

SUBSCRIPTS

C - Corner conditions

E - Evader

P - Pursuer

h - Horizontal plane value

0 - Zero-order value

1 - First-order value

b - Value at termination of the boundary layer

SUPERSCRIPTS

o - Reduced game

i - Outer boundary layer

j - Inner boundary layer

c - Composite variable

3. FIRST ORDER EQUATIONS

$$\frac{d\tilde{r}}{d\tilde{t}} = -v_P \cos(\varphi_P - \theta_h) + \Omega v_E \sin(\varphi_E - \theta_h) \tag{9.1}$$

$$\frac{d\theta_h}{d\tilde{t}} = \frac{1}{r}\left[-v_P \sin(\varphi_P - \theta_h) + \Omega v_E \sin(\varphi_E - \theta_h)\right] \tag{9.2}$$

$$\varepsilon \frac{dv_P}{d\tilde{t}} = \phi_P - N_P\left(\eta_{P_0} + \varepsilon\eta_{P_1}\right)^2 \tag{9.3}$$

$$\varepsilon \frac{dv_E}{d\tilde{t}} = \Gamma\Omega\left[\phi_E - N_E\left(\eta_{E_0} + \varepsilon\eta_{E_1}\right)^2\right] \tag{9.4}$$

$$\varepsilon^2 \frac{d\varphi_P}{d\tilde{t}} = \eta_{P_0} + \varepsilon\eta_{P_1} \tag{9.5}$$

$$\varepsilon^2 \frac{d\varphi_E}{d\tilde{t}} = \Gamma\Omega\left[\eta_{E_0} + \varepsilon\eta_{E_1}\right] \tag{9.6}$$

The Hamiltonian is:

$$\begin{aligned}\mathcal{H} = 1 &+ \left(J_{r_0} + \varepsilon J_{r_1}\right)\frac{d\tilde{r}}{d\tilde{t}} + \left(J_{\theta_0} + \varepsilon J_{\theta_1}\right)\frac{d\theta_n}{d\tilde{t}} + \\ &+ \left(J_{v_{P_0}} + \varepsilon J_{v_{P_1}}\right)\frac{dv_P}{d\tilde{t}} + \left(J_{v_{E_0}} + \varepsilon J_{v_{E_1}}\right)\frac{dv_E}{d\tilde{t}} + \\ &+ \left(J_{\varphi_{P_0}} + \varepsilon J_{\varphi_{P_1}}\right)\left(\eta_{P_0} + \varepsilon\eta_{P_1}\right) + \left(J_{\varphi_{E_0}} + \varepsilon J_{\varphi_{E_1}}\right)\Gamma\Omega\left(\eta_{E_0} + \varepsilon\eta_{E_1}\right)\end{aligned} \tag{9.7}$$

Since time does not appear explicitly in the equations of motion:

$$\mathcal{H} = \mathcal{H}_0 + \varepsilon\mathcal{H}_1 = 0 \tag{9.8}$$

where:

$$\mathcal{H}_0 = 1 + J_{r_0}\frac{dr}{d\tilde{t}} + J_{\theta_0}\frac{d\theta}{d\tilde{t}} + J_{v_{P_0}}\left(\frac{dv_P}{d\tilde{t}}\right)_0 + \tag{9.9}$$

$$+ J_{v_{E_0}}\left(\frac{dv_E}{d\tilde{t}}\right)_0 + J_{\varphi_{P_0}}\eta_{P_0} + J_{\varphi_{E_0}}\Gamma\Omega\,\eta_{E_0} = 0$$

$\left(\frac{dv_E}{d\tilde{t}}\right)_0$, $\left(\frac{dv_P}{d\tilde{t}}\right)_0$ — zero-order terms of the aircraft accelerations

$$\left(\frac{dv_P}{d\tilde{t}}\right) = \left(\frac{dv_P}{d\tilde{t}}\right)_0 + \varepsilon\left(\frac{dv_P}{d\tilde{t}}\right)_1 \tag{9.10}$$

$$\left(\frac{dv_E}{d\tilde{t}}\right) = \left(\frac{dv_E}{d\tilde{t}}\right)_0 + \varepsilon\left(\frac{dv_E}{d\tilde{t}}\right)_1 \tag{9.11}$$

$$\mathcal{H}_1 = J_{r_1}\left(\frac{dr}{d\tilde{t}}\right) + J_{\theta_1}\left(\frac{d\theta}{d\tilde{t}}\right) + J_{v_{P_0}}\left(\frac{dv_P}{d\tilde{t}}\right)_1 +$$

$$+ J_{v_{P_1}}\left(\frac{dv_P}{d\tilde{t}}\right)_0 + \Gamma\Omega\left[J_{v_{E_0}}\left(\frac{dv_E}{d\tilde{t}}\right)_1 + J_{v_{E_1}}\left(\frac{dv_E}{d\tilde{t}}\right)_0\right] +$$

$$+ J_{\varphi_{P_0}}\eta_{P_1} + J_{\varphi_{P_1}}\eta_{P_0} + \Gamma\Omega\left[J_{\varphi_{E_0}}\eta_{E_1} + J_{\varphi_{E_1}}\eta_{E_0}\right] = 0 \tag{9.12}$$

The adjoint equations are:

$$\frac{dJ_{r_0}}{d\tilde{t}} + \varepsilon\frac{dJ_{r_1}}{d\tilde{t}} = \left(J_{\theta_0} + \varepsilon J_{\theta_1}\right)\frac{1}{r^2}\left[-v_P\sin(\varphi_P - \theta_h) + \Omega v_E\sin(\varphi_E - \theta_h)\right] \tag{9.13}$$

$$\frac{dJ_{\theta_0}}{d\tilde{t}} + \varepsilon\frac{dJ_{\theta_1}}{d\tilde{t}} = \left(J_{r_0} + \varepsilon J_{r_1}\right)\left[v_P\sin(\varphi_P - \theta_h) - \Omega v_E\sin(\varphi_E - \theta_h)\right] +$$

$$+ \left(J_{\theta_0} + \varepsilon J_{\theta_1}\right)\frac{1}{\tilde{r}}\left[-v_P\cos(\varphi_P - \theta_h) + \Omega v_E\cos(\varphi_E - \theta_h)\right] \tag{9.14}$$

$$\varepsilon\left[\frac{dJ_{v_{P_0}}}{d\tilde{t}} + \varepsilon\frac{dJ_{v_{P_1}}}{d\tilde{t}}\right] = \left(J_{r_0} + \varepsilon J_{r_1}\right)\cos(\varphi_p - \theta_h) +$$

$$+ \left(J_{\theta_0} + \varepsilon J_{\theta_1}\right)\frac{1}{\tilde{r}}\sin(\varphi_p - \theta_h) - \left(J_{v_{P_0}} + \varepsilon J_{v_{P_1}}\right)\frac{\partial\Lambda_p}{\partial v_p} \qquad (9.15)$$

$$\varepsilon\left[\frac{dJ_{v_{E_0}}}{d\tilde{t}} + \varepsilon\frac{dJ_{v_{E_1}}}{d\tilde{t}}\right] = -\Omega\left[\left(J_{r_0} + \varepsilon J_{r_1}\right)\cos(\varphi_E - \theta_h) +\right.$$

$$\left. + \left(J_{\theta_0} + \varepsilon J_{\theta_1}\right)\frac{1}{\tilde{r}}\sin(\varphi_E - \theta_h) - \left(J_{v_{E_0}} + \varepsilon J_{v_{E_1}}\right)\Gamma\Omega\frac{\partial\Lambda_E}{\partial v_E}\right] \qquad (9.16)$$

$$\varepsilon^2\left[\frac{dJ_{\varphi_{P_0}}}{d\tilde{t}} + \varepsilon\frac{dJ_{\varphi_{P_1}}}{d\tilde{t}}\right] = v_p\left[-\left(J_{r_0} + \varepsilon J_{r_1}\right)\sin(\varphi_p - \theta_h) +\right.$$

$$\left. + \left(J_{\theta_0} + \varepsilon J_{\theta_1}\right)\frac{1}{\tilde{r}}\cos(\varphi_p - \theta_h)\right] \qquad (9.17)$$

$$\varepsilon^2\left[\frac{dJ_{\varphi_{E_0}}}{d\tilde{t}} + \varepsilon\frac{dJ_{\varphi_{E_1}}}{d\tilde{t}}\right] = \Omega v_E\left[\left(J_{r_0} + \varepsilon J_{r_1}\right)\sin(\varphi_E - \theta_h) -\right.$$

$$\left. - \left(J_{\theta_0} + \varepsilon J_{\theta_1}\right)\frac{1}{\tilde{r}}\cos(\varphi_E - \theta_h)\right] \qquad (9.18)$$

4. THE REDUCED GAME

During the reduced order game:

$$\left(\frac{d\theta}{d\tilde{t}}\right)^o = \left(\frac{dv_P}{d\tilde{t}}\right)^o = \left(\frac{dv_E}{d\tilde{t}}\right)^o = \left(\frac{d\varphi_P}{d\tilde{t}}\right)^o = \left(\frac{d\varphi_E}{d\tilde{t}}\right)^o = 0 \qquad (9.19)$$

AD-A121 379 IMPROVED DYNAMIC MODELS FOR AIR COMBAT ANALYSIS(U) 2/2
TECHNION - ISRAEL INST OF TECH HAIFA DEPT OF
AERONAUTICAL ENGINEERING N FARBER ET AL. JUL 82
UNCLASSIFIED AFWAL-TR-82-3057 F33615-81-K-3007 F/G 15/7 NL

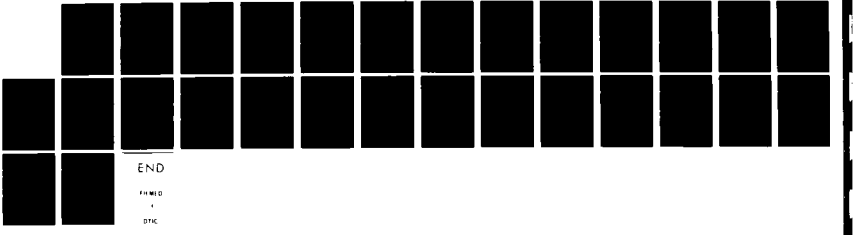

END

FILMED
4
DTIC

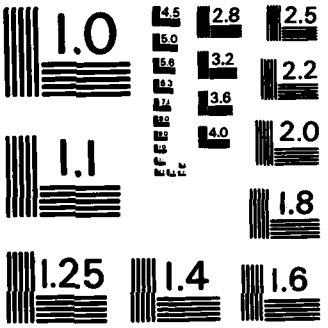

MICROCOPY RESOLUTION TEST CHART
NATIONAL BUREAU OF STANDARDS-1963-A

From (9.6), (9.5)

$$\eta_P^o = \eta_E^o = 0 \tag{9.20}$$

Substituting (9.20), (9.19) into (9.12)

$$\mathcal{H}_1^o = J_{r_1}^o \left(\frac{d\tilde{r}}{d\tilde{t}}\right)^o \tag{9.21}$$

However, since $\left(\frac{d\tilde{r}}{d\tilde{t}}\right)^o \neq 0$

$$J_{r_1}^o = 0 \tag{9.22}$$

Optimality condition of the reduced game (Eq. (69) of [3]) is:

$$J_r^o v_p \sin(\varphi_p - \theta_h) - J_\theta^o \frac{v_p}{\tilde{r}} \cos(\varphi_p - \theta_h) = 0 \tag{9.23}$$

During the reduced game:

$$J_\theta^o = J_{\theta_0}^o + \varepsilon J_{\theta_1}^o = 0 \tag{9.24}$$

Therefore:

$$J_{\theta_0}^o = J_{\theta_1}^o = 0 \tag{9.25}$$

Finally, from (9.9), (9.19), we obtain:

$$J_{r_0}^o = \frac{1}{v_P^o - \Omega v_E^o} \tag{9.26}$$

5. THE OUTER BOUNDARY LAYER

Using the stretching transformation $\tau = t/\varepsilon$, the following adjoint equations are obtained:

$$\frac{dJ^i_{r_0}}{d\tau} + \varepsilon \frac{dJ^i_{r_1}}{d\tau} = \varepsilon \left(J^i_{\theta_0} + \varepsilon J^i_{\theta_1}\right) \frac{1}{r^2} \left[-v_p \sin(\varphi_p - \theta_h) + \Omega v \sin(\varphi_E - \theta_h)\right] \tag{9.27}$$

$$\frac{dJ^i_{\theta_0}}{d\tau} + \varepsilon \frac{dJ^i_{\theta_1}}{d\tau} = \varepsilon \left(J^i_{r_0} + \varepsilon J^i_{r_1}\right) \left[v_p \sin(\varphi_p - \theta_h) - \right.$$

$$\left. -\Omega v_E \sin(\varphi_E - \theta_h)\right] + \varepsilon \left(J^i_{\theta_0} + J^i_{\theta_1}\right) \frac{1}{\tilde{r}} \left[-v_p \cos(\varphi_p - \theta_h) + \right.$$

$$\left. + \Omega v_E \cos(\varphi_E - \theta_h)\right] \tag{9.28}$$

$$\frac{dJ^i_{v_{P_0}}}{d\tau} + \varepsilon \frac{dJ^i_{v_{P_1}}}{d\tau} = \left(J^i_{r_0} + \varepsilon J^i_{r_1}\right) \cos(\varphi_p - \theta_h) +$$

$$+ \left(J^i_{\theta_0} + \varepsilon J^i_{\theta_1}\right) \frac{1}{\tilde{r}} \sin(\varphi_p - \theta_h) - \left(J^i_{v_{P_0}} + \varepsilon J^i_{v_{P_1}}\right) \frac{\partial \Lambda_p}{\partial v_p} \tag{9.29}$$

$$\frac{dJ^i_{v_{E_0}}}{d\tau} + \varepsilon \frac{dJ^i_{v_{E_1}}}{d\tau} = -\Omega \left[\left(J^i_{r_0} + \varepsilon J^i_{r_1}\right) \cos(\varphi_E - \theta_h) + \right.$$

$$\left. + \left(J^i_{\theta_0} + \varepsilon J^i_{\theta_1}\right) \frac{1}{\tilde{r}} \sin(\varphi_E - \theta_h)\right] - \left(J^i_{v_{E_0}} + \varepsilon J^i_{v_{E_1}}\right) \Gamma\Omega \frac{\partial \Lambda_E}{\partial v_E} \tag{9.30}$$

$$\varepsilon \left[\frac{dJ^i_{\varphi_{P_0}}}{d\tau} + \varepsilon \frac{dJ^i_{\varphi_{P_1}}}{d\tau}\right] = v_p \left[-\left(J^i_{r_0} + \varepsilon J^i_{r_1}\right) \sin(\varphi_p - \theta_h) + \right.$$

$$\left. + \left(J^i_{\theta_0} + \varepsilon J^i_{\theta_1}\right) \frac{1}{\tilde{r}} \cos(\varphi_p - \theta_h)\right] \tag{9.31}$$

$$\varepsilon \left[\frac{dJ_{\varphi_{E_0}}}{d\tau} + \varepsilon \frac{dJ_{\varphi_{p_1}}}{d\tau} \right] = \Omega v_E \left(\left[J^i_{r_0} + \varepsilon J^i_{r_1} \right) \sin(\varphi_E - \theta_h) - \right.$$

$$\left. - \left(J^i_{\theta_0} + \varepsilon J^i_{\theta_1} \right) \frac{1}{\tilde{r}} \cos(\varphi_E - \theta_h) \right] \tag{9.32}$$

From the zero-order terms of (9.27) we have:

$$\frac{dJ^i_{r_0}}{d\tau} = 0 \sim J^i_{r_0} = \text{const.} \tag{9.33}$$

$$\frac{dJ^i_{r_1}}{d\tau} = J^i_{\theta_0} \frac{1}{\tilde{r}^2} \left[-v_p \sin(\varphi_p - \theta_h) + \Omega v_E \sin(\varphi_E - \theta_h) \right] \tag{9.34}$$

and from the zero-order terms of (9.28):

$$\frac{dJ^i_{\theta_0}}{d\tau} = 0 \sim J_{\theta_0} = \text{const.} \tag{9.35}$$

$$\frac{dJ^i_{\theta_1}}{d\tau} = J^i_{r_0} \left[-v_p \sin(\varphi_p - \theta_h) + \Omega v_E \sin(\varphi_E - \theta_h) \right] +$$

$$+ J^i_{\theta_0} \frac{1}{\tilde{r}} \left[-v_p \cos(\varphi_p - \theta_h) + \Omega v_E \cos(\varphi_E - \theta_h) \right] \tag{9.36}$$

Using (9.33) and the matching condition:

$$\lim_{\tau \to \tau_b} J^i_{r_0} = J^o_{r_0} \Big|_{\tilde{t}=0} = \frac{1}{v^o_p - \Omega v^o_E} \tag{9.37}$$

From (9.35) and the matching condition:

$$J^i_{\theta_0} = J^o_{\theta_0} = 0 \tag{9.38}$$

From (9.34) and (9.38):

$$\frac{dJ^i_{r_1}}{d\tau} = 0 \sim J^i_{r_1} = \text{const.} \tag{9.39}$$

Use of the matching conditions leads to:

$$J^i_{r_1} = J^o_{r_1} = 0 \tag{9.40}$$

Finally, from (9.36), (9.37), and (9.38):

$$\frac{dJ^i_{\theta_1}}{d\tau} = \frac{1}{v^o_P - \Omega v^o_E}\left[v_P \sin(\varphi_P - \theta_h) - \Omega v_E \sin(\varphi_E - \theta_h)\right] \tag{9.41}$$

Integrating (9.41):

$$J^i_{\theta_1} = \frac{1}{v^o_P - \Omega v^o_E} \int_0^{\tau} \left[v_P \sin(\varphi_P - \theta_h) - \Omega v_E \sin(\varphi_E - \theta_h)\right] d\tau + C \tag{9.42}$$

The constant of integration (C) is found by use of the matching condition:

$$\lim_{\tau \to \tau_b} J^i_{\theta_1} = J^o_{\theta_1}\Big|_{\tilde{t}=0} = 0 \tag{9.43}$$

or:

$$C = \frac{1}{v^o_P - \Omega v^o_E} \int_0^{\tau_b} \left[v_P \sin(\varphi_P - \theta_h) - \Omega v_E \sin(\varphi_E - \theta_h)\right] d\tau \tag{9.44}$$

The final expression for $J^i_{\theta_1}$ is:

$$J^i_{\theta_1} = \frac{1}{v^o_P - \Omega v^o_E} \int_{\tau}^{\tau_b} \left[-v_P \sin(\varphi_P - \theta_h) + \Omega v_E \sin(\varphi_E - \theta_h)\right] d\tau \tag{9.45}$$

This integral can be computed only if the zero-order trajectory (i.e., $v_p(\tau)$, $\varphi_p(\tau)$, $\theta_h(\tau)$, $v_e(\tau)$, $\varphi_E(\tau)$) are known.

At this point it is necessary to show that in this boundary layer:

$$\Lambda_p = \phi_p + O(\varepsilon^2) \tag{9.46}$$

From (9.5):

$$\varepsilon \frac{d\varphi_p^i}{d\tau} = \eta_{p_0}^i + \varepsilon\eta_{p_1}^i \tag{9.47}$$

It is clear that:

$$\eta_{p_0}^i = 0 \tag{9.48}$$

Substituting (9.46) into:

$$\Lambda_p = \phi_p - N_p \left(\eta_{p_0}^i + \varepsilon\eta_{p_1}^i\right)^2 \tag{9.49}$$

we get

$$\frac{\partial \Lambda_p}{\partial v_p} = \frac{\partial \phi_p}{\partial v_p} \tag{9.50}$$

First-order terms of (9.29) are:

$$\frac{dJ_{v_{p_1}}^i}{d\tau} = J_{\theta_1}^i \frac{1}{\tilde{r}} \sin(\varphi_p - \theta_h) - J_{v_{p_1}}^i \left(\frac{\partial \phi_p}{\partial v_p}\right) \tag{9.51}$$

(9.51) can be integrated, now, starting from the terminal surface and using the boundary condition:

$$\left[J_{v_{p_1}}^i + J_{v_{p_0}}^o\right]^{TS} = 0 \tag{9.52}$$

This integration can be done only if the zero-order trajectory is known.

6. THE INNER BOUNDARY LAYER

Using the stretching transformation $\sigma = t/\varepsilon^2$, the following adjoint equations are obtained:

$$\frac{dJ^j_{r_0}}{d\sigma} + \varepsilon \frac{dJ^j_{r_1}}{d\sigma} = \varepsilon^2 \left(J^j_{\theta_0} + \varepsilon J^j_{\theta_1}\right) \frac{1}{\tilde{r}} \left(\frac{d\theta}{d\tilde{t}}\right) \tag{9.53}$$

$$\frac{dJ^j_{\theta_0}}{d\sigma} + \varepsilon \frac{dJ^j_{\theta_1}}{d\sigma} = -\varepsilon^2 \left(J^j_{r_0} + \varepsilon J^j_{r_1}\right) \tilde{r} \left(\frac{d\theta}{d\tilde{t}}\right) + \varepsilon^2 \left(J^j_{\theta_0} + \varepsilon J^j_{\theta_1}\right) \frac{1}{r} \left(\frac{dr}{d\tilde{t}}\right) \tag{9.54}$$

From (9.53), (9.54), the following system of equations is obtained:

$$\frac{dJ^j_{r_0}}{d\sigma} = 0 \sim J^j_{r_0} = J^i_{r_0}\Big|_{\tau=0} = J^o_{r_0} \tag{9.55}$$

$$\frac{dJ^j_{r_1}}{d\sigma} = 0 \sim J^j_{r_1} = J^i_{r_1} = 0 \tag{9.56}$$

$$\frac{dJ^j_{\theta_0}}{d\sigma} = 0 \sim J^j_{\theta_0} = J^i_{\theta_0} = 0 \tag{9.57}$$

$$\frac{dJ^j_{\theta_1}}{d\sigma} = 0 \sim J^j_{\theta_1} = J^i_{\theta_1}\Big|_{\tau=0} = J^o_{r_0} \int_0^{\tau_b} \left[-v_p \sin(\varphi_p - \theta_h) + \Omega v_E \sin(\varphi_E - \theta_h)\right] d\tau \tag{9.58}$$

$J^j_{v_p}$ adjoint equation is:

$$\frac{dJ^j_{v_{p_0}}}{d\sigma} + \varepsilon \frac{dJ^j_{v_{p_1}}}{d\sigma} = \varepsilon \left(J^j_{r_0} + \varepsilon J^j_{r_1}\right) \cos(\varphi_p - \theta_h) +$$

$$+ \varepsilon \left(J^j_{\theta_0} + \varepsilon J^j_{\theta_1}\right) \frac{1}{\tilde{r}} \sin(\varphi_p - \theta_h) - \varepsilon \left(J^j_{v_{p_0}} + \varepsilon J^j_{v_{p_1}}\right) \frac{\partial \Lambda_p}{\partial v_p} \tag{9.59}$$

The first order equation (using (9.55) and (9.57)) is:

$$\frac{dJ^j_{v_{P_1}}}{d\sigma} = J^o_{r_0} \cos(\varphi_p - \theta_h) - J_{v_{P_0}} \left(\frac{\partial \Lambda_P}{\partial v_P}\right)_0 \tag{9.60}$$

$$\Lambda_P = \phi_P - N_P \left(\eta^{j\,2}_{P_0} + 2\varepsilon \eta^j_{P_0} \eta^j_{P_1} + \varepsilon^2 \eta^{j\,2}_{P_1}\right) \tag{9.61}$$

when G = const.

$$\left(\frac{\partial \Lambda_P}{\partial v_P}\right)_0 = \left(\frac{\partial \phi_P}{\partial v_P}\right) \tag{9.62}$$

Integrating (9.60) along the zero-order trajectory:

$$J^j_{v_{P_1}} = \int_0^\sigma J^o_{r_0} \cos(\varphi_p - \theta_h)\, d\sigma - \int_0^\sigma J^o_{v_{P_0}} \left(\frac{\partial \phi_P}{\partial v_P}\right) d\sigma \tag{9.63}$$

Boundary condition:

$$J^j_{v_{P_1}}\Big|_{\sigma=\sigma_b} = J^i_{v_{P_1}}\Big|_{\tau=0} \tag{9.64}$$

$$J^i_{v_{P_1}}\Big|_{\tau=0} = \int_0^{\sigma_b} J^o_{r_0} \cos(\varphi_p - \theta_h)\, d\sigma - \int_0^{\sigma_b} J^o_{v_{P_0}} \left(\frac{\partial \phi_P}{\partial v_P}\right) d\sigma \tag{9.65}$$

$$J^j_{v_{P_1}} = J^i_{v_{P_1}}\Big|_{\tau=0} - \int_\sigma^{\sigma_b} J^o_{r_0} \cos(\varphi_p - \theta_h) d\sigma + \int_\sigma^{\sigma_b} J^o_{v_{P_0}} \left(\frac{\partial \phi_P}{\partial v_P}\right) d\sigma \tag{9.66}$$

$$J^c_{v_{P_1}} = J^j_{v_{P_1}} + J^i_{v_{P_1}} - J^i_{v_{P_1}}\Big|_{\tau=0} \tag{9.67}$$

The inner boundary layer Hamiltonian:

$$\mathcal{H}^j = 1 + J^j_r \dot{r} + J^j_\theta \dot{\theta} + J^j_{v_p} \Lambda^j_P + J^j_{\varphi_p} \eta^j_P + J^j_{v_E} \Gamma\Omega\Lambda^j_E + J^j_{\varphi_E} \Gamma\Omega\eta^j_E = 0 \tag{9.68}$$

$$\mathcal{H}_1^j = J_\theta^j \dot{\theta} + \left(J_{v_P}^j \Lambda_P^j\right)_1 + J_{\varphi_{P_0}}^j \eta_{P_1}^j + J_{\varphi_{P_1}}^j \eta_{P_0}^j + \Gamma\Omega \left(J_{v_E}^j \Lambda_P^j\right)_1 +$$

$$+ \Gamma\Omega \left(J_{\varphi_{E_0}}^j \eta_{E_1}^j + J_{\varphi_{E_1}}^j \eta_{E_0}^j\right) = 0 \tag{9.69}$$

Let us calculate the first order terms of the following expression:

$$J_{v_P}^j \Lambda_P^j = \left(J_{v_P}^j \Lambda_P^j\right)_0 + \varepsilon \left(J_{v_P}^j \Lambda_P^j\right)_1 =$$

$$= \left(J_{v_{P_0}}^j + \varepsilon J_{v_{P_1}}^j\right) \left[\phi_P - N_P \left(\eta_{P_0}^j + \varepsilon \eta_{P_1}^j\right)^2\right] =$$

$$= J_{v_{P_0}}^j \left(\phi_P - N_P \eta_{P_0}^{j\,2}\right) + \varepsilon \left\{J_{v_{P_1}}^j \left(\phi_P - N_P \eta_{P_0}^{j\,2}\right) - 2N_P J_{v_{P_0}}^j \eta_{P_0}^j \eta_{P_1}^j\right\} +$$

$$+ O(\varepsilon^2) \tag{9.70}$$

i.e.,

$$\left(J_{v_P}^j \Lambda_P^j\right)_1 = J_{v_{P_1}}^j \left(\phi_P - N_P \eta_{P_0}^{j\,2}\right) - 2N_P J_{v_{P_0}}^j \eta_{P_0}^j \eta_{P_1}^j \tag{9.71}$$

The optimality condition is:

$$2N_P \left(J_{v_{P_0}}^j + \varepsilon J_{v_{P_1}}^j\right)\left(\eta_{P_0}^j + \varepsilon \eta_{P_1}^j\right) = J_{\varphi_{P_0}}^j + \varepsilon J_{\varphi_{P_1}}^j \tag{9.72}$$

The first order terms satisfy:

$$2N_P \left(J_{v_{P_0}}^j \eta_{P_1}^j + J_{v_{P_1}}^j \eta_{P_0}^j\right) = J_{\varphi_{P_1}}^j \tag{9.73}$$

Multiplying both sides by $-\eta_{P_0}^j$ we obtain:

$$-2N_P J_{v_{P_0}}^j \eta_{P_1}^j \eta_{P_0}^j = -J_{\varphi_{P_1}}^j \eta_{P_0}^j + 2N_P J_{v_{P_1}}^j \eta_{P_0}^{j\,2} \tag{9.74}$$

Substituting (9.73) into (9.71)

$$\left(J^j_{v_p} \Lambda^j_P\right)_1 = J^j_{v_{P_1}} \left(\phi_P - N_P \eta^{j\,2}_{P_0}\right) - J^j_{\varphi_{P_1}} \eta^j_{P_0} +$$

$$+ 2N_P\, J^j_{v_{P_1}} \eta^{j\,2}_{P_0} = J_{v_{P_1}} \left(\phi_P + N_P \eta^{j\,2}_{P_0}\right) - J^j_{\varphi_{P_1}} \eta^j_{P_0} \qquad (9.75)$$

Substituting (9.75) into (9.69) we get:

$$J^j_1 = J^j_\theta\, \dot{\theta} + J^j_{v_{P_1}} \left(\phi_P + N_P \eta^{j\,2}_{P_0}\right) + J^j_{\varphi_{P_0}} \eta^j_{P_1} +$$

$$+ \Gamma\Omega\, J^j_{v_{E_1}} \left(\phi_E + N_E \eta^{j\,2}_{E_0}\right) + \Gamma\Omega\, J^j_{\varphi_{E_0}} \eta^j_{E_1} = 0 \qquad (9.76)$$

The first order correction term for the pursuer's turn rate control is:

$$\eta^j_{P_1} = \frac{-\left\{J^j_{\theta_1} \left[\frac{-v_P \sin(\varphi_P - \theta_h)}{r}\right] + \left(\phi_P + N_P \eta^{j\,2}_{P_0}\right) J^j_{v_{P_1}}\right\}}{J^j_{\varphi_{P_0}}} \qquad (9.77)$$

Similar expression can be derived for the evader.

Finally it can be observed that the entire right-hand side of (9.77) is derived from the zero-order trajectory.

$J^j_{\theta_1}$ is calculated from (9.58) and $J^j_{v_{P_1}}$ from (9.64) and (9.51).

Both expressions require integration along the zero-order solution which is an off-line operation.

7. CONCLUSIONS

Due to the inherent complexity of the approach outlined in this chapter, even for the relatively simple 2-D (horizontal) case, it seems that other methods for approving the zero-order FSPT approximation need to be investigated.

An example for such an improvement technique, motivated by a recent work [32] is presented in the next chapter.

SECTION X

IMPROVEMENT OF THE ZERO-ORDER GAME SOLUTION BY PARAMETER OPTIMIZATION

1. GENERAL DISCUSSION

As mentioned in Chapter 9, the functional structure of the suboptimal control strategies (i.e., the dependence on the state and the adjoint variables) is identical to the optimal control strategies.

The difference is that the adjoint variables being based on the time scale separation assumption, are approximate.

One way to improve the approximation of zero-order is to compute higher order terms as demonstrated in the previous chapter. However, the complexity of this approach renders it a hardly practical engineering tool.

In this chapter a different approach is presented. Motivated by a recently reported investigation by ONERA [32] on approximating a game saddle-point solution by results of respective minmax and maxmin optimization it is proposed to optimize parameters in the feedback expressions of the FSPT control strategies.

The most important parameters in this respect are the maximum velocities of the respective airplanes, determined for each of them by

$$V_{max} = \arg \max_{E,h} [T_{max} - D_0 + D_i] \tag{10.1}$$

In the reduced order game it has been assumed that both aircraft reach this maximum velocity before termination, i.e.,

$$V_E^o = V_E(t_f) = V_{E_{max}} \quad , \quad V_P^o = V_P = V_P(t_f) = V_{P_{max}} \tag{10.2}$$

In reality these conditions are rarely satisfied. Consequently the value of

$$\lambda_R^o = 1/(V_P^o - V_E^o) = 1/[(V_P)_{max} - (V_E)_{max}] \tag{10.3}$$

is not correct, violating the transversality condition

$$\mathcal{H}(t_f) = 0 \tag{10.4}$$

Using the uncorrect values for $V_p(t_f)$ and $V_E(t_f)$ leads to further violations of other transversality conditions as

$$\lambda_{E_p}(t_f) = \lambda_{E_E}(t_f) = 0 \tag{10.5}$$

resulting in a deviation from optimality.

An educated guess of the actual final velocities of the opponent airplanes (which are not known a priori) $V_p(t_f)$ and $V_E(t_f)$, and their use in the zero-order feedback control expressions instead of $(V_p)_{max}$ and $(V_p)_{max}$, should provide an improved approximation for the game solution. Such a correction should also lead to improve the performance of the individual aircraft.

For purposes of performance assessment by off-line computation this correction can be easily carried out by successive approximation starting with the zero-order feedback solution. At each step the values of V_P^o and V_E^o are approximated by the actual final values obtained from the previous step. The convergence of this process is very fast. Experience gained using the examples of Chapter 7 indicates that only 2 or 3 additional integrations are necessary and the improvement can be of importance.

For a real time (on-line) airborne implementation (one of the most attractive features of the FSPT approach), simple algorithms can be developed, based on range measurements and estimations of own and opponent acceleration capabilities, to predict approximatively $V(t_f)$ of each airplane. The type of feasible algorithm depends on the available measurements onboard the airplane. Further exploration and assessment of such algorithms are out of the scope of the reported research activity.

2. THE PARAMETER OPTIMIZATION PROCESS

In this section the effect of varying the value of V_P^o and V_E^o on the outcome of the game is demonstrated. In order to analyse the respective performance improvements and verify that optimal value of V^o the approach of minmax (maxmin) parameter optimization, motivated by [32], was selected. The example for this analysis was the one used in Chapter 7 with the following set of initial conditions:

$R_0 = 20.000$ m, $\psi_0 = 0°$, $\chi_{P_0} = 0°$, $\chi_{E_0} = 180°$, $V_{P_0} = 280$ m/sec, $V_{E_0} = 370$ m/sec,

$h_{P_0} = 4000$ m, $h_{E_0} = 2000$ m, and with $R_F = 4000$ m.

The results of the uncorrected zero-order solution are summarized in Table 10.1.

TABLE 10.1. RESULTS OF THE UNCORRECTED GAME, t_f = 149 sec.

	$V^o = V_{max}$	$V(t_f)$	$\Delta V^o = V^o - V(t_f)$	$\Delta V^o/V(t_f)$
Pursuer	555 m/sec	496 m/sec	59 m/sec	12%
Evader	604 m/sec	464 m/sec	140 m/sec	30%

The large discrepancies (especially for the evader) indicate that this particular zero-order game solution may not be a good approximation of an optimal game.

To evaluate the influence of V^o on the individual aircraft performance first the evader's V_E^o was varied as a parameter, keeping $V_P^o = (V_P)_{max}$ = 555 m/sec constant. Results of these computations are depicted by a solid line on Fig. 10.1 as a function of the speed ratio (V^o/V_{max}). The same excercise was repeated by varying V_P^o and keeping $V_E^o = (V_E)_{max}$ = 604 m/sec. This results are shown in Fig. 10.1 by a dashed line. In Fig. 10.2 the ratio of the actual final velocities $(V(t_f)/(V_{max}))$ are plotted as a function of (V^o/V_{max}) for each case.

These results confirm the expected performance improvements as $V^o \to V(t_f)$, amounting to an individual sensitivity, defined as the ratio of the relative change in capture time to the relative change in the value of own V^o (while the opponent's $V^o = V_{max}$).

$$\sigma_E \triangleq \left.\frac{(\Delta t_f / t_f)}{[\Delta V_E^o / V_E(t_f)]}\right|_{V_P^o = (V_P)_{max}} = -0.33 \tag{10.6}$$

$$\sigma_P = \left.\frac{(\Delta t_f / t_f)}{[\Delta V_P^o / V_P(t_f)]}\right|_{V_E^o = (V_E)_{max}} = 0.13 \tag{10.7}$$

As expected by optimizing the parameter V^o for the evader (the maximizer) the capture time increases and conversely by varying V_P^o to the right direction the capture time is decreasing.

The result of a simultaneous parameter optimization is not obvious from the beginning, but due to the higher sensitivity of the evader it can be expected that the corrected game solution would favourably shift to its direction.

Indeed the outcome of the engagement with converged values of $V_P^o = V_p(t_f) = 507$ m/sec and $V_E = V_E(t_f) = 476$ m/sec resulted in $\underline{t_f = 163 \text{ sec}}$ an improvement of 8.5% for the evader compared to the uncorrected zero-order estimate of 149 sec.

3. A QUALITATIVE ANALYSIS

In Fig. 10.3 and 10.4 the velocity profiles of the evader and the pursuer for the parameter optimized engagement are respectively compared to their profiles in the uncorrected game.

Since the initial conditions of the engagement are very unfavourable for the evader ($\chi_{E_0} = 180°$) its turning performance at the initial phase is predominant. The corrected lower value of V_E^o (see Eq. 5.103 and 6.12) requires higher turning rate and consequently a smaller gain, or even some loss, of specific energy. Inspite of the fact that the game terminates later, the final speed of the evader is less than in the uncorrected version. The relative advantage gained by this faster initial turn, and demonstrated by the increased "capture time", is illustrated in Fig. 10.5 where the histories of the relative range of separation of the engagements are compared.

The variations in the speed profile of the pursuer in Fig. 10.4 are much less impressive for the following reasons: (i) the pursuer starts with the most favourable initial geometry ($\chi_{P_0} = \psi_0$) and almost does not have to turn in the horizontal plane; (ii) the difference ΔV_P^o given in Table 10.1 is much smaller than ΔV_E^o. Consequently due to the longer flight time the final velocity is higher than in the uncorrected game.

The comparison also indicates that the relatively large improvement is very probably due to the asymmetry of initial conditions of the example selected and to the fact that the evader has a higher maximum velocity than the pursuer, i.e., that reduced order game does not predict capture.

The additional insight gained from this comparison and the demonstrated improvement, indicate the potential of this simple technique and the need for further, more detailed investigation in this direction.

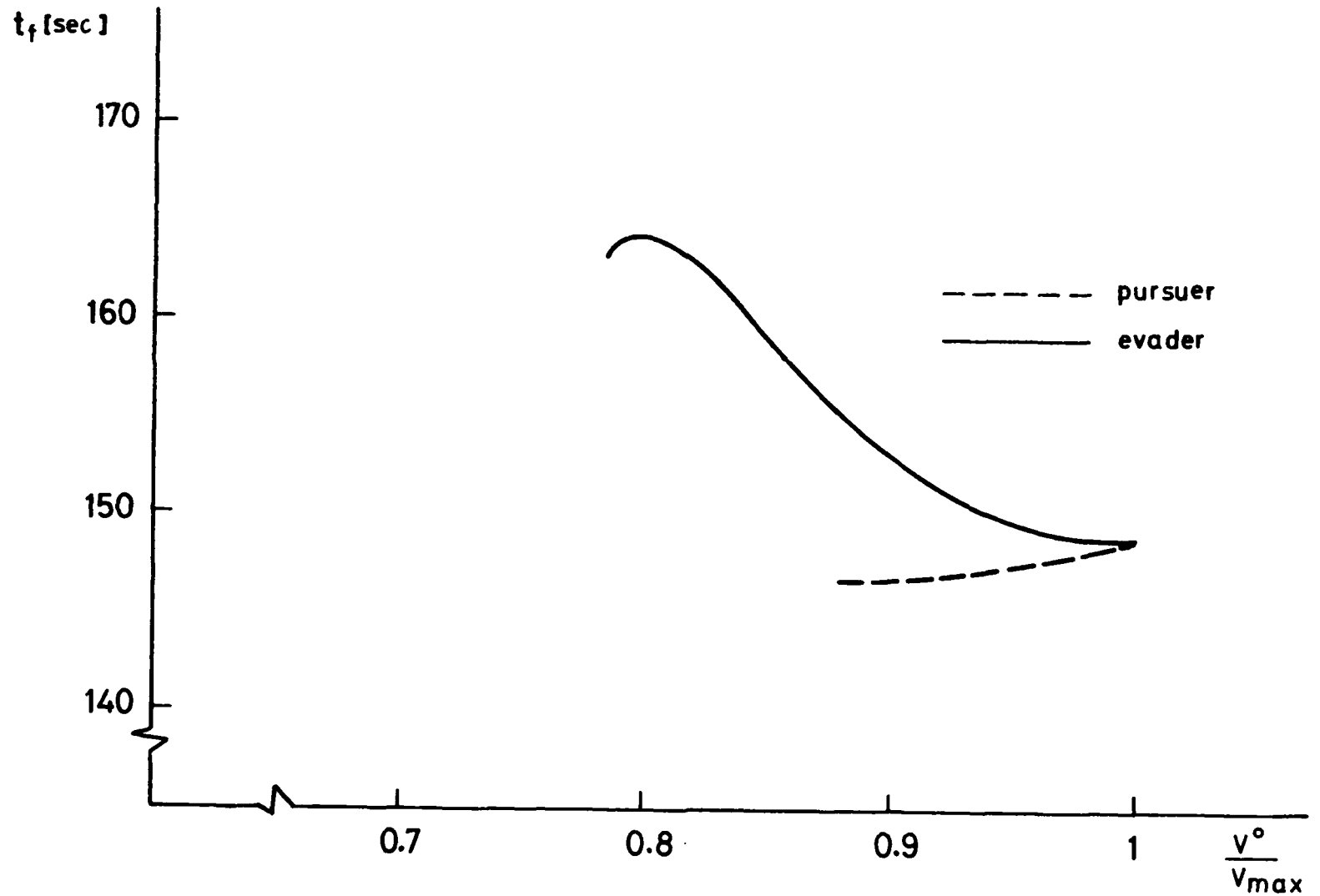

Fig. 10.1: Effect of V^o variation on the capture time.

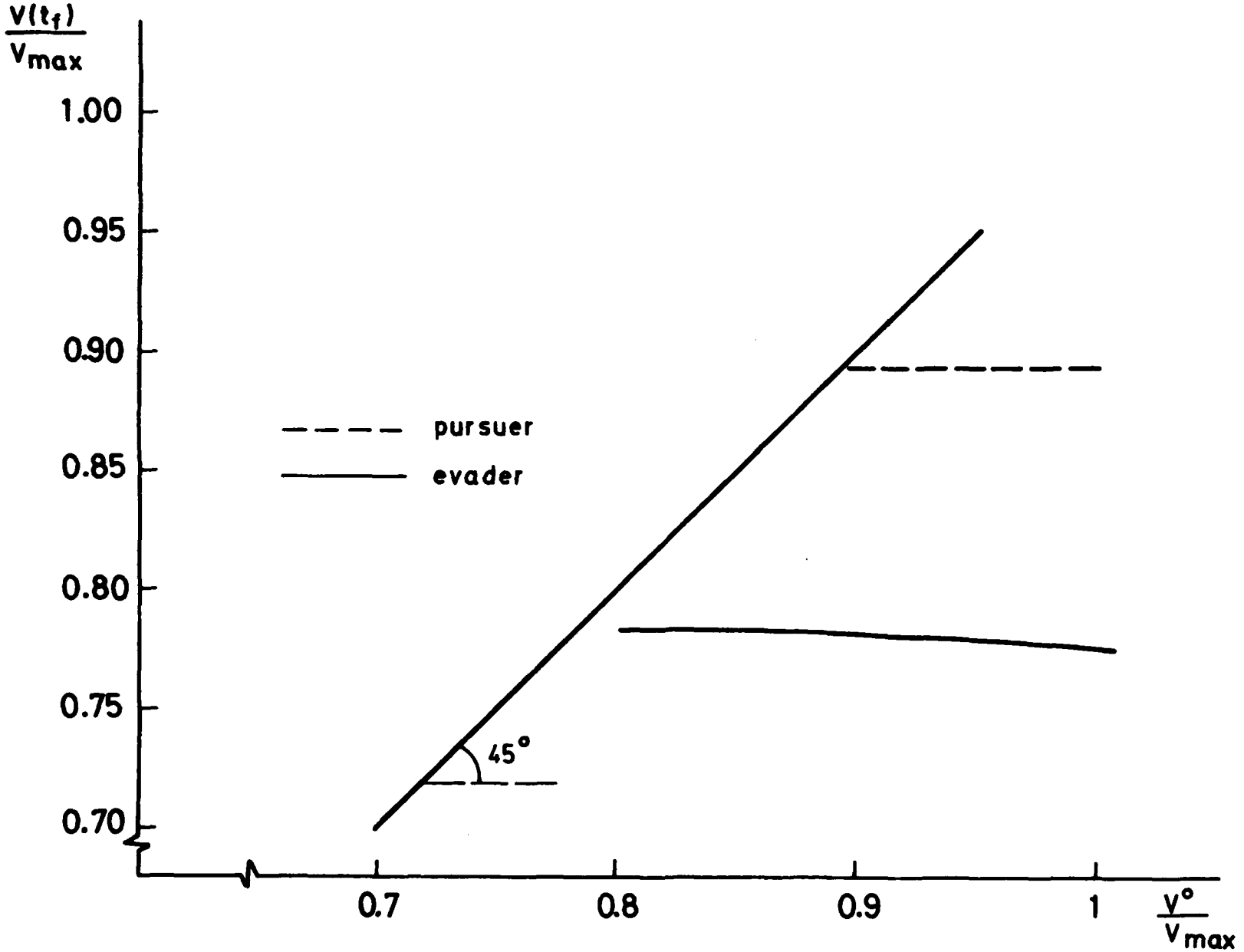

Fig. 10.2: Effect of V^o variation on the final velocities.

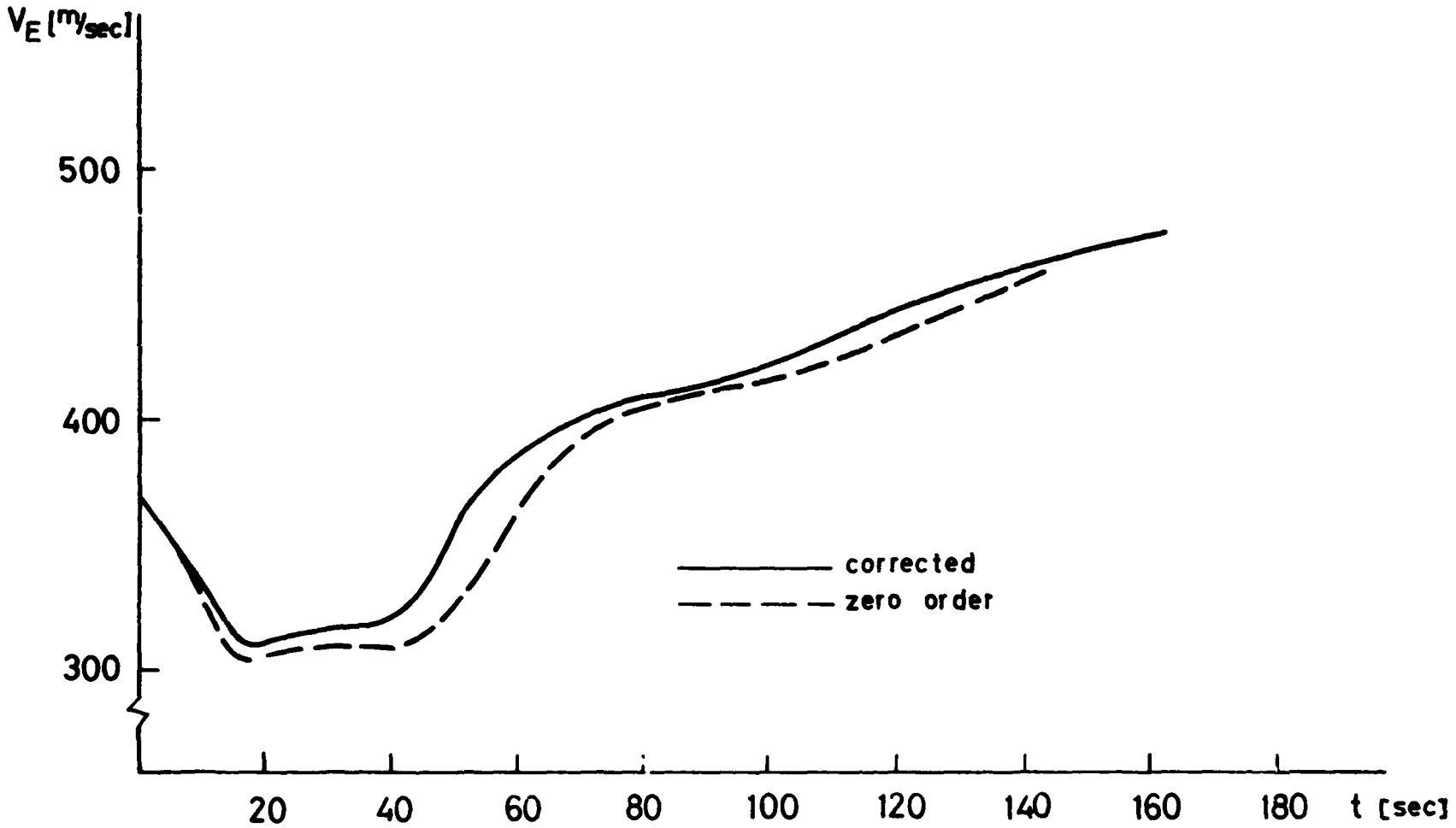

Fig. 10.3: Evader's velocity profile for zero-order and corrected games.

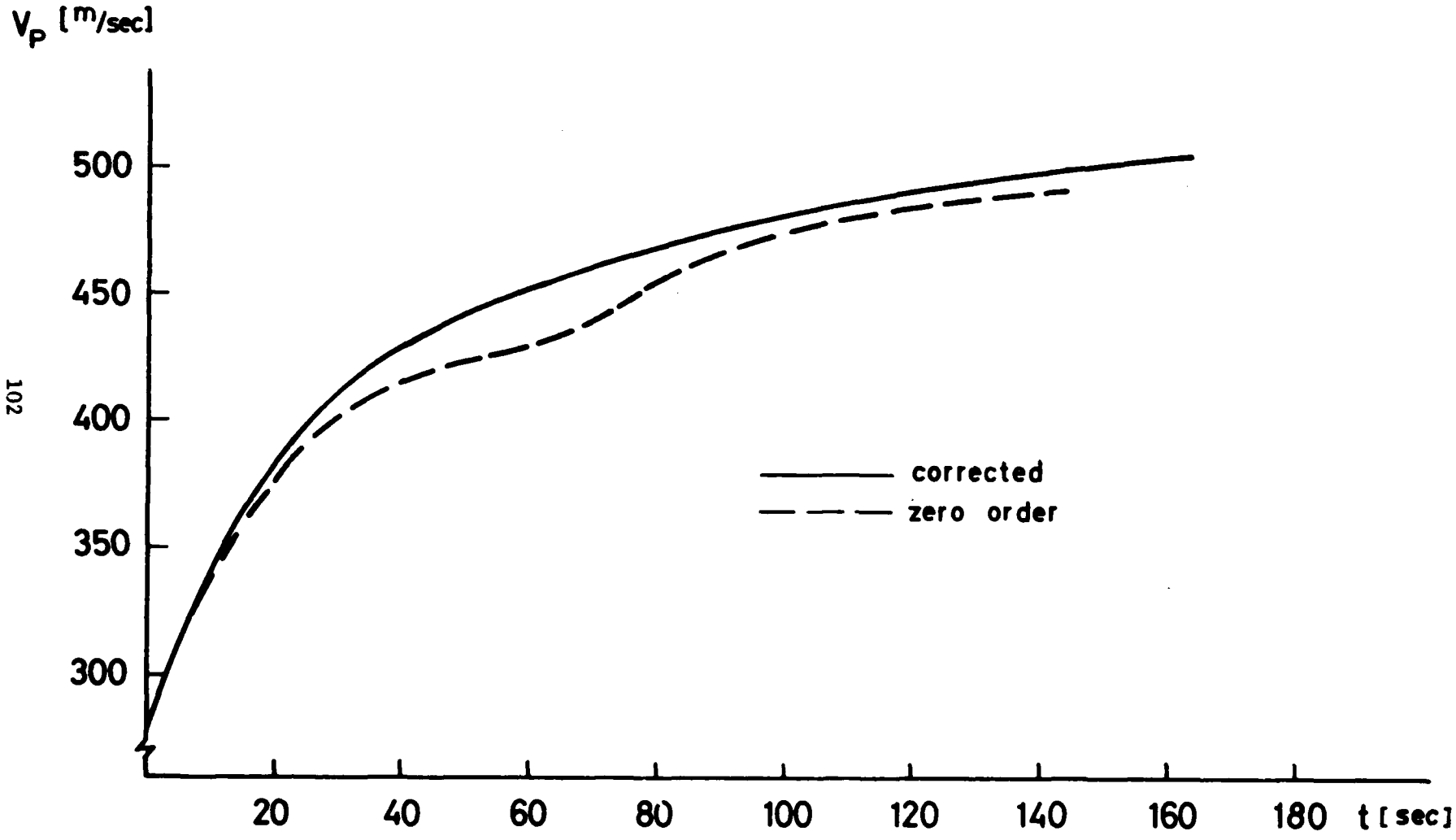

Fig. 10.4: Pursuer's velocity profile for zero-order and corrected games.

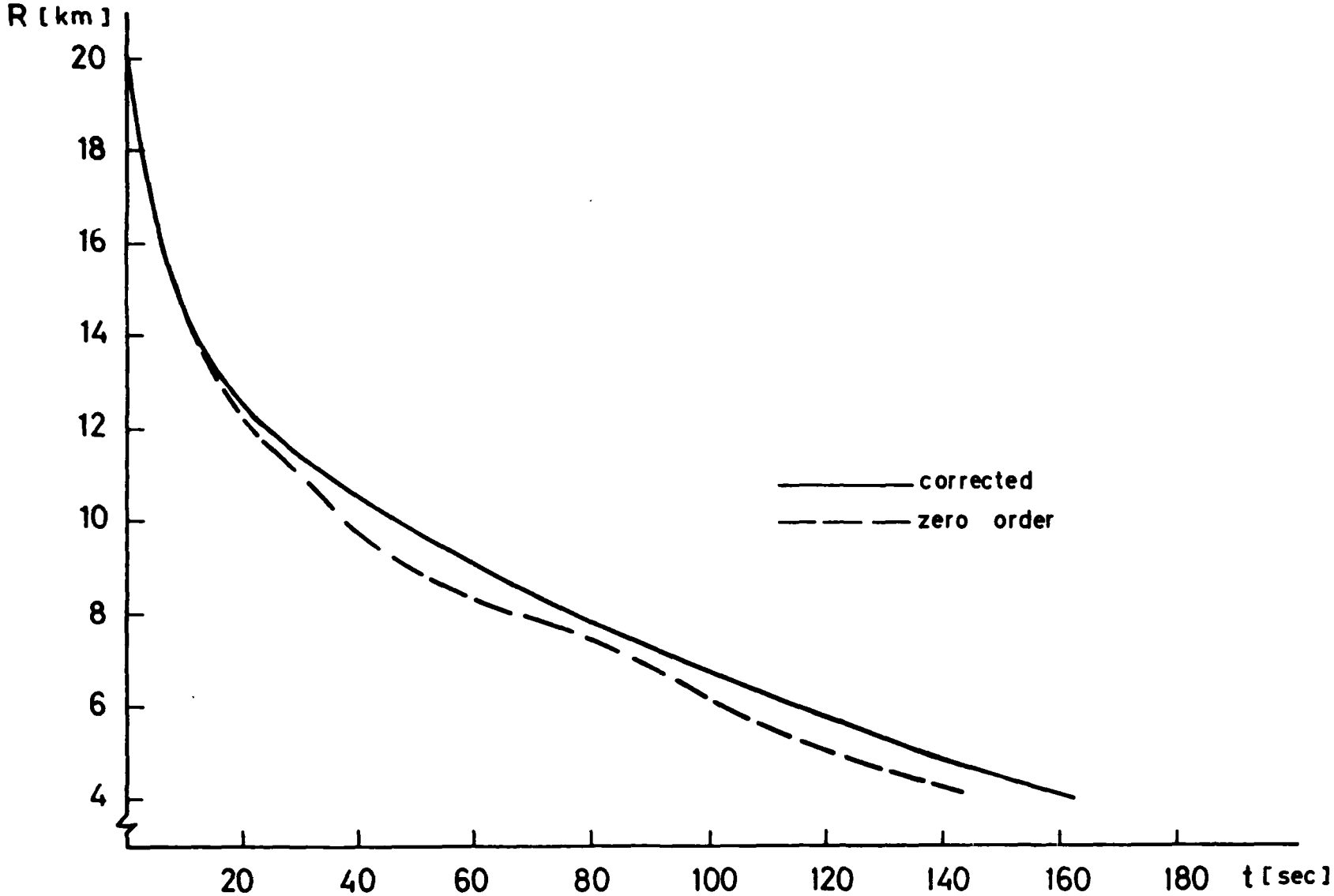

Fig. 10.5: Time histories of separation distance in zero-order and corrected games.

SECTION XI

CONCLUSIONS AND RECOMMENDATIONS

1. CONCLUSIONS

From the results presented in this report it can be first of all be concluded that modern air combat can be meaningfully investigated by an analytical method. An air combat problem of considerable importance: the three-dimensional medium range air to air interception, with advanced guided missiles, was successfully analyzed using realistic airplane models, by combining the technique of forced singular perturbation and differential game theory. This methodology has provided a zero-order feedback control strategy, closely approximating the exact solution. The attractiveness of the feedback solution for airborne implementation cannot be overemphasized. (This aspect of the solution merits some additional effort, outlined in the sequel). The feedback solution can serve also as a very efficient tool for rapid but systematical assessment of several operational problems of interest as demonstrated by the analysis of an imaginary air defence scenario.

The numerical accuracy of the zero-order FSPT solution for a three-dimensional interception game could not be directly assessed due to the non-existence of any operating numerical algorithm to provide the exact game solution for comparison. There is however a very strong "circumstantial evidence", based on similar but not identical comparisons, that the zero-order FSPT solution has a sufficient level of accuracy for medium range air combat analysis. Consequently higher order correction terms in many cases may not be required.

Nevertheless, the methodology to obtain the first (and higher) order terms of the FSPT expansion has been developed, indicating that such correction can be carried out only by an off-line computation. The considerable computational complexity, demonstrated by the relatively simple horizontal example, makes the usefulness of such correction questionable. As an alternative, a technique of parameter optimization is proposed and its potential for improvements is demonstrated. On-board implementation of this technique seems possible but requires, however, further investigation.

Another problem addressed in the research program was the solution of "terminal boundary layer". It was found that terminal boundary layer solutions, though they may exist and computed in open loop, cannot be implemented in a feedback form. Moreover, it has been demonstrated that solution of terminal boundary layers can be avoided by using a judiciously formulated dual modelling (see Chapter 5). This approach enables to keep the zero-order control strategies in a pure feedback form and make airborne implementation of these strategies a simple task.

The topic of airborne implementation, being the ultimate objective of an applicable analysis, merits further elaboration.

2. AIRBORNE IMPLEMENTATION

As mentioned earlier, the feedback form of the FSPT solution makes it an extremely attractive candidate for implementation onboard future advanced aircraft. There are several ongoing experimental programs exploring concepts and technologies for advanced integrated fire and flight control systems. Incorporating elements of optimal air combat strategy in such a system seems to be an obvious step. The simplicity of the FSPT control algorithm and its

accuracy for medium range air combat lead to strongly recommend its airborne implementation.

In order to provide a preliminary tool for evaluating such effort, the requirements for the airborne implementation are briefly obtained. It has to be noted that this outline is by itself an introductory one and does not pretend to substitute a more profound assessment. For airborne implementation the following requirements can be listed:

a) storage of aircraft performance data and results of some off-line computations;

b) measurement, filtering and data reduction of the state variables involved;

c) computation and synthesis of the control algorithm;

d) display of the required control strategy or its application as an input of the flight control system.

2.1 Storage Requirement

The largest storage requirement relates to the aircraft aerodynamic and propulsive model as a function of speed, altitude, and plane configuration. Either tabulated data, requiring some interpolation scheme or a polynomial approximation can be used, as it has been done for a ground base simulation. Such data can be also used, and in some airplanes it has been already done, for other purposes such as automatic weapon delivery, flight path managements, etc. The additional data to be stored, useful mostly for medium range interception, is the precomputed "optimal" altitude for best acceleration "h_1", as a function of specific energy. The eventual constraints of the flight envelop are included in any modern flight control system.

2.2 Measurement Requirements

In order to compute the FSPT control strategy the knowledge of the following variables is needed:

a. velocity vector, magnitude and direction in a fixed (inertial) coordinate system,

b. altitude (pressure altitude is sufficient),

c. angle of attack,

d. bank angle,

e. radar range to the target,

f. line of sight orientation in aircraft body axes,

g. aircraft actual weight,

h. weapon system envelope.

It is easy to see, without further detail, that the required measurements do exist in every modern military airplane. If line of sight angles are beyond the usual range of airborne radar gimbals, this information has to be either a manual input of the pilot or a data linked message by a ground based controller (giving the interception command).

2.3 Computations

Filtering, transformation of coordinates and other phases of data reduction may require some computational load as for any other automated system. It is strongly dependent on the type of the airplane considered for implementation. The computation of the control algorithm is extremely simple. Three different types of optimal load factors $(n_h, \bar{n}_v, \hat{n}_v)$ have to be computed. The number of arithmetical operations in each computation is relatively small depending

slightly on the type of stored data. Based on these three values the synthesis of the required optimal load factor and bank angle is obtained.

2.4 Display

The outputs of the control algorithm are the required values of variables already displayed in almost every aircraft. It is very simple to use the already existing symbols of a HUD or other type of display, by selecting a proper mode of operation (i.e., medium range air-to-air) in order to indicate to the pilot the required control action minimizing the time for air-to-air weapon deployment. Simultaneously, the signals of the required maneuver can be used as inputs to an automatic flight control system.

3. RECOMMENDATIONS

In spite of the preliminary nature of the airborne implementation scheme it is clear that it does not present any particular difficulty. Moreover, very probably it can be carried out without substantial complication and additional cost in a planned integrated fire and flight control system. Therefore it is strongly recommended to make the necessary steps that the airborne implementation of the FSPT algorithm for medium range air combat would be included in a future experimental flight test program. The real merits of the algorithm can be fully evaluated based on the results of flight experience.

Further investigation of simple correction techniques of the basic zero-order FSPT solution, which seem to lead to important improvements, are also recommended.

REFERENCES

1. Farber, N., and Shinar, J., "Approximate Solution of Singularly Perturbed Nonlinear Pursuit-Evasion Games", Journal of Optimization Theory and Applications. Vol. 32, No. 1, Sept. 1980.
2. Simakova, E.N., "Differential Pursuit Game", Automatika i Telemekhannika, No. 2, pp. 5-14, Feb. 1967.
3. Farber, N., and Shinar, J., "An Approximate Feedback Solution of a Variable Speed Nonlinear Pursuit-Evasion Game Between Two Airplanes in a Horizontal Plane", AIAA Paper 80-1597, Atmospheric Flight Mechanics Conference, Danvers, Massachusetts, Aug. 1980.
4. Ardema, M.D., Singular Perturbations in Flight Mechanics, NASA TM X 62-380, Aug. 1974.
5. Calise, A.J., "Singular Perturbations Methods for Variational Problems in Aircraft Flight", IEEE Transactions on Automatic Control, AC 21, No. 3, June 1976.
6. Calise, A.J., "Extended Energy Management Methods for Flight Performance Optimization", AIAA J., 15, No. 3, March 1977.
7. Calise, A.J., Singular Perturbations Analysis Approach for Systems with Highly Coupled Dynamics, Dynamics Research Corporation, 1977.
8. Shinar, J., "Remarks on Singular Perturbation Technique Applied in Nonlinear Optimal Control", 2nd IFAC Workshop on Control Application of Nonlinear Programming and Optimization, Oberpfaffenhofen, W. Germany, Sept. 1980.
9. Farber, N., and Shinar, J., A Variable Modeling Approach for Singularly Perturbed Pursuit-Evasion Problems, TAE Report No. 433. Feb., 1981. Department of Aeronautical Engineering, Technion - Israel Institute of Technology.
10. Farber, N., Improved Dynamic Models for Air Combat Analysis as a Zero-Sum Differential Game, D.Sc. Dissertation. Department of Aeronautical Engineering, Technion - Israel Institute of Technology, May 1981 (in Hebrew).
11. Lynch, U.H.D., Games Barriers and their Application in Air to Air Combat, Ph.D. Dissertation, Air Force Institute of Technology, Wright-Patterson AFB, 1973.
12. Miloh, T., "A Note on Three Dimensional Pursuit-Evasion Game with Bounded Curvature", to be published in the IEEE Journal of Guidance and Control.
13. Miller, E.L., Application of Differential Game to Air-to-Air Combat Problems AFFDL-TR-7547, 1975.
14. Mehra, R.K., Washburn, R.B., Sagon, S., A Study of the Application of Singular Perturbation Theory, Final Report on Contract NAS1-15113, 1979.

15. Shinar, J.,"Solution Techniques for Realistic Pursuit-Evasion Games", Chapter 3, Advances in Control and Dynamic Systems, Vol. 17, (Ed. C.T. Leondes), Academic Press, 1980.

16. Shinar, J., and Merari, A., "Aircraft Performance Optimization by Forced Singular Perturbations", 12th Congress of ICAS, 12-17 October, 1980, Munich, Germany.

17. Bryson, A.E. Jr., Desai, M.N., and Hoffman, W.C., "Energy State Approximation in Performance of Supersonic Aircraft", Journal of Aircraft, Vol. 6, No. 6, Nov. 1969, pp. 481-488.

18. Negrin, M., Solution of Optimal Three Dimensional Interceptions by the Method of Singular Perturbations, M.Sc. Thesis, Department of Aeronautical Engineering, Technion - Israel Institute of Technology, June 1981 (In Hebrew).

19. Shinar, J., Negrin, M., Well, K., and Berger, E., "Comparison Between the Exact and an Approximate Feedback Solution for Medium Range Interception Problems," Joint Automatic Control Conference, University of Virginia, Charlottesville, Va., June 17-19, 1981.

20. Roberts, D.A., and Montgomery, R.C., "Development and Application of a Gradient Method for Solving Differential Games," NASA TN-D 6502, 1971.

21. Leathman, A.L., A Neighboring Optimal Method to Solve Differential Games Involving Realistic Aerodynamic Vehicle Models, AFFDL-TM-73-56-FXG. Air Force Flight Dynamics Laboratory, Wright-Patterson Air Force Base, Ohio, 1973.

22. Lynch, U.H.D., The Simultaneous Minmax Gradient Technique for Solving the Air-to-Air Combat Differential Game," AFFDL TM-73-57-FXG, Air Force Flight Dynamics Laboratory, Wright-Patterson AFB, Ohio, 1973.

23. Anderson, G.M., "A Near Optimal Closed Loop Solution Method for Non-Singular Zero-Sum Differential Games," JOTA, 13, No. 3, 1974.

24. Neeland, R.P., The Numerical Solution of a Nonlinear, Control Constrained, Air-to-Air Combat Differential Game," Ph.D. Dissertation, University of California, Los Angeles, 1974.

25. Miller, L.E., "Differential Game Computer Program," AFFDL TM 75-66-FXG, November 1977.

26. Jamark, B., "Convergence Control in Differential Dynamic Programming Applied to Air-to-Air Combat," AIAA J., 14, No1

27. Fajalbert, B., Resolution Numériques pour les Problèmes de Jeux Differentiels. Thèse de 3ème cycle, Universite de Paris, 1979.

28. Shinar, J., Validation of Zero-Order Feedback Strategies for Medium Range Horizontal Air-to-Air Interception. NASA-TM (in preparation).

29. Rajan, N., Prasad, U.R., and Rao, N.J., "Pursuit-Evasion of Two Aircraft in a Horizontal Plane", Journal of G. and C. Vol. 3, No. 3, May-June 1980, pp. 261-267.

30. Prasad, U.R., Rajan, N., and Rao, N.J., "Planar Pursuit-Evasion with Variable Speeds, Part 1. JOTA. Vol. 33, No. 3, March 1981, pp. 401-418.

31. Rajan, N., Prasad, U.R., and Rao, N.J., "Planar Pursuit-Evasion with Variable Speeds, Part 2, JOTA, Vol. 33, No. 3, March 1981, pp. 419-432.

32. Marchal, C., Resolution des Jeux Differentiels Deterministes. - La Methode de la Strategie Approchée, ONERA Rapport Technique 3/3437 SN. Avril 1981.